Alma Mater Studiorum – Università di Bologna

DOTTORATO DI RICERCA IN

Scienze Biomediche e Neuromotorie

Ciclo XXXIV

Settore Concorsuale: 06/D3

Settore Scientifico Disciplinare: MED/06

Modeling the natural history of bone metastasis from breast cancer in a 3D biomimetic scaffold.

Presentata da: Chiara Spadazzi

Coordinatore Dottorato

Prof.ssa Matilde Yung Follo

Supervisore

Prof. Nicola Baldini

Co-Supervisore

Dott.ssa Laura Mercatali

Esame finale anno 2021

Abstract

The study of bone metastasis from breast carcinoma is hampered by the lack of *in vitro* models that recapitulate the complex sequential stages and interactions between tumor cells and microenvironment. Indeed, molecular interactions, between tumor and stromal cells, are critical regulators of every steps of progression. However, cells typically grown on two-dimensional (2D) platforms poorly reflect the microenvironment context of the tumor, hampering the translation of the data to the human disease. Indeed, the extracellular matrix of both primary tumor and metastatic site plays a crucial role in orchestrating tumor progression. Animal models could be useful for evaluating the complexity of the bone metastasis process, but this model suffers of being time-consuming and labor intensive. Moreover, to date, there is no ideal animal model able to replicate different aspects of the metastasis. Indeed, it remains impossible to analyze the initial phase of the process, such as the pre-metastatic niche formation in the host secondary organ. More reliable systems able to deconstruct the sequential cascade of events involved in bone metastasis pathogenesis would lead the opportunity to identify new therapeutic strategies to block the metastatic spread, at an early stage. Hence, it emerges the need to fill the gap between *in vitro* and *in vivo* model with a reliable *in vitro* three-dimensional (3D) system that closely recapitulates the complexity of the bone microenvironment and its interaction with cancer cells. With a step-by-step approach, we aimed to mimic the mechanisms involved in the natural history of breast cancer bone metastasis, from the establishment of the pre-metastatic niche in the host environment, to the bone metastasis. To achieve this aim, we developed a bone biomimetic scaffold, made of collagen, and functionalized with hydroxyapatite material (3D mineralized scaffold), able to mimic the composition of the bone matrix *in vitro*. Firstly, we demonstrated that this platform is suitable for the culture and differentiation, from their respective precursor cells, of osteoclasts and osteoblasts, the crucial players in the maintenance of bone homeostasis. Then, we investigated how the bone biomimetic extracellular matrix can affect dynamics of cell growth, genetic and phenotypic characteristics of three breast cancer cell lines, different for their molecular profile and clinical behavior: MDA-MB-231 (triple negative breast cancer), SCP2 (a bone-tropic subclone of the MDA-MB-231 cell line, *in vivo* selected) and the MCF7 cell line (luminal A breast cancer). Interestingly, breast cancer cells, cultured in the presence of HA, showed a lower growth rate compared to when cultured in collagen matrix. By gene expression analysis, we showed that breast cancer cells cultured in 3D mineralized scaffold express at higher level pro-inflammatory genes and that ER- breast cancer cells showed an upregulation of the osteomimetic genes

CXCR4, JAG1. Moreover, we showed that breast cancer cells, cultured in the 3D mineralized scaffold, secrete soluble factors able to induce osteoclasts differentiation from their precursor cells. TNF-α, which has been found to be highly expressed by breast cancer cells cultured in 3D mineralized scaffold, could support this differentiation. Interestingly, different ECM seems to affect breast cancer and osteoclasts sensitivity to bone targeted drugs. The mechanisms underlying this different response still need to be clarified. Finally, the direct co-culture of osteoclasts and tumor cells in the 3D mineralized model enabled to demonstrate their mutual interactions in bone microenvironment, showing a different behavior and phenotypic plasticity for ER- and ER+ tumors. Indeed, ER- tumors seem to acquire a more epithelial-like phenotype, as demonstrated by the downregulation of EMT markers; ER+ tumors shift towards a more mesenchymal phenotype, with the significant upregulation of EMT markers and the acquisition of a spheroid-like morphology in the 3D mineralized scaffold.

In conclusion, we developed an *in vitro* three-dimensional bone biomimetic model, demonstrating that it is a feasible platform to mimic bone microenvironment and to investigate the interaction between tumors and bone cells, in the establishment of metastasis. To increase its translational value, it would need to be confirmed with patients' clinical samples and implemented with a tri co-culture of osteoblasts, osteoclasts, and tumor cells. The achieved results represent a first step which laid the ground to a more comprehensive model. We demonstrated that the mechanical structure and mineral phase of the extracellular matrix can affect breast cancer cells behavior in bone metastatic progression. Moreover, we showed that each breast cancer subtypes are differently affected by the host microenvironment. A more understanding of the mechanisms underlying these processes would help the identification of future therapeutic strategies that specifically target defined components of the bone microenvironment to prevent or treat skeletal metastases.

Index

1. Introduction

1.1 Breast Cancer

Breast cancer is the most common neoplastic pathology in the female population and the second leading cause of death in women[1]. Due to its incidence and mortality rate, it represents a public health problem in Europe and the USA. In 2020, it is estimated that 2.3 million women were diagnosed with breast cancer and 685.000 deaths globally. At the end of 2020, 7.8 million women were diagnosed with breast cancer in the past 5 years, making it the world's most prevalent cancer. The epidemiology of breast cancer has undergone substantial changes during the years, following the introduction of screening programs, the discovery of more effective and personalized therapeutic strategies and life-style changes in women. The trends show an incidence growth in the younger age group (<49 years), a decreased incidence in women aged between 50 and 69, and stable trend in the elderly. However, survival is higher compared to the past. Indeed, it is estimated a survival rate of about 85% 5 years after diagnosis, compared to 76.3% in the years 1985-87. This improvement mainly concerns younger women (20-40 years). This effect can be accounted to the early diagnosis by efficient screening programs implemented in recent years and to the more efficient therapeutic strategies, which contributed to a significant improvement of survival in breast cancer patients. Despite the numerous improvements in therapeutic and management of breast cancer patients, this tumor is still the leading cause of cancer-related deaths in European women[1].

1.1.1 Classification

The initial clinical evaluation should determine the clinical stage of the disease and allow for treatment planning by defining the indications for initial surgery, conservative or not, or for systemic treatment in case of advanced disease. The extent of the disease is described with conventional classification criteria, among which the most used is from the International Union against Cancer; the TNM system[2].

- T → stands for tumor size.
- N → it concerns lymph node involvement.
- M→ it is evaluated for the presence of metastases.

Besides the initial clinical evaluation, the increased understanding of morphological and intrinsic molecular features of breast cancer has led to a more accurate categorization of each tumor subtype, leading to a significant improvement in prevention, early detection, and personalized breast cancer therapy. Indeed, breast cancer classification has become always

more accurate over the years, moving towards an integrative categorization which combines a histological and molecular classification[3]. This enables a better understanding of breast cancer heterogeneity, to better stratify patients and personalize treatment. Moreover, it is an ongoing-dynamic process which continues to evolve with the integration of new and updated scientific knowledge[4]. According to the latest World Health Organization (WHO) classification of tumors series' fifth edition, breast carcinomas are divided into 19 different major subtypes which includes: invasive carcinomas of no special type, which is a carcinoma that does not fit into a specific histotype (formerly ductal carcinoma) and it is estimated as the 70–80% of all subtypes; lobular carcinomas (10–15%) and the other carcinomas of special type (including 17 different rare histotypes and their subclassifiers)[5,6]. The histological and morphological classification is insufficient to predict the behavior of breast tumor pathophysiology[6]. Indeed, these breast cancer subtypes can be molecularly classified into distinct groups, analyzing their gene and markers expression patterns. Four clinically relevant molecular subtypes have been identified: Luminal A, Luminal B, enriched HER2 (HER2+), and Triple Negative (TNBC)[7] (Table 1). The expression of estrogen receptors (ER), progesterone receptors (PR), Human epidermal growth factor receptor 2 (HER2), and cell proliferation regulator (Ki-67) are the main indicator to classify the distinct molecular subgroups. Luminal A is defined as: ER+ (≥ 1%), high expression of PR (≥ 20%), HER2- (≤ 10%), and low levels of Ki-67 (< 14%)[8]. These tumors have characteristics of luminal epithelial cells of the breast, such as the high expression of cytokeratins 7/8/18/19[9]. The Luminal B (approximately the 20% to 30% of invasive breast cancer cases) is defined as: ER+ (≥ 1%), PR- or < 20%, HER2- (≤ 10%) and high levels of Ki-67 (≥ 20%); or Luminal B (HER2+): ER+ (≥ 1%), HER2+ (> 10%) and any level of PR and Ki-67[8]. The HER2+ subtype represents 15% to 20% of newly diagnosed breast cancer cases and it is characterized by a high expression of HER2 (> 10%), negativity for ER (< 1%) and PR (< 20%), and high expression of Ki-67 (> 20%). Finally, the triple negative subtype represents the 10%-20% of all breast cancer types and it is characterized by the lack of expression of the hormone receptors ER (< 1%) and PR (< 20%) and the oncoprotein HER2 (≤ 10%); moreover, they are highly proliferative tumors, according to the Ki-67 index (> 30%).

Table 1 Definitions of intrinsic subtypes of breast cancer[8]	
Intrinsic subtype	**Clinicopathological surrogate definition**
Luminal A	‘Luminal A-like’ ER-positive HER2-negative Ki67 low [a] PgR high [b] Low-risk molecular signature (if available)
Luminal B	‘Luminal B-like (HER2-negative)’ ER-positive HER2-negative and either Ki67 high or PgR low High-risk molecular signature (if available)
	‘Luminal B-like (HER2-positive)’ ER-positive HER2-positive Any Ki67 Any PgR
HER2	‘HER2-positive (non-luminal)’ HER2-positive ER and PgR absent
‘Basal-like’	‘Triple-negative’[c] ER and PgR absent[c] HER2-negative[c]

Adapted from the 2013 St Gallen Consensus Conference[8].
ER, oestrogen receptor; HER2, human epidermal growth factor receptor 2; PgR, progesterone receptor.
[a] Ki-67 scores should be interpreted in light of local laboratory values: as an example, if a laboratory has a median Ki-67 score in receptor-positive disease of 20%, values of 30% or above could be considered clearly high; those of 10% or less clearly low.
[b] Suggested cut-off value is 20%; quality assurance programmes are essential for laboratories reporting these results.
[c] There is ~80% overlap between ‘triple-negative’ and intrinsic ‘basal’ subtype, but ‘triple-negative’ also includes some special histological types such as carcinoma with a rich lymphocytic stroma (former medullary), secretory carcinoma, low-grade metaplastic carcinoma, and adenoid cystic carcinoma.

Besides the immunohistochemical markers (ER/PR/HER2/Ki-67), the growing molecular technologies support the evolution of this classification, leading to the improvement of patients' stratification and selection for treatment, with the development of many multigenic assays, such as Oncotype DX, Prosigna PAM50 and Mammaprint[7,10–12] .These multigenic signatures are being used to distinguish patients who may have an increased risk of recurrence and to identify who more likely could benefit of neoadjuvant or adjuvant chemotherapy. The molecular classification has also a prognostic value[6] (Fig. 1). Indeed, the intrinsic features can affect the profile (timing, sites) of metastatic disease. Luminal A tumors tend to relapse late (after 5 years of diagnosis) and they show a bone and lymph node tropism (as do luminal B, HER2-negative tumors). Instead, TNBCs tend to relapse early (within 2–3 years of diagnosis) showing a visceral (lung) and brain tropism. Since the era of anti-HER2 targeted therapy, HER2-positive breast cancers show better prognosis, but they can escape therapy through brain metastasis[7].

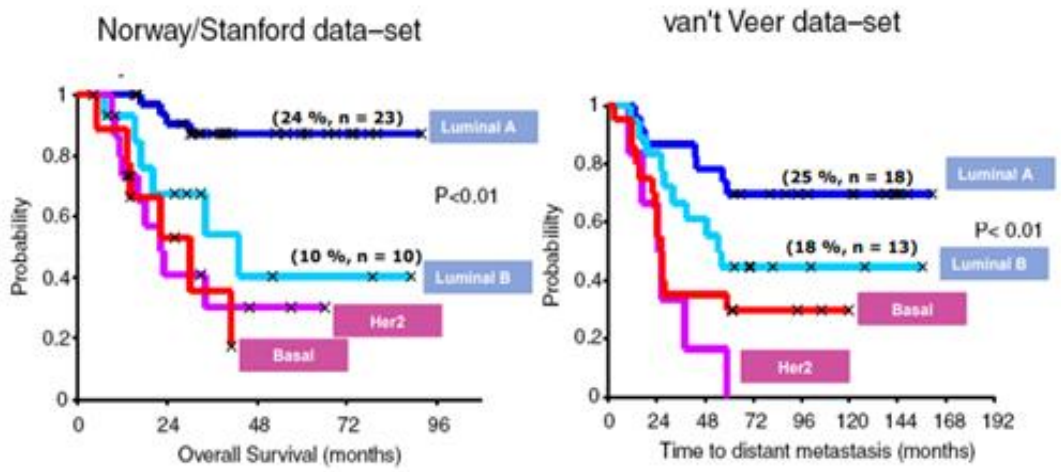

Fig. 1 Significant Prognostic Value of Intrinsic classification[6]

1.1.2 Current and Emerging Therapeutic Strategies

The strategies for the treatment of early breast cancer today can be guided by the integration of various multidisciplinary therapeutic modalities: surgery, radiotherapy (RT), pharmacological treatments, and consequently, by the optimal collaboration of various specialists[13]. It is also essential to know the prognostic, clinical and biological indicators that allow clinicians to evaluate the opportunity and the adequate options of systemic treatment[14]. Not least is the evaluation of the possibility of hereditary cancer. Treatment of early breast cancer is complex and involves combination of local modalities [surgery, radiotherapy, systemic anticancer treatments (chemotherapy, endocrine therapy, molecularly targeted therapies)] and supportive measures, delivered in diverse sequences. The use of predictive biomarkers such as ER, PgR, HER2 and Ki67 and approved genomic signatures is well established to help in determining the treatment of choice[14].

Neoadjuvant Treatment

Before surgery, neoadjuvant systemic treatment can be performed to render some inoperable patients eligible for it and to reduce the extent and morbidity of curative surgery. Indeed, multiple studies showed that both chemotherapy and endocrine therapy can increase the possibility of breast-conserving surgery[15–19]. The appropriate neoadjuvant treatment can be selected according to the breast cancer subtype and predictive biomarkers (Fig. 2). All modalities (chemotherapy, endocrine therapy, and targeted therapy) used in adjuvant treatment may also be used preoperatively. Thus, endocrine therapy should be used in all luminal-like cancers (ER+). Indications for chemotherapy within this subtype depend on the individual's risk of relapse, considering the tumor burden and features of biological aggressiveness (grade, proliferation, vascular invasion). Moreover, chemotherapy sensitivity is dependent on the intrinsic phenotype. ER-positive/HER2-negative carcinomas, especially of the lobular histology and luminal A-like subtype, are generally less responsive to primary chemotherapy and may benefit more from primary endocrine therapy[20,21]. Instead, chemotherapy is indicated in HER2+ breast cancer, for which neoadjuvant treatment is highly effective, and TNBC since their sensitivity to chemotherapy is high[20,21]. In particular, the pathological complete response rate is higher in TNBC patients treated with Carboplatin in the neo-adjuvant setting[22]. However, there are still no validated predictive markers to allow the tailoring of the regimen to the individual patient[23].

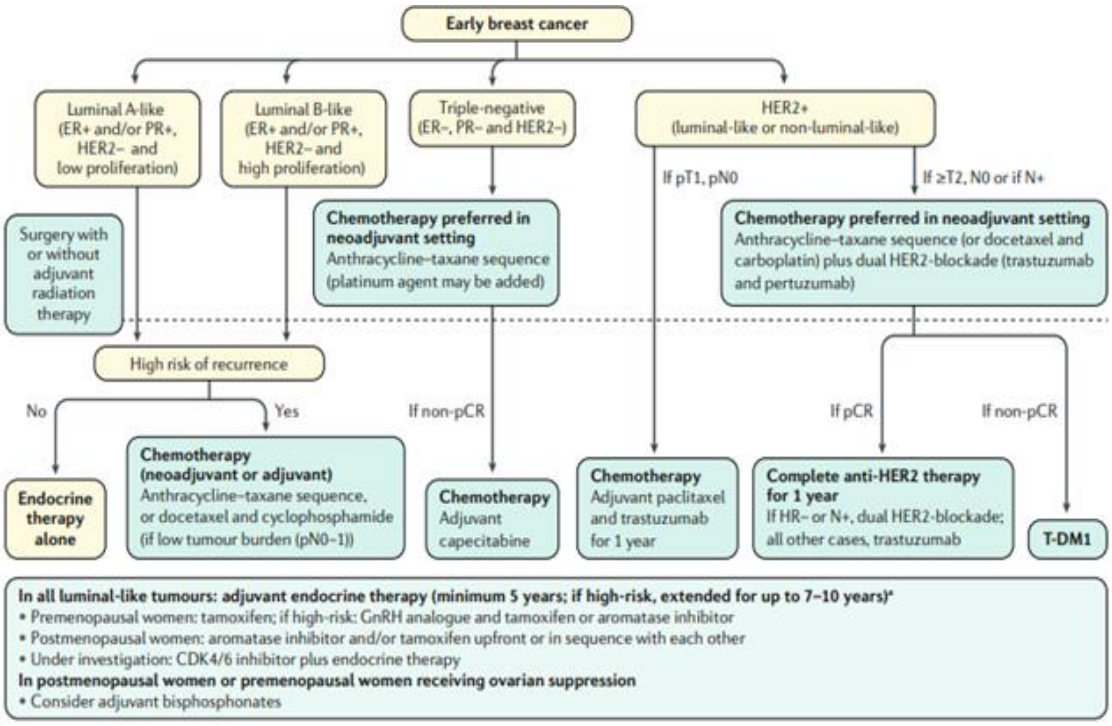

Fig. 2 Management of early breast cancer based on tumor burden and subtype[7]

Local Treatment (Surgery and Radiotherapy)

After neoadjuvant treatment, breast cancer surgery is the first treatment that is performed[24]. Currently, the surgical procedure is aimed at a conservative purpose, which is equivalent from a therapeutic point of view to radical surgery but with satisfactory cosmetic results. In Europe, 2/3 of breast carcinomas are treated with conservative surgery while the remaining 1/3, due to size (≥ 4 cm), is treated with mastectomy, position and multifocal / multicentricity of the tumor. After conservative surgical practice, the histological and pathological evaluation of the resection margins is important and a radiation treatment is strongly recommended[13,25]. The omission of radiotherapy is associated with a significant increase in local relapses; highlighting that post-surgical radiotherapy has an important effect on survival. In the standard application, the dosage for local or regional irradiation is 45-50 Gy divided into 25-28 fractions of 1.8-2.0 Gy/day. Complementary radiotherapy often must be integrated with adjuvant medical treatment, preferably not concomitantly[13,14].

Adjuvant Treatment

Adjuvant treatment is recommended if a relevant reduction in the estimated risk of recurrence or death can be expected. Estrogen Receptor (ER) and HER2 status are the most relevant predictors for choosing the most appropriate treatment modality (Table 2). As for the neoadjuvant setting, patients with hormone receptor positive tumors are treated with endocrine

therapy alone or in combination with chemotherapy depending on other biological characteristics of the tumor (Grading, index of proliferation, HER2 expression). For example, patients with amplification or overexpression of the HER2 gene receive in addition to endocrine therapy also chemotherapy with the dual anti-HER2 blockade Trastuzumab (Herceptin) and Pertuzumab (Perjeta). The choice of adjuvant therapy must consider the benefits, potential side effects and patient preferences. Standard endocrine therapy is characterized by the administration of tamoxifen (20 mg/day for 5 years) alone or in combination with ovarian function inhibitors [i.e. Gonadotropin-releasing hormone analogs (GnRHAs)]. The optimal duration of adjuvant hormonal treatment is between 5 and 10 years even if the benefit of using the therapy for a duration of more than 5 years has not been proven[26]. Other anti-hormonal strategies are used in clinical practice beside Tamoxifen. Adjuvant chemotherapy is recommended in ER-negative tumors. The most frequently used regimens contain anthracyclines and/or taxanes, although in selected patients, cyclophosphamide/ methotrexate/5-fluorouracil (CMF) may still be used. In particular, four cycles of doxorubicin and cyclophosphamide (AC) are considered to have equal efficacy to 6 cycles of CMF. The optimal duration of adjuvant chemotherapy is usually 18-24 weeks for patients with a high probability of relapse[27].

Table 2 Systemic treatment recommendations for early breast cancer subtype[14]

Subtype	Recommended therapy	Comments
Luminal A-like	Endocrine Therapy alone in most cases	Consider Chemotherapy if high tumour burden (≥ 4 LNs, T3 or higher)
Luminal B-like (HER2-negative)	Chemotherapy followed by ET for most cases	
Luminal B-like (HER2-positive)	Chemotherapy + anti-HER2 followed by Endocrine Therapy for all patients	If contraindications for Chemotherapy, it may be considered Endocrine Therapy + anti-HER2 therapy
HER2-positive (non-luminal)	Chemotherapy+ anti-HER2	
Triple-negative (ductal)	Chemotherapy	

Even if chemotherapy and endocrine therapy are still the basic regimen treatment for HER2 breast cancer patients, new therapeutic options are necessary since many patients with early-stage disease still relapse despite the use of currently available therapies. Currently, advanced breast cancer it is a treatable but incurable disease, with metastases being the cause of death in almost all patients, with a median overall survival (OS) of about 3 years and a 5-year survival rate of around 25%[26]. Survival is strongly related to breast cancer subtype, with the major advances seen in human epidermal growth factor receptor 2 (HER2)-positive. Endocrine therapy, with or without targeted therapy, is the mainstay for luminal-like disease, and several lines are to be used before commencing chemotherapy (Fig. 3). When chemotherapy is used, sequential monotherapy is advised. For triple-negative disease, chemotherapy is the main treatment, with no specific recommendations except that platinum is one of the preferred options. Moreover, triple-negative tumors may be candidates for first-line immunotherapy. For HER2-positive disease, it is crucial to continue blocking the HER2 pathway, with a sequence of anti-HER2 agents and chemotherapy; combinations of endocrine therapy with anti-HER2 therapy can also be used in ER-positive, HER2-positive disease, preferentially as maintenance therapy. For women harboring germline BRCA mutations, poly(ADP-ribose) polymerase (PARP) inhibitors are an additional therapy option.

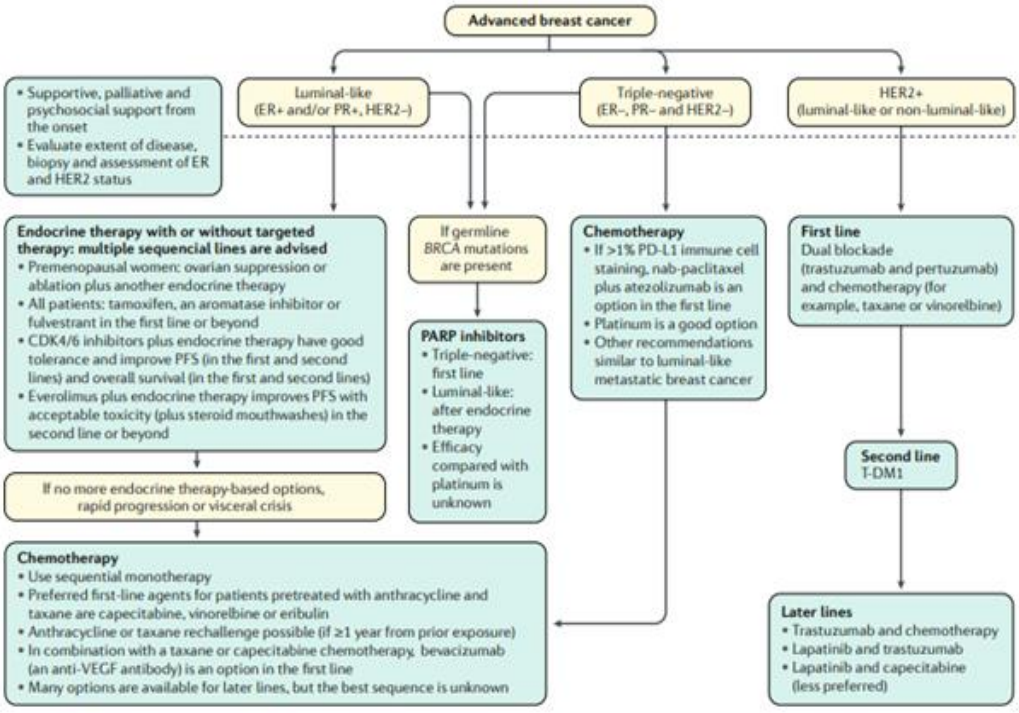

Fig. 3 Management of advanced breast cancer with distant metastases[7]

New promising drugs under evaluation, which would enhance the management of these diseases, raise increasing interests (Fig. 4). These drugs comprise novel oral small molecules (Neratinib, anti HER-receptor inhibitor, ONT-380, HER2-selective inhibitor); antibody-drug conjugates (T-DM1, the first antibody-drug conjugate (ADC) approved for metastatic HER2-positive breast cancer), inhibitors of downstream signaling pathways (mTOR/Phosphoinositide 3-Kinase/Akt Inhibitors, CDK4/6 Inhibitors, a key pathway downstream to HER2[28–31]. Moreover, the recent advances in tumor biology and immunology are owing valuable insight into breast cancer heterogeneity and the interplay of cancer cells with stromal and immune system in the natural history of breast cancer progression[32–34]. Although breast cancer is not considered a highly immunogenic disease, novel therapeutic strategies to boost the immune system and educate it to attack cancer cells are being successfully in clinical trials, especially among patients with triple negative breast cancer (TNBC)[35,36]. The most successful immunotherapeutic agents consist of immune checkpoint inhibitors (ICIs), which block immunosuppressive receptors, such as cytotoxic T lymphocyte antigen-4 (CTLA-4) and PD-1, to improve the cytotoxicity and proliferative capacity of tumor-infiltrating lymphocytes (TILs). ICIs, including monoclonal antibodies against PD-1 (i.e. pembrolizumab, nivolumab), PD-L1 (i.e. atezolizumab, durvalumab, avelumab), and CTLA-4 (i.e. ipilimumab). Interestingly, the clinical testing of ICI in breast cancer has been recently extended to HER2-positive breast cancer patients, in a phase IB/II trial (PANACEA; NCT02129556) that evaluate the efficacy of pembrolizumab and trastuzumab in trastuzumab-resistant metastatic breast cancer[37]. However, the response rate to these immunomodulatory agents varies significantly between patients[38,39]. For this reason, the identification of predictive markers, such as the tumor mutational burden score, is essential to select patients who can benefit from it[40]. Finally, vaccine-based therapy is now under investigation to stimulate the intrinsic anti-tumor immune response[41]. The long-term effect expected by these therapies is the strong immunity which establish an immunological memory, preventing tumor recurrence. For example, CAR-T therapy is an innovative form of immunotherapies wherein autologous T cells are genetically modified to express chimeric receptors encoding an antigen-specific single-chain variable fragment and various costimulatory molecules[42,43]. In breast cancer, HER2 is a receptor currently under investigation as tumor associated antigen for CAR-T cell therapy. However, concerns about serious adverse effects and high risk of autoimmunity hinder their clinical development, and investigation about them, still remains in early experimental stage.

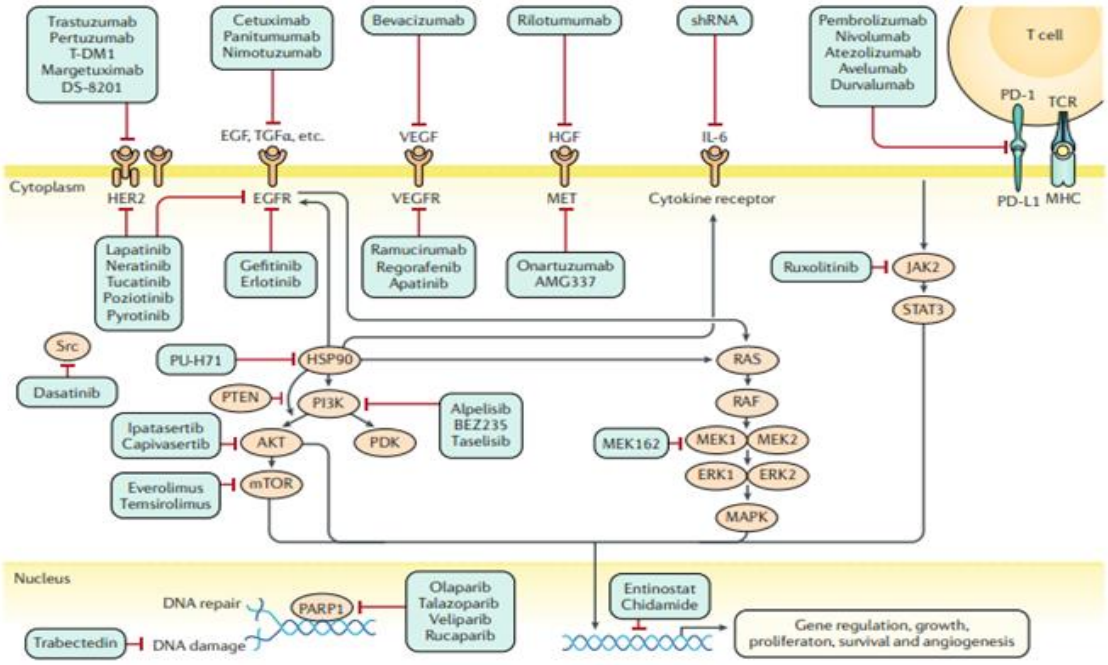

Fig. 4 Emerging targetable pathways in breast cancer[7]

1.1.3 Features of Breast Tumors that Form Bone Metastasis

Certain tumors show a unique predilection to form bone metastasis, despite the similar circulatory system and dissemination pathways. This suggest that, at primary tumor level, it is the combination of features of the cell of origin and the stromal influence that guide the metastasis to bone rather than other sites[44]. Indeed, stromal cells can support tumor cell plasticity, cancer stemness and the epithelial-to-mesenchymal transition, which promotes the extravasation and dissemination of tumor cells from the primary tumors[45]. Moreover, a recent study showed that cancer-associated fibroblasts (CAFs) might play a critical role in tumor progression. CAFs can secrete CXCL12 which prime tumor cells for metastasis to organs wherein host cells express CXCL12 at high levels, leading to the selection of tumor cells with high SRC activity[46]. Breast cancers metastasize to distant sites differently according to data from the US Surveillance, Epidemiology, and End Results Program (SEER) database[47,48] (Fig. 5). Bone is the most frequent site of breast cancer metastasis[49]. Indeed, about 65–75% of advanced breast cancer patients could develop bone metastasis[50]. Usually, metastasis to bone is associated with accelerated bone resorption leading to increased morbidity due to different skeletal-related events (SREs) including bone pain (BP), pathological fracture (PF), spinal cord compression (SCC) and tumor-induced hypercalcemia[50]. At molecular basis, different genes have been identified in primary breast cancer as associated with bone metastatic potential[51–53].

These genes can play a different role in the bone metastatic process. Moreover, even within breast cancer, different clinical subtypes show a different degree's propensity to develop bone metastasis, demonstrating that stromal influence and site of origin cannot fully explain and predict the mechanisms of metastasis. For example, brain metastases are more frequent in TNBC than luminal tumors. Instead, in a 15-year retrospective study comprising 1357 patients with breast cancer metastatic disease, bone metastasis is observed in 71% of patients with estrogen receptor-positive (ER+) tumors, meanwhile only in 47% of patients with estrogen receptor-negative (ER-) tumors[47]. Another important difference between subtypes and their propensity to bone metastasis, is their clinical behavior. Indeed, patients with ER− breast cancer tend to manifest overt metastasis within 5 years of diagnosis, meanwhile those with ER+ breast cancer can show bone metastasis 10 years after the primary tumor diagnosis[47]. This evidence suggests that mechanisms underlining the bone metastatic process are different even within one type of cancer. Identification of the mechanisms guiding the dormant phenotype in ER+ breast cancer is an unmet clinical need. Recently, it has been found that those molecular determinants could act as biomarker to predict breast cancer bone metastasis in ER+ breast cancer and that could play a role in regulating their dormant phenotype[52]. However, this still needs to be confirmed and the mechanisms still need to be clarified.

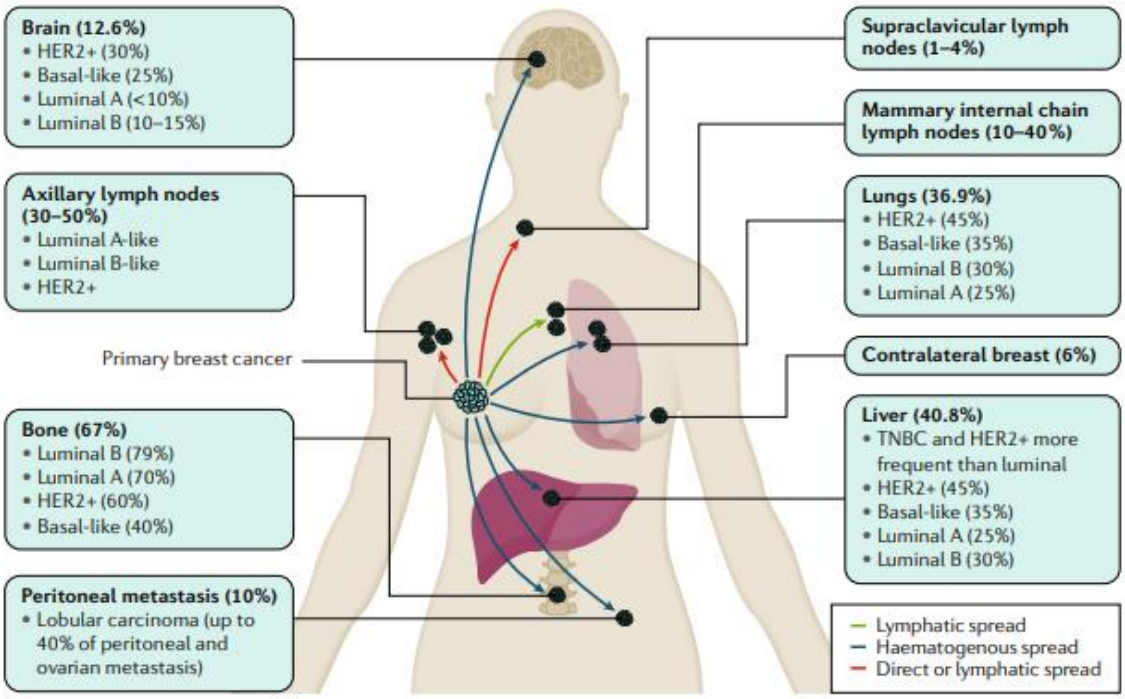

Fig. 5 Common metastatic sites in breast cancer[7]

1.2 Bone Tissue and Bone Metastasis

1.2.1 Bone Physiology

Bone tissue is a supporting connective tissue consisting of cells dispersed in an abundant extracellular matrix structure, fibers, and an amorphous substance of glycoprotein origin; this has the particularity of being calcified and formed by minerals[54,55]. Bone is a dynamic tissue which supports structural, protective, mechanical, and trophic functions since it acts as a deposit of mineral salts, in particular the calcium ion which plays an important role in various cellular activities. It is composed of various cell types: in addition to stromal, hematopoietic, and endothelial cells, osteoclasts and osteoblasts are involved in the development and regulation of bone remodeling[56,57]. Indeed, to accomplish all its functions, bone is an extremely dynamic tissue in a constant state of remodeling. The main cell actors in the regulation of bone homeostasis are osteoclasts and osteoblasts. Bone undergoes destruction, called resorption, carried out by osteoclasts cells, and formation, carried out by osteoblasts. In the adult skeleton this process is strictly balanced maintaining a constant, homeostatic controlled amount of bone[57]. Multiple factors are involved in the maintenance of bone homeostasis[58]. For example, growth factors trapped in the bone, such as insulin-like growth factors (IGFs) and Transforming Growth Factor-β (TGFB), are released during the bone resorption carried out by osteoclasts and they promote differentiation of osteoblasts leading to the production of new bone tissue[59]. In pathological conditions, the composition and the activity of osteoclasts and osteoblasts can be altered, leading to an imbalance in bone homeostasis. For example, excessive bone resorption due to a hyperactivity of osteoclasts not balanced by osteoblasts activity leads to reduced mass and undermined structure of bone, which is frequently called osteoporosis[60]. At the contrary, osteopetrosis is a genetic disease characterized by the lack of function of osteoclasts or by their absence, which leads to an excessive bone formation and high bone density[61,62].

Osteoclasts are giant, multinucleated cells that form from the fusion of their mononuclear progenitors from the granulocyte-macrophage lineage, in a process called osteoclastogenesis[63,56]. Their primary function consists in the degradation of the bone matrix during the remodeling process; this activity takes place in three phases: adhesion to the bone matrix to be reabsorbed, creation of an acidic environment that solubilizes the mineral matrix and enzymatic digestion of the organic matrix. Adhesion to the matrix occurs through integrins, receptors located in the cell membrane of the osteoclast, capable of recognizing peptide sequences in the matrix. Osteoclastogenesis is strictly regulated: hematopoietic stem cells give rise to precursors of osteoclasts. These cells require additional factors to be able to differentiate,

secreted from stromal cells of the marrow, osteoblasts, T lymphocytes. Two of these factors are necessary and sufficient to promote osteoclastogenesis: macrophage colony-stimulating factor (M-CSF) and receptor activator of nuclear factor kappa-B ligand (RANKL). While M-CSF is essential for the early stages of osteoclastogenesis, RANKL is critically involved in the maturation and activation of osteoclasts. M-CSF is produced by stromal cells and osteoblasts and binds to its receptor c-fms expressed on the surface of the macrophage precursors and stimulates proliferation[64,65]. RANKL has been first discovered as the osteoprotegerin ligand and it is expressed by osteoblasts, osteocytes and stromal cells[66]. It interacts with the receptor RANK localized on the membrane of the monocyte - macrophage precursors and induces differentiation into osteoclasts and their activation[67,68].

Osteoclastogenesis is indirectly stimulated by the increased RANKL expression from osteoblasts and bone marrow stromal cells, induced by different cytokines produced locally in bone as well as systemic calciotropic hormones, including parathyroid hormone (PTH), the 1,25 dihydroxyvitamin D3 and prostaglandins. In addition, other cytokines such as Interleukin-1 (IL-1) and Tumor Necrosis Factor-α (TNF-α) can act directly on osteoclasts[69,70]. Osteoblasts are cells of mesenchymal derivation responsible for the synthesis and mineralization of bone matrix. For osteoblast differentiation, mesenchymal stem cell (MSC) first undergoes proliferation, it becomes the commitment and therefore differentiate in pre-osteoblast (which produces alkaline phosphatase) and later in a mature osteoblast which produces an increasing amount of osteocalcin and calcified matrix. Runx2 and Osterix (Osx) are two transcription factors that determine the expression of many genes associated with osteoblast differentiation. The commitment of MSCs into the osteoblast line is controlled by three morphogenetic pathways: the Bone Morphogenetic Protein (BMP) pathway, Hedgehog signaling (HH) and the Wnt pathway[71–73]. Once formed the matrix, numerous osteoblasts become trapped in bone lacunae and thus they become osteocytes. Osteocytes are not inert cells for bone metabolism. Indeed, they could participate in the exchange of minerals from the bone, then intervening in the homeostatic regulation of the concentration of calcium in the body and, working as mechano-sensors, can modulate the bone resorption in response to different stimuli[74,75]. Bone matrix is constituted by the organic matrix reinforced by the deposition of calcium salts. The type I collagen constitutes about 90-95% of the organic matrix while non-collagenous proteins constitute the remaining 5-10%. The crystalline salts deposited in the matrix are primarily calcium and phosphate in the form of hydroxyapatite[76]. The proteins can be divided into non-collagenous proteins of cell adhesion, proteoglycans, γ-carboxylated and growth factors. Each of the adhesion proteins as osteopontin, integrin binding sialoprotein (IBSP), vitronectin and

type I collagen facilitate interactions with integrins that are expressed by hematopoietic stem cells and specialized cells of the bone, as well as osteotropic tumor cells. Because of bone remodeling, growth factors stored in the bone such as fibroblast growth factor (FGF), platelet-derived growth factor (PDGF), IGF, TGF-β and BMP, are released into the medullary cavity and act on metastatic cancer cell growth[55,77,78].

1.2.2 Pathophysiology of Bone Metastasis

The process of bone cancer metastasis consists of a long series of sequential, interrelated steps (Fig. 6). Each of these can be rate limiting, as a failure or an insufficiency at any of the steps can stop the entire process[44,79,80]. The outcome of the process is dependent on both the intrinsic properties of the tumor cells and the responses of the host[44].

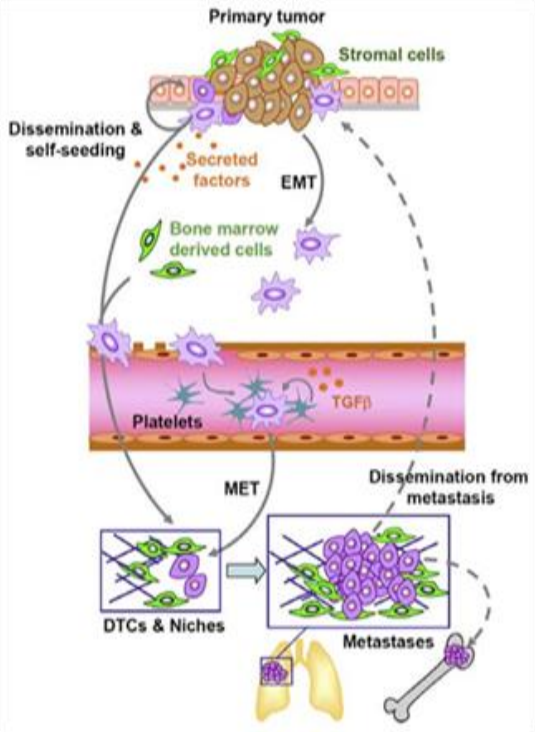

Fig. 6 Schematic Representation of the Steps in the Dissemination, Survival, and Expansion of Metastatic Tumor Cells[45]

Dissemination and Local Invasion: The EMT Process

The first step of the metastatic process is the successful escape from the primary tumor of single tumor cells. This phase requires the acquisition from the primary tumor of motility and invasiveness capability. Indeed, they must undergo a drastic transformation which is called epithelial to mesenchymal transition (EMT). This term defines a set of events through which epithelial cells lose many of their epithelial characteristics and acquire mesenchymal properties[81,82]. Polarized epithelial cells, which normally interact with the basement membrane,

undergo numerous biochemical changes, which allow them to assume a mesenchymal phenotype, characterized by a greater migratory capacity, invasiveness, high resistance to apoptosis and a significant increase in the components of the extracellular matrix[83,84]. EMT is a highly conserved process that governs the morphogenesis of multicellular organisms. This process normally occurs during the early stages of embryonic development where the mesenchymal cells do not derive only from the mesoderm but also from the epithelial cells of the endoderm that undergo EMT[85,86]. The importance of this process in embryogenesis is highlighted by the fact that the failure or malfunction of the EMT determines the developmental block at the blastula stage[86]. Epithelial cells have well defined phenotypic and morpho-functional characteristics[87] (Fig. 7). Mesenchymal cells, on the other hand, form unorganized structures of different shape and density and between them there are only focal adhesion points and no stable junctions as between epithelial cells. Mesenchymal cells are also endowed with a high mobility that allows them to migrate either as single cells or as chains of cells. When the EMT process is completed, the epithelial cell has regained the mesenchymal phenotype by losing some epithelial markers, which are replaced by mesenchymal markers.

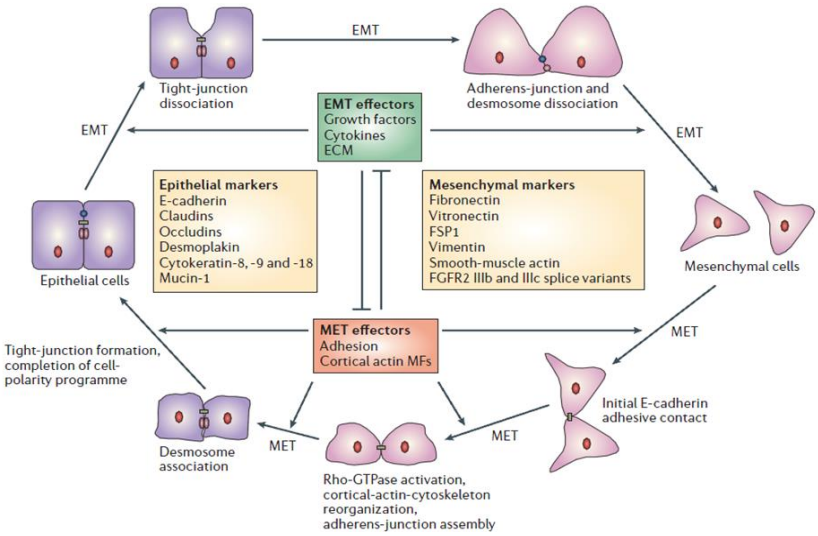

Fig. 7 Cancer Cell Plasticity (EMT-MET)[88]

The consequent acquisition of an invasive mesenchymal phenotype by cancer cells leads to the rupture of the basal lamina and invasion of the underlying stromal compartments. The acquisition of the invasive mesenchymal phenotype by epithelial tumor cells does not occur only because of somatic mutations and epigenetic alterations in the tumor cells themselves, but changes in the stroma surrounding the tumor are also required to guide neoplastic progression[89,90]. Indeed, EMT is also activated by some extracellular signals deriving from the

interaction of cancer cells with components of the extracellular matrix such as collagen and hyaluronic acid. For examples, it has been demonstrated that ovarian and prostate cancer cells can be affected by the contact with type I collagen, which induce an up-regulation of EMT-TFs markers (Snail and Slug) leading to a shift towards a mesenchymal phenotype[91]. EMT plasticity can be affected also by mechanobiology stimuli from the extracellular matrix, such as the matrix stiffness[92–94]. Indeed, it has been shown that breast cancer cells can activate EMT programs with the nuclear translocation of Twist1 (EMT transcription factor) in response to the increased stiffness of collagen fibrils[95]. EMT programs activation, induces changes at the intracellular level of various effector proteins such as the GTPases Ras, Rho, Rac and the MAPK and Src kinases which cause a change in the organization of the cytoskeleton and the disassembly of the different junctional complexes. Two of the main targets of Ras and MAPKs are Slug and Snail, transcription factors that inhibit the expression of genes that have an E-box in the promoter region such as E-cadherin and the proteins that make up the occluding junctions (occludin and claudine)[96]. However, the precise requirements for EMT in metastasis have not been fully delineated, with different tumor types relying on discrete EMT effectors. Most tumor cells do not undergo a full EMT, but rather adopt some qualities of mesenchymal cells and maintain some epithelial characteristics. Emerging evidence suggests that partial EMT can drive distinct migratory properties and enhance the epithelial-mesenchymal plasticity of cancer cells as well as cell fate plasticity[97] (Fig. 8).

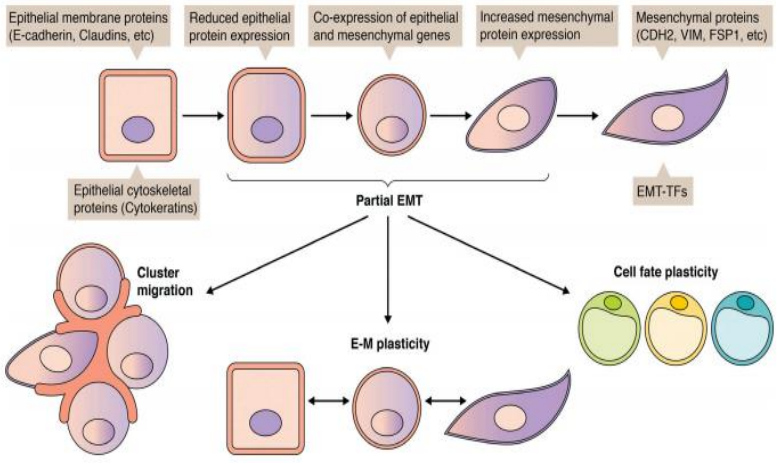

Fig. 8 Partial EMT: Heterogeneity and functional consequences[97].

Blood and Lymphatic Dissemination

The arrival of cells at the level of a secondary organ is therefore not a random process. The first contact between the "seed" and the "soil" consists in the interaction between the tumor cells that circulate in the blood and in the lymphatic vessels and the endothelium of a specific tissue

of the organ they colonize. Regarding bone metastases, cancer cells must reach, colonize, and grow in the bone marrow. This phenomenon also depends on the presence of receptors for cytokines and growth factors, located on the surface of tumor cells[98]. It has been observed that breast cancer cells can express the RANK receptor which plays a role in tumor etiopathology. Tumor cells expressing the receptor are chemo-attracted by the RANKL factor expressed by the cells of the bone tissue[99]. Another data that supports the role of the RANK-RANKL pathway in tumor cells is the finding that a higher expression of RANK confers to the MDA-MB-231 cells increased metastatic growth in bone compared to MDA-MB-231 cells that do not express high levels of the receptor[100]. Osteomimicry describes the phenomenon whereby osteotropic metastatic cancer cells, once they reach the bone microenvironment, can express proteins and receptors usually expressed by the cells and the bone matrix[101]. Among the most important factors, the CXCR4 and CCR-7 receptors were found mainly expressed by breast and prostate carcinoma cells[102,103], which interact with the chemokines like monocyte chemoattractant protein 1 (MCP-1) and the stromal cell-derived factor 1 (SDF-1), chemoattractive cytokines and chemokines constitutively expressed by endothelial cells, osteoblasts and other stromal cells of the bone marrow. The SDF-1 / CXCR4 axis, used physiologically by HSC (Hematopoietic Stem Cells) to be recalled to the bone marrow, plays a fundamental role in the development of metastasis; in normal breast tissue low levels of CXCR4 are expressed while in breast cancer high levels of this receptor are present[102]. SDF-1 in the bone marrow is produced abundantly by osteoblasts especially during the bone remodeling process and its production is increased by factors such as PTH, PDGF, IL-1, VEGF and TNF-α (TNF-alpha)[104]. SDF-1 also recruits the precursors of osteoclasts by inducing chemotaxis, the activity of MMP-9 and the transmigration of collagen. Activation of the SDF-1 / CXCR4 pathway not only regulates the homing and migration of cancer cells into the bone, but also the adhesion, invasion, and rearrangement of the cytoskeleton of cancer cells[105,106].

Bone Colonization: the MET Process

A critical step in successful bone colonization is the engagement of specific stromal components in distant organ for the survival and outgrowth of tumor cells. Osteopontin, bone sialoprotein and type I collagen are the predominant components of mineralized bone; these proteins mediate local adhesion, motility, survival, and growth by interacting with integrins, adhesion molecules expressed by different types of cells[107,108]. Integrin αvβ3 is the receptor for vitronectin (another molecule of the extracellular matrix) and it is an essential component for the adhesion of osteoclasts to bone[109]. This integrin is expressed at high levels on the surface

of breast cancer cells and appears to cooperate with bone sialoprotein and MMP-2 and -9 in the invasion of cancer cells into bone[110,111]. Moreover, ITGA5 has been recently found as a promoter of bone metastatic dissemination in breast cells[53]. The engagement of disseminated cancer cells in the bone leads to the activation of cell plasticity programs crucial for their survival and outgrowth[112]. Indeed, meanwhile EMT programs seem to be necessary for the escape of tumor cells from the primary tumor, these cells must revert to an epithelial state for the successfully metastatic outgrowth, when they colonize the host organ[113,114]. The stimuli that drive activation of MET (Mesenchymal to Epithelial Transition) programs are not fully elucidated. In breast cancer, different mechanisms have been proposed, for example the mir-200 which target the transcription factors of EMT[115,116]. In the context of bone metastasis, an interesting explanation of the paradoxical requirement for simultaneous induction of both MET and cancer stem cell traits in DTCs has been proposed[117]. Indeed, the engagement by metastatic breast cancer cells of E-selectin, expressed in the vascular bone niche, guide the promotion of MET programs in breast cancer cells, which shift to an epithelial state and simultaneously activate the Wnt signaling, a classical pathway linked to self-renewal and stemness, which induce the expression of Sox2/Sox9. This non-canonical MET resolves the paradoxical requirement of stemness and epithelial state during the metastatic colonization, paving the way to new therapeutic strategies that target the bone microenvironment to prevent the breast cancer cell colonization[118].

1.2.3 Metastasis Classification

Bone metastases can be classified into three different types[119] (Fig. 9):

- Osteolytic metastases,
- Osteoblastic metastases,
- Mixed metastases.

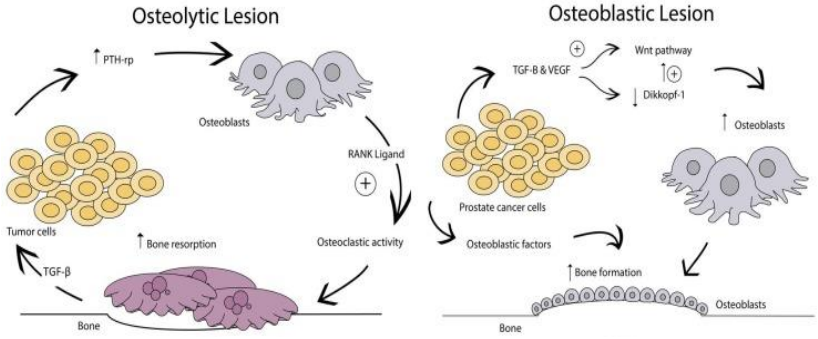

Fig. 9 Types of Bone Metastasis[120].

Osteolytic Bone Metastasis

Osteolytic metastasis occurs mainly in subjects with solid tumors such as those of the breast, prostate, lungs, kidney, and thyroid; although breast cancer remains the neoplasm most involved in the onset of this type of metastasis[119,121].

The dominant lesion is lytic and destructive although there is also a local bone formation which probably represents an attempt to repair the bone itself. This increase in bone formation in patients with osteolytic metastases is reflected by an increase in serum levels of the enzyme alkaline phosphatase (enzyme located at the osteoblast surface, involved in bone mineralization), used as a serum marker for the determination of activity of osteoblasts[122]. Specific and sensitive markers have been identified to assess the response in the bone: turnover and formation. These include bone-specific alkaline phosphatase and type I collagen pro-peptides, used to evaluate bone formation. Many *in vivo* studies have shown that osteolysis is associated with an increase in the activity of osteoclasts and a reduction in the activity of osteoblasts and not by the direct effect of neoplastic cells on bone tissue[123].

Osteolytic metastasis arises following a complex interaction between tumor cells and the bone microenvironment which gives rise to a "vicious cycle" which is self-sustaining (Fig. 10)[112]. Bone homeostasis is regulated by the direct interaction between osteoblasts and osteoclasts; in particular, the RANK / RANKL / OPG axis plays an important role. RANKL, expressed on the surface of osteoblasts and medullary stroma cells, induces the recruitment, activation, and differentiation of osteoclasts by binding to its RANK receptor located on the surface of osteoclast precursors[68].

The process is controlled by the production, by osteoblasts and other types of cells of the bone microenvironment, of OPG (osteoproteogerin or osteoclastogenesis inhibition factor)[124]. OPG is a "receptor-bait" capable of binding RANKL limiting its biological activity and thus inhibiting development, mainly by blocking the stages of fusion and differentiation of osteoclasts, and their bone resorption activity[125]. Once activated, osteoclasts begin the bone resorption process by secreting proteases and forming an acidic environment between the plasma membrane and the bone surface. Cancer cells that reach the bone microenvironment secrete factors that influence the bone resorption process.

The PTHrP (parathyroid hormone-related protein) peptide is the most important mediator in the activation of osteoclasts in metastatic breast cancer[126]. It has a 70% homology with the first 13 amino acids of the parathyroid hormone (PTH), it binds to the same receptor as PTH showing a biological activity like PTH itself. 50-60% of primary breast cancers produce PTHrP but its expression is higher in the bone microenvironment (90% of bone metastases from breast cancer

express PTHrP) compared to the primary tumor site and other metastatic sites (only 17% of metastases in anatomical sites other than bone express PTHrP)[127].

PTHrP stimulates the production of RANKL by osteoblasts and inhibits the production of OPG, increasing osteoclastogenesis. The signal activated in the precursors of osteoclasts following the binding of RANKL to RANK leads to the increase in the expression of some transcription factors such as AP1 (activated by the N-terminal kinase JUN) and NF-κB (activated by the inhibitor of the κB kinase IKK) leading to the maturation of the progenitors of osteoclasts[128]. The newly formed osteoclasts then begin the process of bone resorption. Osteoclast-induced osteolysis is related to the release from the bone matrix of growth factors such as TGF-β and IGF1 and to an increase in the extracellular concentration of calcium. These growth factors, in particular TGF-β, bind to their own receptors on the surface of tumor cells and induce signal transduction mechanisms mediated by SMAD and MAPK proteins[129,130]. This leads to an increase in the proliferation of tumor cells and an increase in the production of PTHrP which in turn increases the production of RANKL by the osteoblasts, closing this vicious cycle which in this way feeds itself.

In addition to PTHrP, the expression of RANKL by osteoblasts and stromal cells is increased by other factors produced by tumor cells such as IL-1, IL-6, IL-8, IL-11 and Prostaglandin E2 (PGE2)[131]. Some of these factors not only stimulate osteoclasts via RANKL, but also independently of it. In fact, IL-8 binds directly to the CXCR1 receptor located on the surface of the precursors of osteoclasts[132], promoting their differentiation.

Also, COX-2, overexpressed in bone metastases deriving from breast cancer, can activate osteoclasts directly by inducing PGE2[133], or indirectly through the up-regulation of RANKL in osteoblasts and/or bone marrow stromal cells[134]. Secreted factors produced by cancer cells recruit and activate T cells, which in turn support osteoclastogenesis by producing TNF-α and TRAIL (which inhibits the anti-osteoclastogenic effect of OPG)[135,136]. It has recently been found that high expression of Jagged-1 in breast cancer cells promotes bone metastasis by activating the Notch pathway in supporting bone cells[137]. Jagged-1 is overexpressed in metastatic tumor cells and is further activated by the cytokine TGF-β released from the bone matrix during the osteolysis. Cancer cells expressing Jagged-1 have a growth advantage in the bone microenvironment by promoting the expression and release of IL-6 by osteoblasts and increasing osteolysis, stimulating the maturation of osteoclasts[137]. Jagged-1 is not expressed only by tumor cells, but also by bone cells which regulate the niche of hematopoietic stem cells through Notch[138]. Besides TGF- β pathway, the activation of another developmental pathway, the Wnt signaling, is crucial in bone metastasis formation[139]. However, the two pathways

usually play opposing role, raising paradoxical concern in bone metastasis development[140]. Indeed, TGF- β sustains osteolytic outgrowth through induction of JAG1 and DKK1 (Dickkopf-Related Protein 1), a Wnt inhibitor, by contrast the Wnt signaling is essential for the initial metastatic dissemination and it is activated by the engagement of E-selectin by disseminated tumor cells in sinusoid vasculature in the bone. This implies a complex crosstalk and context-dependent regulation between TGF-β and Wnt signaling in different stages of bone metastasis that enables efficient colonization, dormancy, and outgrowth. Recently, a key connection node between the two pathways and a novel mechanism has been proposed to explain this paradoxical concern[141]. It has been shown that TGF-β spatially inhibits WNT in bone metastatic cells by promoting the expression of DACT1 which through liquid–liquid phase separation is necessary for compartmentalizing Casein Kinase 2 (CK2), a potent inductor of Wnt signaling. By sequestering CK2 into biomolecular condensates, DACT1 can constrain WNT/TCF activation in the dormancy stage. Then, metastatic outgrowth stimulates osteoclastogenesis which further increase TGF- β concentration, leading to DACT1 induction and Wnt signaling suppression which is important for the development of the osteolytic metastasis[141].

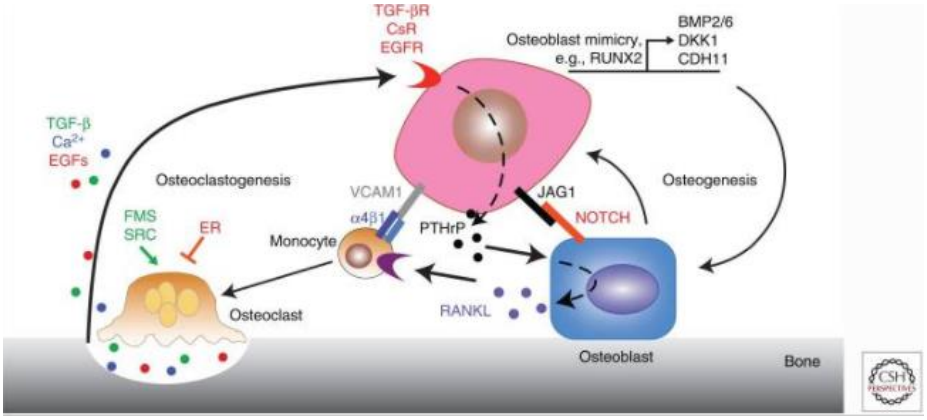

Fig. 10 The "vicious cycle" of osteolytic and osteogenic bone metastases[112]

Osteoblastic Bone Metastasis

Although osteoblastic metastases mainly arise in bone secondary to prostate cancer, 15-20% of subjects with breast cancer develop this type of metastasis[142]. It should be noted that in breast cancer metastases, however, there is a prevalence of mixed metastases characterized by a lytic component and a thickening component.

In osteoblastic or osteo-thickening metastasis there is a prevalence in the process of bone formation compared to resorption, even if the osteoid that is deposited and subsequently

mineralized is of poor quality and this leads to the onset of fractures which are a common event[123]. The formation of osteo-thickening metastases depends on an overstimulation of the osteoblasts or an inhibition of the osteoclasts (or both) by the tumor cells.

The mechanisms underlying the formation of osteoblastic metastasis are not yet well defined but it is thought that the massive production of bone matrix in the region surrounding the tumor cell deposit is due to the abundant production and secretion of growth factors that induce recruitment, proliferation, and differentiation of osteoblast progenitors by metastatic tumor cells[143]. Among the factors most involved in the development of osteo-thickening metastasis are the BMPs, bone morphogenetic proteins (BMP2, BMP3, BMP4, BMP6 and BMP7), members of the TGF-β superfamily, mainly produced by tumor cells[144]. These bone morphogenic proteins stimulate the differentiation of osteoblasts by activating transcription factors such as Runx-2 and indirectly induce angiogenesis. The expression pattern of BMPs plays an important role in the etiology of osteoblastic metastases resulting mainly from prostate cancer. Primary tumor and metastasis have been found to have different BMP expression patterns; BMP6 is expressed at high levels both in the primary tumor and in metastasis, while BMP7 is expressed at high levels only in bone metastasis. Another important factor is endothelin-1 (ET-1), a vasoactive peptide of 21 amino acids produced by cancer cells[145]. The pathophysiological role of ET-1 in the development of metastasis has been demonstrated in preclinical models for both breast and prostate cancer[146,147]. ET-1 binds to its receptor, Endothelin A (ETA) expressed by both tumor cells and bone cells (osteoblasts and osteoclasts) suggesting both paracrine and autocrine activity. ET-1 increases the activity of cancer cells and improves the mitogenic effect of other growth factors such as IGF-1, PDGF and EGF; it also leads to the formation of bone tissue by stimulating osteoblasts and inhibiting osteoclast-mediated resorption[148]. Some proteases, such as the serine protease urockinase (uPA) and the prostate-specific antigen (PSA), appear to be involved in the formation of osteoblastic metastases. uPA, produced by cancer cells, is synthesized as a precursor (pro-uPA) but subsequently undergoes a proteolytic cut which leads to its activation. The carboxy-terminal proteolytic domain of uPA contains 2 domains: a growth factor domain (GDF), so called because it is structurally like EGF, and a Kringle domain. This domain is essential for the activation and proliferation of osteoblasts. Furthermore, uPA cuts and activates TGF-β, which regulates the differentiation of osteoclasts and osteoblasts and promotes the growth of the tumor cells themselves[149], and hydrolyzes the proteins that bind IGF, increasing the concentration of free IGF[150].

1.3 Role of bone microenvironment in tumor progression

1.3.1 Bone as Pre-Metastatic Niche

Bone is the main site that houses hematopoiesis and osteogenesis in healthy individuals. For this reason, inside the bone there is a unique environment composed of various stem cells, progenitor cells, mature immune cells strictly regulated by a dynamic balance. This concept describes the existence of two primary niches in the bone marrow (BM): the osteoblastic and the perivascular niche[151] (Fig. 11). These contrasting niches house two types of adult stem cells and their progeny: mesenchymal stem cells (MSCs) and hematopoietic stem cells (HSCs), respectively[152–154]. MSCs cells differentiate into the mesenchymal lineage cells which include osteoblasts, adipocytes, chondrocytes, fibroblasts, and other stromal cells. Instead, HSCs differentiate to form the entire immune systems. These two cell lineages interact with each other in the bone niche to sustain normal bone homeostasis, which is impaired during pathological conditions. Moreover, these bone niches can be hijacked to support the growth of both primary and metastatic cancers[155].

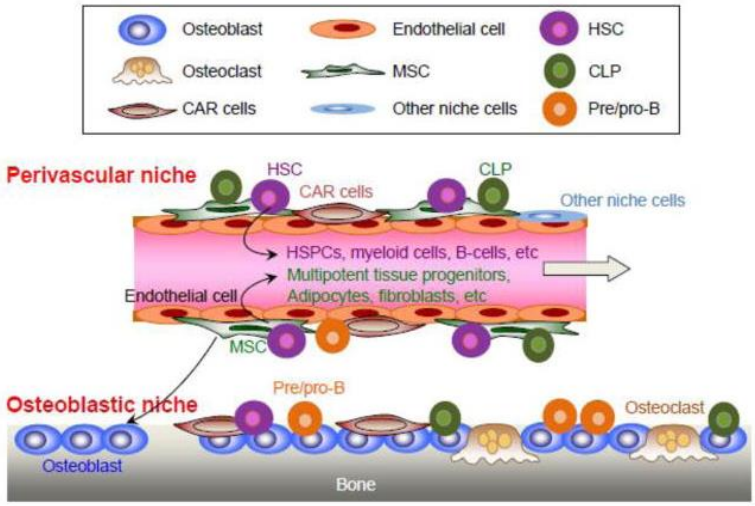

Fig. 11 The normal bone niche and homeostasis[151]

A pre-metastatic niche in the bone can also be induced by tumor cells[156]. Indeed, recent studies show that microenvironments distant from the primary tumor site are prepared for the arrival of metastatic cells from tumor cells themselves, to create a suitable and favorable site for future metastatic growth. This implies that metastasis to a distant site is not a random event, as already anticipated by Paget's theory more than a hundred years ago, but rather a predetermined event, in which cancer cells colonize an already defined site[157]. The modified microenvironment that will become the site of metastases is called the pre-metastatic niche. In the process of formation

of the pre-metastatic niche, bone has the dual role of a possible metastatic site, but also of "director" (or helper) of the primary tumor. In fact, it has been seen that the factors secreted by primary tumor cells induce the mobilization of bone marrow cells towards the organs of metastasis, in which they induce molecular changes in the stromal cells that favor colonization by cancer cells[44,158]. Regarding the formation of the premetastatic bone niche, the secretion of enzymes, growth factors and cytokines by the tumor alters the bone microenvironment at a distance to promote metastasis. Primary tumor-derived exosomes may increase hepatocyte growth factor-activated MET (receptor tyrosine kinase) signaling in bone marrow cells while other factors, yet unknown, inhibit osteoblast differentiation by increasing plasma levels of DKK1. Proteases such as HPSE (Heparanase) alter the bone stroma by degrading proteins of the extracellular matrix[159]. Recently, Erler and colleagues found that lysyl oxidase (LOX) plays an important role in the formation of the pre-metastatic niche[160]. Once secreted from the hypoxic microenvironment of the primary tumor, LOX co-localizes with fibronectin at the sites of metastasis, contributing to the generation of a suitable extracellular matrix to facilitate the recruitment of bone marrow endothelial cells and other mesenchymal cells, important for the subsequent development of metastasis.

In the bone metastasis development, primary tumor cells could condition the bone marrow to produce factors targeting the cells of the microenvironment to favor the migration and colonization of tumor cells.

In conclusion, during tumor progression, cells co-evolve with the surrounding microenvironment, promoting the development of metastasis.

1.3.2 Bone as Metastatic Niche

The bone microenvironment comprises a mineralized extracellular matrix and specific cells that are under the control of systemic and local factors. Its composition makes the bone tissue a suitable site for its colonization by aggressive solid tumors capable of metastasizing. Cancer cells modify the bone microenvironment during invasion and expansion through the recruitment and modulation of osteoclasts, osteoblasts, immune system cells, vascular elements, and bone matrix. Cancer cells that metastasize to bone can use the same physiological mechanisms used by hematopoietic stem cells for homing to bone[155]. Osteoblasts and bone marrow stromal cells regulate and attract hematopoietic stem cells by creating a niche through protein interactions including the CXCL12-CXCR4 axis. CXCL12 is expressed at high levels by osteoblasts and stromal cells, and the expression of CXCR4 by cancer cells is crucial for homing to bone. CXCR4 was found to be highly overexpressed in a subpopulation of a selected and highly

metastatic human breast cancer line[51]. The bone marrow can also serve as a support site for dormant cancer cells, neoplastic cells that can reside in the bone for a long time before generating a new tumor and that often acquire resistance to chemotherapy attacks[155] (Fig. 12).

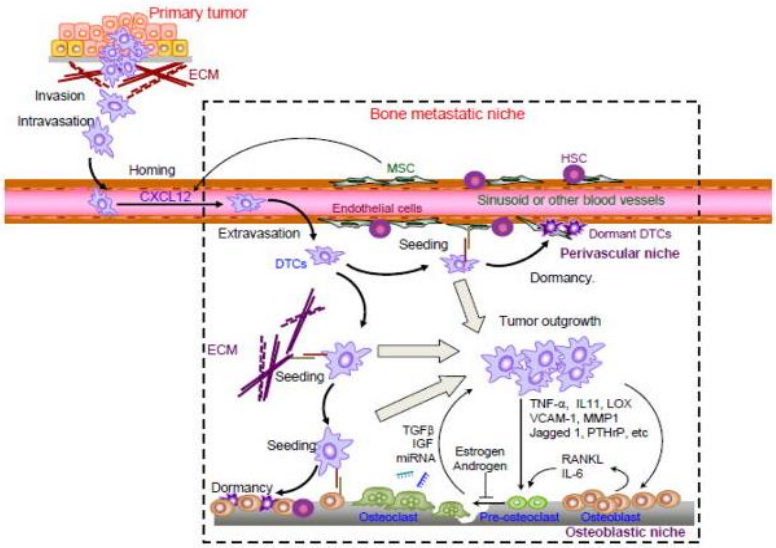

Fig. 12 Bone metastatic niche in distinct steps of bone metastasis[151]

1.3.3 Role of ECM and Microenvironment in Bone Metastasis

Bone microenvironment is a highly heterogenous and dynamic niche that hosts different bone cells (osteoblasts, osteoclasts, osteocytes, and their precursor), stromal cells, hematopoietic and immune cells, adipocytes, endothelial and fibroblasts cells, which orchestrate the bone remodeling process and immune function during the development (Fig. 13). All these cells are surrounded in an extracellular matrix (ECM) which is composed of organic and inorganic components[161]. The main organic component is represented by type I collagen fibrils, which gave the strength and stiffness to the bone matrix and the structural support for cell attachment. Collagen fibers are strictly organized in a hierarchical and directional manner corresponding to cellular orientation. It has been shown that, in pathological conditions, this organization can be altered, and the stiffness provided by the collagen fibrils is modulated, affecting cell behavior, proliferation, survival, and differentiation[162]. Besides collagen, which provides the structural support, there are other organic proteins that form the bone matrix[107]. The most characterized in the bone are Bone Sialoprotein (BSP), osteopontin (OPN), fibronectin (FN1), proteoglycans, and matrix metalloproteinases (MMPs). These proteins play a crucial role in modulating the bone microenvironment in physiological and pathological conditions[161]. The inorganic components of the bone matrix are instead represented by different minerals including calcium,

phosphate, that are released during the bone remodeling. The most represented inorganic component of the bone matrix are the hydroxyapatite crystals which regulate the bone matrix mineralization[76,163]. It has been shown that the structure and orientation of the hydroxyapatite crystals, in conjunction with the collagen fibrils, are critical for bone matrix organization[108,164]. In pathological conditions, the alignment of apatite crystals and collagen can be altered, affecting cell behavior and differentiation. For this reason, emerging evidence highlights the ECM key role in bone metastasis progression. Indeed, its biochemical and mechanical properties can affect the plasticity of disseminated cancer cells, which adapt to the hostile microenvironment fostering their growth and survival. The identification of the mechanisms by which cancer cells induce tumor-promoting ECM could provide new avenue in the therapeutic strategies to inhibit the formation of bone metastasis[165]. Thus, prevention of cancer cells dissemination in the bone could be pursued in the adjuvant setting by the identification of therapeutic strategies that act on the bone microenvironment, making it a hostile niche for cancer cells colonization and survival at an early stage.

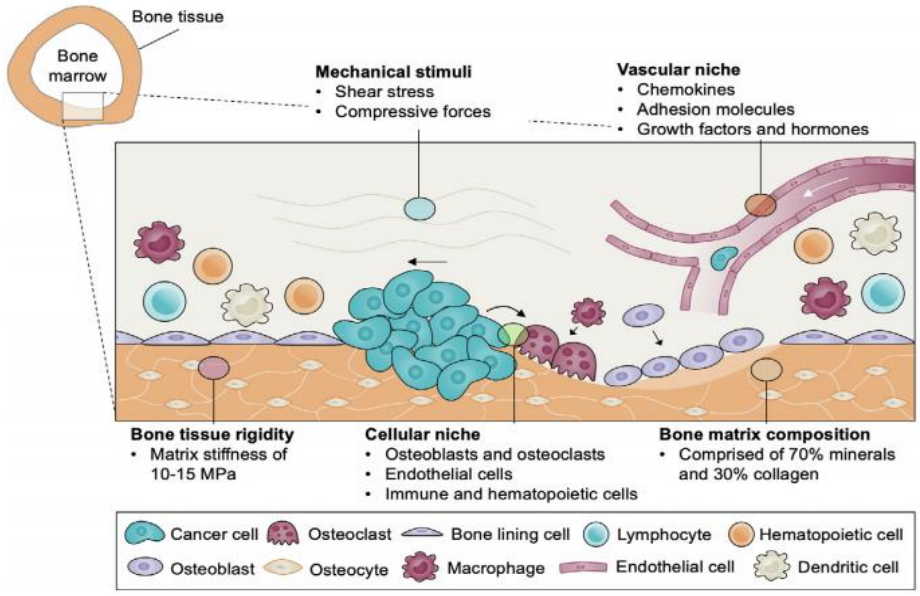

Fig. 13. Bone Tissue and Microenvironment[166]

1.3.4 Therapies to target bone microenvironment in breast cancer bone metastasis

A more understanding of the osteogenic and oncogenic pathway involved in the establishment of bone metastasis allowed the development of new therapeutic strategies based on the biology of the bone microenvironment[167] (Fig. 14). These advances, allowed by single cell gene expression analyses and high-resolution imaging, which shed the light to novel pleiotropic roles of bone cells. Moreover, recent technologies made possible a more understanding of circulating tumor cells (CTCs) and disseminated tumor cells (DTCs) from the primary tumors, reveling new potential predictors of bone metastasis[168]. These include PDL-1 expression[169] and alteration of the RANKL-OPG ratio[170]. These discoveries provided the rationale for incorporating antibody-based therapies targeting PD-1 (pembrolizumab and nivolumab) and CTLA4 (ipilimumab) into the therapeutic strategies against bone metastasis, which include bone targeting agents and radium-223 dichloride[167].

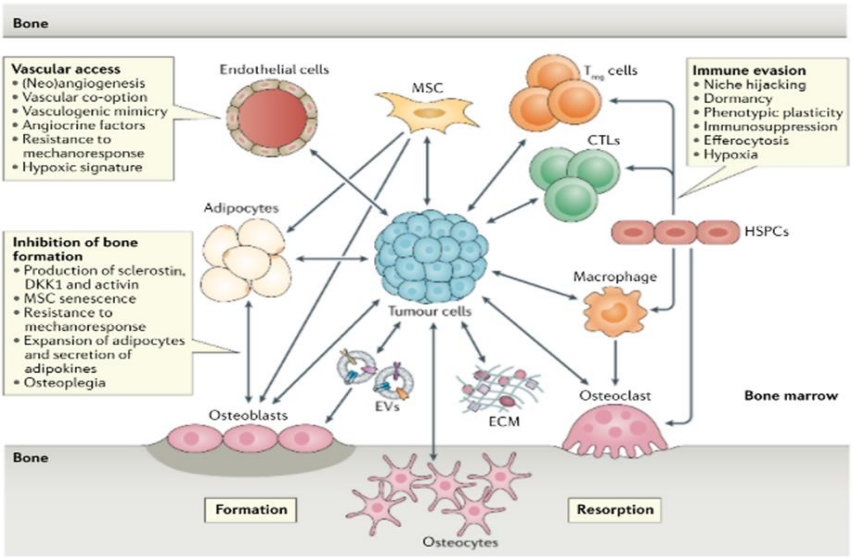

Fig. 14 Interactions of tumor cells with the bone microenvironment.[167]

1.3.5 Bone Targeted Therapies

Bone lesions compromise patients' quality of life by causing pathological fractures, nerve compression syndromes, hypercalcemia, and reduced mobility: events named SRE (Skeletal related event)[171]. It is therefore important to better understand the molecular mechanisms associated with the metastasis process in the bone to improve existing therapies and develop therapies on new targets. The treatments currently used, in addition to anti-tumor and anti-hormonal therapy, consist of the use of 2 drugs: Zoledronic Acid (Zometa®, Novartis) and Denosumab (Prolia®, Amgen).

Zoledronic Acid

Zoledronic Acid is a third-generation nitrogen bisphosphonate (NBP) characterized by the presence of an imidazole ring containing 2 nitrogen atoms[172]. Nitrogen bisphosphonates inhibit the mevalonate pathway and in particular farnesyl diphosphate (FPP) synthase[173]. The inhibition of FPP synthase determines the production and accumulation of triphosphoric acid 1-adenosine-5-yl ester and 3- (3-methylbut-3-enyl) ester (ApppI). This intracellular analogue of ATP can induce apoptosis of osteoclasts *in vitro*, inhibiting mitochondrial translocase ADP/ATP[174].

Proteins covalently modified by isoprenylation are involved in numerous cellular functions of osteoclasts, such as the control of endosomal trafficking, integrin signaling, membrane wrinkling, control of cell morphology and apoptosis. Zoledronic Acid reduces the risk of skeletal complications by 30-50% and not only for breast cancer but for a wide range of solid tumors[175].

Indeed, it can reduce the production of numerous growth factors and cytokines at the level of the bone microenvironment (IGF-1 and IGF-2, FGFs), making it less attractive as a site for migration, colonization, adhesion and invasion, proliferation, and survival for cancer cells[176,177]. Zoledronic Acid can have both direct and indirect effects on tumor cells, comprising immunomodulatory response and ECM modulation. Indeed, it has been shown that alteration of the bone ECM by Zoledronic Acid can impair the adhesive capacity of tumor cells[178].

Regarding the anti-tumor direct effect, Zoledronic Acid can induce cancer cells apoptosis by preventing the translocation of Ras on the cell membrane. However, it can have also indirect effect, modulating the immune system. Indeed, it promotes reprogramming of M2- like TAMs (tumor associated macrophages), which support tumor proliferation, angiogenesis, and metastasis[179] and it leads to the immune system's activation by the recruitment of the Λδ T cell population, an anti- tumor subset of T cells. The recruitment occurs through the recognition by these cells of the nitrogenous bisphosphonate which is exposed on the surface of the tumor cells[180]. The Λδ T cells therefore inhibit tumor induced osteolysis by inducing the lysis of neoplastic cells. Zoledronic Acid shows anti-tumor activity even outside the bone microenvironment, especially when administered in combination with other anticancer drugs such as taxanes, doxorubicin and platinum-derived compounds, showing either synergies or additivity in anti-neoplastic activity[181]. In some studies, it has been shown that the administration first of the classic anticancer and then of the Zoledronic Acid sensitizes the neoplastic cells to the action of Zoledronic Acid, thus inhibiting the spread of the tumor in the body[182].

Denosumab

Denosumab is a monoclonal antibody directed against RANKL which mimics the endogenous effect of OPG[183]. It binds to RANKL with high affinity, preventing its binding with its RANK receptor and this leads to the inhibition of the processes of recruitment, differentiation, and activation of osteoclasts with a consequent reduction in bone resorption[184]. In the United States, Denosumab was initially approved only for the treatment of patients with postmenopausal osteoporosis, while its use has recently been authorized for the prevention of SREs in patients with bone metastases from solid tumors[185]. Phase III clinical trials comparing treatment with Zoledronic Acid and Denosumab were conducted in patients with bone metastases from breast and prostate cancer[186,187]. The efficacy of treatment with Denosumab appears to be superior to that with Zoledronic Acid in terms of the risk of developing SRE. The time interval observed for the appearance of the first and subsequent SREs is longer after treatment with Denosumab compared to treatment with Zoledronic Acid. Furthermore, there is also a significantly higher reduction in bone turnover markers (uNTX / Cr) in treatment with Denosumab (uNTX / Cr -80% with Denosumab versus -68% with Zoledronic Acid)[184].

1.3.6 Bone Metastasis Experimental Modeling

Given the co-protagonist role played by the microenvironment in the formation of bone metastasis, it becomes essential to develop new models for the study of the interactions between stroma and tumor cells to identify new therapeutic targets. Bone metastasis is a complicated process to reproduce and monitor both *in vitro* and *in vivo* because, in addition to the poor accessibility of the tissue, it involves many different types of cells that take part in the process at different stages of its development[188]. Although animal models are certainly useful for evaluating tumor expansion in bone, using aggressive metastatic cell lines, they suffer from significant criticalities, including the fact that although the excised tissue represents well the final phase of bone metastasis, it remains impossible to analyze the initial phase of the process. Animal models need to be improved to study the metastatic progression of cancer cells in the bone. Regarding *in vitro* models that reproduce the bone environment, both two-dimensional and three-dimensional culture models have been developed[189].

2D models

Among the two-dimensional models, interactions between the microenvironment and cancer cells can be reproduced by indirect co-culture, which consists in using the culture medium of the cancer cells to condition the growth of cells in the microenvironment[190]. A two-dimensional

model has been developed in which a medium conditioned at 10% by MDA-MB-231 breast carcinoma cells is able to induce the differentiation in osteoclasts of human monocytes isolated from peripheral blood. This system allowed to evaluate the mechanism of action of bone and anti-tumor drugs, studying possible therapeutic combinations to block the vicious cycle of bone metastases. Other two-dimensional models set up indirect co-culture through transwell supports, that allow the growth of different cells on different planes but with the sharing of the same culture medium[191,192]. It has been demonstrated their validity to study therapeutic strategies to block the vicious cycle of bone metastasis from different primary tumors[193]. The main problems are due to the lack of structural architecture and the difficult exchange of nutrients. To overcome these main limitations, attempts are being made to recreate a model that mimics the pathophysiology of bone metastasis, and which maintains the characteristic three-dimensional architecture of the tissue.

3D models

The study of the interactions of metastatic cells with the tissue microenvironment requires a system capable of reproducing not only the complexity of the bone tissue but also the interactions between tumor cells and cells of the tissue itself[194,195]. In some studies, a three-dimensional *in vitro* model has been developed that supports the growth and co-culture of different cell types[196,197]. It allows an efficient exchange of cytokines and factors that recreate both paracrine and autocrine signaling effects and, in some cases, also allows the production of an extra-cellular matrix to give mechanical stability. Depending on the different three-dimensional system adopted, the culture offers rapid and significant experimental manipulations and allows real-time monitoring of cell-cell and cell-matrix interactions. In one study, a bioreactor was developed that enables the growth and formation of a three-dimensional and multilayer osteogenic tissue, starting from isolated osteoblasts[197]. Mouse bone marrow-derived osteoclasts were co-cultured with osteoblasts and led to differentiate. The introduction of cells from the metastatic breast cancer line MDA-MB-231 made it possible to follow the early stages of tissue colonization in real time with confocal microscopy. In this way, it was possible to observe the adhesion of tumor cells to osteoblastic tissue, their proliferation, the tissue penetration, the formation of non-vascularized micro tumors and the degradation of the extracellular matrix derived from osteoblasts. Other models use 3D scaffolds, supports made of biodegradable polymers such as type I collagen or matrix derived from extracellular matrix subjected to decellularization[198]. In addition to mimicking the tissue architecture and being easily accessible, a further advantage is the possibility to recreate the hypoxic

microenvironment present in the tumor tissue, with poor availability of nutrients and oxygen. Although the two-dimensional model constitutes a simplified model of the bone microenvironment, 3D models, which comprise the interaction between tumor cells and extracellular matrix, could represent a more comprehensive and reliable system for studying the effectiveness of drug treatments and identifying new molecular targets to interfere with the vicious cycle that occurs during the formation of bone metastasis. However, up to date, most *in vitro* models focused on the colonization process by cancer cells of the bone microenvironment and only a few attempted to mimic the initial phases like the pre-metastatic niche, evaluating the ECM-tumor induced changes by tumor cells conditioning factors, or the dissemination of cancer cells from the primary tumors[199]. Future efforts should be made towards the development of an *in vitro* 3D models that would mimic all the sequential phases of the bone metastatic process, taking advantage of a microfluidic system.

2. Aim of the Project

The study of bone metastasis from breast carcinoma is hampered by the lack of *in vitro* models that recapitulate the complex sequential stages and interactions between tumor cells and microenvironment. At an early stage, tumor secreted factors and microvesicles can be released from the primary tumors and directly modify the host stroma to establish a supportive microenvironment before the arrival of cancer cells (pre-metastatic niche). Once cancer cells arrive in the bone (metastatic niche), they can secrete soluble factors able to promote the osteoclasts differentiation and the degradation of the bone matrix, which in turn leads to the release of cytokines and growth molecules that fuel the proliferation and the expansion of cancer cells. Indeed, molecular interactions between tumor and stromal cells are critical regulators of every step of progression. In previous works[191,193],we developed a 2D model of bone metastasis taking advantage of the indirect co-culture system of cancer cells and osteoclasts. However, cells typically grown on two-dimensional (2D) platforms poorly reflect the microenvironment context of the tumor, hampering the translation of the data to the human disease. Animal models could be useful for evaluating the complexity of the bone metastasis process, but this model suffers of being time-consuming and labor intensive. Moreover, to date, there is no ideal animal model able to replicate different aspects of the metastasis. Indeed, it remains impossible to analyze the initial phase of the process, such as the pre-metastatic niche formation in the host secondary organ.

Hence, it emerges the need to fill the gap between *in vitro* and *in vivo* model with a reliable *in vitro* three-dimensional (3D) system that closely recapitulates the complexity of the bone microenvironment and its interaction with cancer cells. It has been demonstrated that a 3D system can better recapitulate the cancer *in vivo* architecture and its behavior compared to the two-dimensional models[200,201]. Another advantage of the 3D model is the possibility to co-culture two or more cell types, which reproduce *in vivo* conditions more closely. Different efforts have been made to develop 3D models able to recapitulate the complexity of the bone microenvironment[199]. However, more reliable systems able to reproduce and deconstructing the sequential cascade of events involved in bone metastasis pathogenesis would lead the opportunity to identify new therapeutic and diagnostic strategies to block the metastatic spread at an early stage.

Thus, this project aimed to develop a three-dimensional *in vitro* model able to mimic the "vicious cycle" of bone metastasis from breast carcinoma. With a step-by-step project, we aimed to highlight the mechanisms involved in the establishment of the pre-metastatic niche

and bone metastasis, leading to the opportunity to identify new therapeutic strategies to block the metastatic spread at an early stage.

To achieve this aim, we developed a bone biomimetic scaffold, made of collagen, and functionalized with hydroxyapatite material (HA, mineralized scaffold) able to mimic the composition of the bone matrix *in vitro*. This would be the platform for the optimization and co-culture of bone cells (osteoclasts and osteoblasts) and breast cancer cell lines, also considering the interaction with the extracellular matrix. This model will be useful to recapitulate the natural history of the bone metastatic vicious cycle *in vitro*, for a better understanding of the molecular mechanisms involved in the crosstalk between tumor and bone cells in the establishment of the sequential stages of the bone metastatic process. The resulting model, mimicking the bone microenvironment *in vivo*, could enable a deeply investigation of the molecular mechanisms involved, and it could provide a more reliable preclinical tool to study the effectiveness of innovative drugs and the discovery of molecular markers useful in the clinical practice.

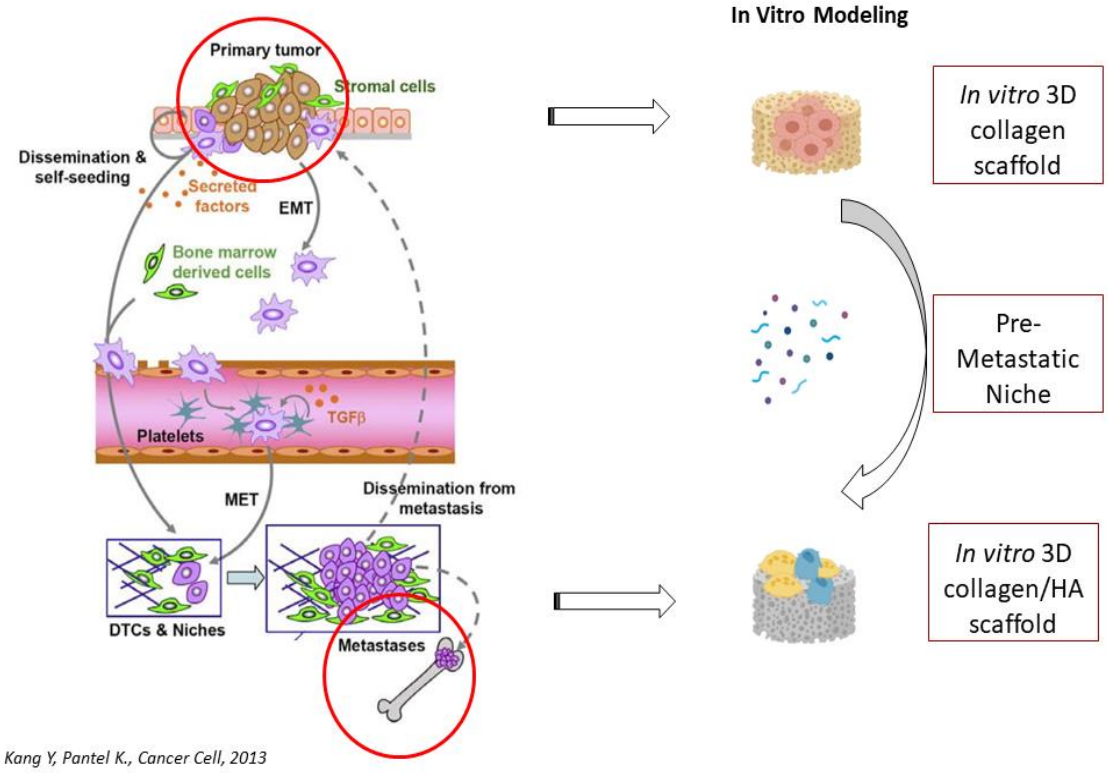

Modeling the Bone Metastatic Process in Vitro.

3. Materials and Methods

3.1 3D Collagen and 3D Mineralized Scaffold Synthesis

All chemicals necessary for scaffold synthesis were purchased from Sigma Aldrich (Merck KGaA, Darmstadt, Germany). Collagen scaffolds were synthesized as followed: a 1wt% suspension of type I collagen in acetic acid was prepared and precipitated to pH 5.5. The material was cross-linked through a 1wt% 1, 4-butanediol diglycidyl eter (BDDGE) to stabilize the collagen matrix and to control porosity and tortuosity. Scaffold's porosity and pore size were obtained through an optimized freeze-drying process, consisting of an established freezing and heating ramp (from 25 °C to −25 °C and from −25 °C to 25 °C in 50min under vacuum conditions, p=0.20 mbar), ultimately ensuring proper pore interconnectivity and orientation.

For 3D collagen/HA scaffolds (3D mineralized scaffold), collagen solution was mixed and cross-linked with hydroxyapatite in a ratio of 70:30 in order to mimic the healthy bone structure, since the bone matrix is composed of 70% of minerals and 30% of collagen[166].

All scaffolds were sterilized by immersion in 70% ethanol for 1hour, followed by three washes in sterile Dulbecco Phosphate Buffered Saline (DPBS) (Thermo Fisher Scientific, Waltham, MA USA).

3.2 Osteoblastogenesis Assay in 2D and 3D Models

Human osteoblasts were obtained from human mesenchymal stem cells (MSC # PT-2501, LONZA, Basel, Switzerland) seeded in bidimensional plates at a concentration of 5700 cells per $2cm^{\wedge 2}$ per well. Mesenchymal Stem Cells were cultured in α-MEM and differentiation was induced by adding to the medium 10 nM dexamethasone, 10mM β-Glycerophosphate, 200μM ascorbic acid for 14 days. Osteoblast's differentiation was confirmed by Alizarin Red S staining performed to evaluate extracellular calcium deposits secreted by differentiated osteoblasts.

For human osteoblasts differentiation in 3D scaffolds $5x10^{\wedge 5}$ human mesenchymal cells at low passage were seeded by adding 50 μl of cell suspension on the scaffold upper surface. Seeding was reached by simple soaking of the cell suspension in the dry scaffolds. Cells were incubated for 1 hour at 37 °C to allow adhesion, after that medium was added. The medium was replaced every two days.

3.3 Osteoclastogenesis Assay in 2D and 3D Models

Human osteoclasts were obtained from the differentiation of peripheral blood mononuclear cells (PBMCs) of healthy donors who gave written informed consent to take part in the study. Monocytes were isolated from buffy coats by Lymphosep™ density gradient[193]. Briefly, EDTA

whole blood (50 mL) was diluted 1:1 with phosphate-buffered saline, layered on lymphocyte separation medium (Lymphosep™, Biowest LLC, Riverside, MO, USA) and centrifuged without brakes at 2200 rpm for 10 min. The PBMCs layer was collected and washed twice with phosphate-buffered saline (PBS) and treated for 4 min on ice with ACK solution. After having washed them twice with phosphate-buffered saline, cells were suspended in complete α-MEM (LONZA, Basel, Switzerland). Cells were counted and plated at a concentration of 1,500,000 PBMCs per 2 cm^2 well. After 4 h, the medium was removed and differentiation into osteoclasts was induced by α-MEM supplemented with 20 ng/mL of M-CSF (Peprotech, Rocky Hill, NJ, USA). From Day 7 of culture, RANKL (20 ng/mL) was added with M-CSF (control positive condition, Ctrl+). The medium was changed every 2–3 days and TRAP+ multinucleated cells were observed after 15 days of differentiation. Each condition was performed in triplicate and experiments were run at least three times.

For human osteoclasts differentiation in 3D scaffolds, 20x10^6 PBMCs, isolated as previously described, were seeded by adding 50 µl of cell suspension on the scaffold upper surface. Seeding was reached by simple soaking of the cell suspension in the dry scaffolds. Cells were incubated for 1 hour at 37 °C to allow adhesion, after that medium was added. The medium was replaced every two days and PBMCs were led to differentiate with different concentrations of MCS-F (20ng/ml or 100ng/mL) and RANKL (20ng/ml or 100ng/mL) to induce osteoclast maturation.

3.4 Tumor Cell Seeding and Culture

The experiments were performed on three human breast cancer cell lines: the triple negative cell line MDA-MB-231 (obtained from the America Type Culture Collection, ATCC, Rockville, Maryland, USA), the SCP2 cell line, a bone-tropic cell line originating from MDA-MB-231 kindly provided by Yibin Kang's laboratory where it was originally isolated[51], and the hormonal receptor positive MCF7, obtained from ATCC. All cells were maintained in DMEM medium supplemented with 10% fetal bovine serum, 1% penicillin-streptomycin and 1% glutamine at 37 °C in a 5% CO2 atmosphere. For standard cultures, 1×10^6 cells were maintained as a monolayer in 25-cm2 flasks in 4 ml of culture medium. For 3D cultures, each scaffold (1×9mm) was placed in a 6-multiwell plate and seeded with 1×10^6 cells by adding 50 µl of cell suspension on the scaffold upper surface. Seeding was reached by simple soaking of the cell suspension in the dry scaffolds. Cells were incubated for 1 hour at 37 °C to allow adhesion, after that 4 ml of culture medium were carefully added. After 24 h, the scaffolds were

gently moved in a new 6-multiwell plate to avoid any contribution of cells that might have attached on the plate surfaces. The medium was replaced every two days.

3.5 Quantification of TRAP-positive Multinucleated Cells

Mature osteoclasts, cultured in 2D plates, were fixed after 15 days of differentiation by incubation in 4% Paraformaldehyde (PFA, Electron Microscopy Sciences, Hatfield, PA, USA) for 20 min at room temperature and then stained for tartrate resistant acid phosphate staining (TRAP kit, Sigma-Aldrich, Darmstadt, Germany). Osteoclasts were counted with a magnification of 10x in an Axiovision Microscope in 5 fields/well as TRAP-positive cells with more than 4 nuclei. Images of mature osteoclasts were acquired at different magnifications with Axiovision Microscope. Each experiment was performed in triplicate and repeated at least three times.

3.6 Indirect and Direct Co-culture of Tumor Cells and Osteoclasts

To evaluate tumor cell's effects on osteoclast's maturation, indirect co-culture was optimized by adding in osteoclasts' medium culture 20% of conditioned medium by breast cancer cell lines. Conditioned medium was collected at 7 days of breast cancer cells' culture in 2D or 3D models. Briefly, cancer cells were seeded at a concentration of $1x10^{\wedge 6}$ cells per 25 cm^2 in bidimensional model or in 3D scaffolds. Then, cells were cultured in α-MEM medium and at day 6^{th} medium was replaced with fresh medium and collected at day 7^{th}.

For direct co-culture $20x10^{\wedge 6}$ cells of PBMCs were seeded by adding 50 µl of cell suspension on the scaffold upper surface. Cells were incubated for 1 hour at 37 °C to allow adhesion. Then, $1x10^{\wedge 6}$ tumor cells were seeded by adding 50 µl of cell suspension on the scaffold upper surface. Cells were allowed to adhere for 1 hour at 37 °C then medium was added. For indirect co-culture, tumor cells and PBMCs were seeded in two different 3D mineralized scaffolds and placed in the same well of a 6-well plate.

3.7 Tumor Cell Growth Assay

Tumor cell growth was assessed by MTT assay. Briefly, at different time points cells within the scaffolds or in monolayer cultures were incubated with 0.5mg/ml of MTT solution (Sigma Aldrich, Darmstadt, Germany) in PBS for 2 hours at 37 °C and the absorbance was determined at 550nm.

3.8 Drug Exposure and Dose Selection

Zoledronic Acid (Zol, Zometa®), was solubilized at a concentration of 50 mM in sterile water, filtered and stored at −20 °C. Denosumab (Deno) 120 mg in 1.7 mL (XGEVA®) was stored at 4 °C. Drugs were diluted in complete α-MEM. Doses of Zol and Den were selected based on plasma levels from pharmacokinetic clinical data. We used 24 μg/mL concentration for Den and 10 μM for Zol, as it was reported to accumulate in bone tissues at a higher concentration than plasmatic peak. Deno and Zol were administered for 72 hours a day 8 (in the latest stages of osteoclasts differentiation). To determine osteoclastogenesis inhibition, the number of osteoclast cells in treated wells was normalized to untreated wells. Inhibition of osteoclastogenesis after drug exposure was reported as percentage (%) of osteoclastogenesis normalized with respect to the untreated control.

Tumor cells were treated at day 4 of culture for 72h, afterwards conditioned medium was collected at day 7 of culture. Survival analysis was performed by MTT assay (Sigma Aldrich, Darmstadt, Germany) according to the manufacturer's instructions and as previously described. For osteoclasts, conditioned medium from treated tumor cells was added to osteoclasts at day 8 of differentiation. Each experiment was performed in triplicate and repeated at least three times.

3.9 Immunofluorescence Staining

For immunofluorescence staining, cells were fixed 20 min in 4% PFA and then blocked to minimize unspecific binding of the primary antibody and permeabilized with PBS + 1%BSA+0.3% Triton X-100. Then, cells were incubated with the h-TRAP primary antibody (abcam ab185716) overnight at 4 °C. Fluorescent secondary antibody was then used to detect the immunoreaction. Dapi staining was used to counterstain the nucleus whereas Phalloidin Staining (Alexa Fluor™ Phalloidin) was used to detect filamentous actin (F-actin). Images were taken by A1 laser confocal microscope (Nikon Corporation, Tokyo, Japan) and analyzed with the NIS Elements software (Nikon Corporation, Tokyo, Japan).

3.10 Quantitative Real Time reverse transcription PCR (qRT-PCR)

The scaffolds were fragmented into small pieces, while 2D culture cells were collected by trypsinization. Total mRNA was isolated using TRIzol Reagent (Invitrogen) following the manufacturer's instructions. Five hundred nanograms of RNA were reverse transcribed using the iScript cDNA Synthesis Kit (BioRad, Hercules, CA, USA). The final mixture was incubated

at 25 °C for 5 min, at 42 °C for 20 min, at 47 °C for 20 min, at 50 °C for 15 min and 5 min at 85 °C. Real-Time PCR was performed on the 7500 Real-Time PCR System (Applied Biosystems, Waltham, MA, USA) using the TaqMan gene expression assay mix (Applied Biosystems, Waltham, MA, USA) or SYBR assay (Applied Biosystems, Waltham, MA, USA). Amplification was performed from 2 µl of cDNA, in a final volume of 20 µl containing 2x Gene expression master Mix (Applied Biosystems, Waltham, MA, USA). The stably expressed endogenous HPRT was used as reference gene. The following markers were analyzed according to cell types: for tumor cells: E-Cadherin (CDH1), Vimentin (VIM), SNAI1, SNAI2, TWIST1, ZEB2, SPARC, LOX, CXCR4, JAG1, RANK, RANKL, OPG, TNF-α, IL-6, IL-8, 1L-11; for osteoclasts: Calcitonin Receptor (CALCR), Carbonic Anhydrase (CA2), Tartrate Resistant Acid Phosphatase (ACP5, TRAP), Cathepsin K (CTSK), OSCAR, RANK; for osteoblasts: ALPL, COL1A1, BGLAP, RUNX2, OSX. The amount of transcripts was normalized to the endogenous reference genes and expressed as n-fold mRNA levels relative to a calibrator using a comparative threshold cycle (Ct) value method (ΔΔCt).

3.11 Statistical Analysis

Each experiment was repeated at least three times with 3 technical replicates for each condition. Data are presented as mean ± S.E.M. (standard error of the mean) or as percentage (%) of osteoclastogenesis or percentage (%) of survival. The differences between groups were assessed by two-tailed Student's t-test or Mann–Whitney test, as appropriated, and accepted as significant when $P < 0.05$.

4. Results

4.1 Development and characterization of a 3D bone biomimetic scaffold.

Previously, we developed and characterized a Type I collagen scaffold as a suitable platform to model *in vitro* some of the key features of primary tumor growth and drugs response[200,201]. Indeed, this model enables to mimic hypoxic condition and it can induce a more aggressive phenotype in breast cancer cell lines. For this reason, to mimic the bone tissue to create a suitable platform and to study bone metastasis *in vitro*, we synthesized scaffolds through a pH-driven method, which enabled the fabrication of a biomimetic material with highly reproducible morphology and tunable macro- and micro-structure. Hence, we incorporated hydroxyapatite mixture in a ratio of 70:30 to mimic the healthy bone tissue. The scaffold has a dimension of 9 mm of diameter and 2 mm of thickness (Fig. 1). Even if mineralized scaffold showed a less porosity than the 3D collagen scaffold, the matrix allows the seeding and the penetration of tumor and bone cells throughout the scaffold.

Fig.1 Development and characterization of a 3D bone biomimetic scaffold.

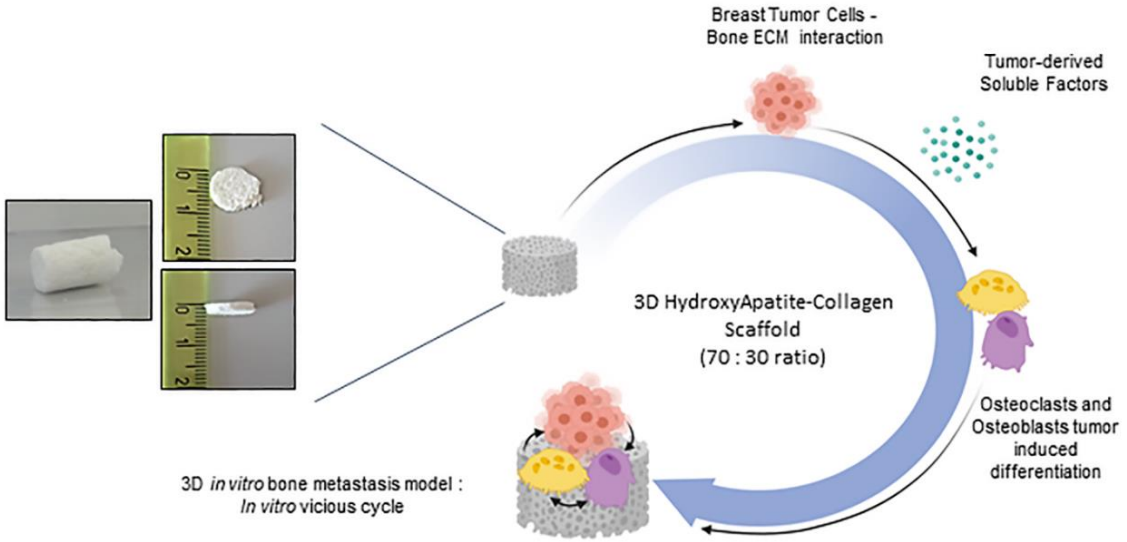

Fig.1 Development and characterization of a 3D bone biomimetic scaffold. *Representative pictures of 3D mineralized scaffold and graphical abstract of study design. The 3D bone biomimetic scaffold is developed from a mixture of Type I collagen and hydroxyapatite in a ratio of 70:30 to mimic the healthy bone composition.*

4.2 3D bone biomimetic model is suitable for osteoblasts and osteoclasts differentiation.

Then, we attempted to evaluate whether the biomineralized scaffold is a suitable *in vitro* platform for osteoclasts and osteoblasts differentiation from their precursor cells (monocytes cells for osteoclasts and mesenchymal stem cells for osteoblasts). To induce osteoblasts differentiation from MSC cells, we seeded 5x10^5 cells/scaffold and we led to differentiate MSC into osteoblasts adding to the medium 10 nM dexamethasone, 10mM β-Glycerophosphate, 200µM ascorbic acid. We could distinguish two different phases in the differentiation process of MSC: an early and a late osteoblastogenesis. Each phase is characterized by the upregulation of specific osteoblastic markers. Then, after 14 days, we evaluated the successful differentiation of cells by immunofluorescence staining of the osteoblast's marker Osteocalcin (Fig. 2A). Hence, at 10 days of the differentiation, cells upregulated the mRNA expression of osteoblasts transcription factor RUNX2, meanwhile at 14 days of differentiation, cells upregulated BGLAP, which encoded the Osteocalcin protein detected also by immunofluorescence. Moreover, osteoblasts cells continuously upregulate the ALPL (Alkaline Phosphatase) mRNA throughout the differentiation period (Fig. 2B).

Fig.2 3D biomineralized model is suitable for osteoblasts differentiation.

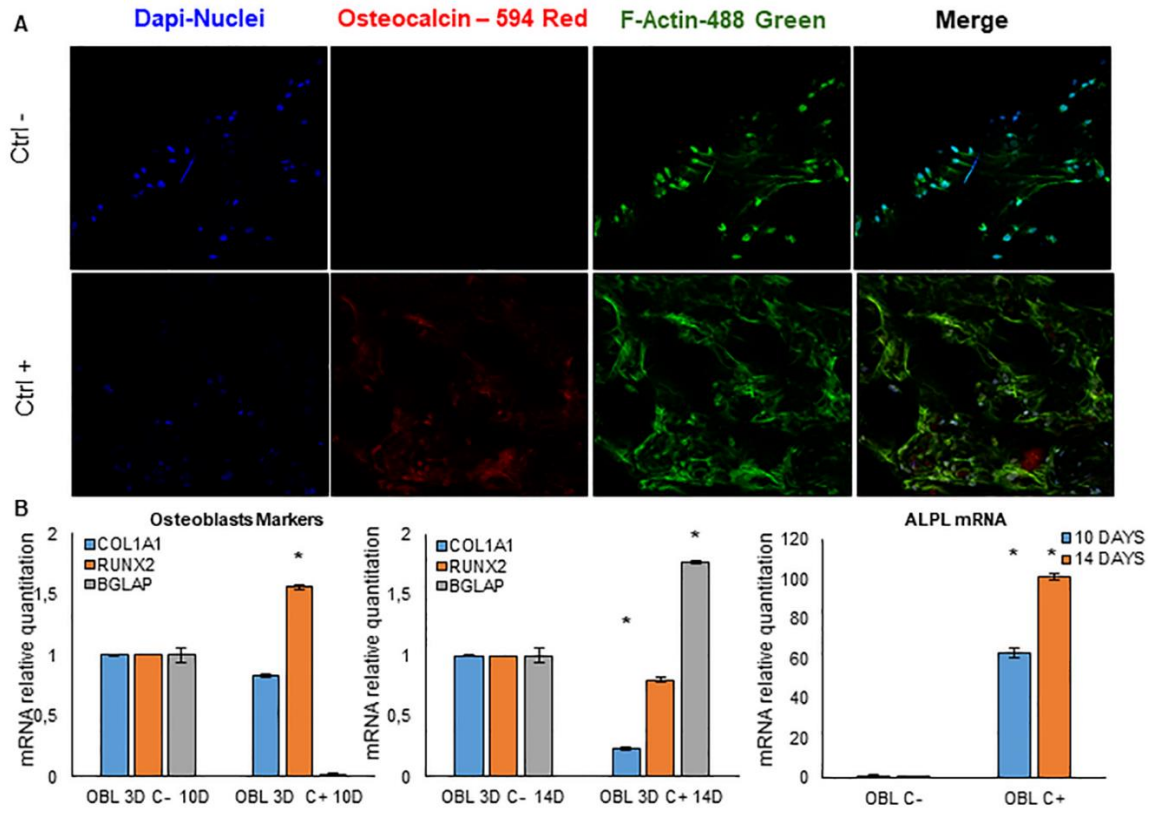

Fig. 2 3D bone biomimetic model is suitable for osteoblasts differentiation. *A) Confocal images of immunofluorescence staining for Osteocalcin as osteoblasts marker in MSCs cells differentiated towards osteoblast lineage at 14 days. Positive staining of Osteocalcin (Alexafluor-594) indicates mature osteoblasts formation in CTRL+ condition. Alexafluor-488 Phalloidin Staining was performed to detect filamentous actin (F-actin) and nuclei were counterstained in DAPI. B) RT–qPCR analysis of Osteoblasts Markers (COL1A1, RUNX2, BGLAP, ALPL) in MSCs cells not differentiated (CTRL-) and differentiated (CTRL+) into osteoblast lineage at 10 and 14 days of differentiation. The values were relative to MSCs cells not differentiated (CTRL-). Data are represented as mean ± S.E.M. (n = 3). *P < 0.05.*

To induce osteoclast differentiation, peripheral-blood mononuclear cells were isolated by healthy donor's blood, and they were seeded in the scaffold. Then, osteoclasts maturation lasts for 15 days, and it consists of two sequential phases: the differentiation of monocytes in pre-osteoclasts (day 0-day 7) and the differentiation of pre-osteoclasts into osteoclasts (day 7-day 15). Hence, the differentiation was induced for 15 days with M-CSF (from day 1 to day 15) and RANKL (from day 7 to day 15). Since it was previously demonstrated that the cellular density is extremely crucial to allow the optimal differentiation, firstly we determined the best concentration of PBMCs to seed in the scaffold to obtain the differentiation. Considering that the optimal concentration to obtain the osteoclasts differentiation from PBMCs in the bidimensional model is $1{,}5x10^{\wedge 6}$ cells/$2cm^{\wedge 2}$, we evaluated three different concentrations: $10x10^{\wedge 6}$ cells/scaffold, $15x10^{\wedge 6}$ cells/scaffold and $20\ x10^{\wedge 6}$ cells/scaffold. By confocal analysis, we evaluated two main features of differentiated osteoclasts: the presence of TRAP protein and the F-actin ring formation. Along this line, we showed that $20\ x10^{\wedge 6}$ cells/scaffold was the optimal concentration to obtain a good cellularity within the scaffold and osteoclasts differentiation at day 15 of differentiation (Fig. 3A-B). Moreover, the concentration of the two soluble factors was determined between 20ng/ml and 100 ng/ml. The differentiation was evaluated by confocal analysis and gene expression analysis of mature osteoclasts markers. Meanwhile 20ng/ml did not enable a good differentiation, 100ng/ml of M-CSF and RANKL was identified as suitable to induce a significant maturation. Indeed, at day 10 and day 15 of differentiation by adding 100 ng/ml of soluble factors, differentiated osteoclasts showed a significant upregulation of the following markers: ACP5 (TRAP), CA2, CTSK, OSCAR, JDP2 at day 10; OSCAR, RANK and NFATC1 at day 15 (Fig. 3C).

Fig.3 3D biomineralized model is suitable for osteoclasts differentiation.

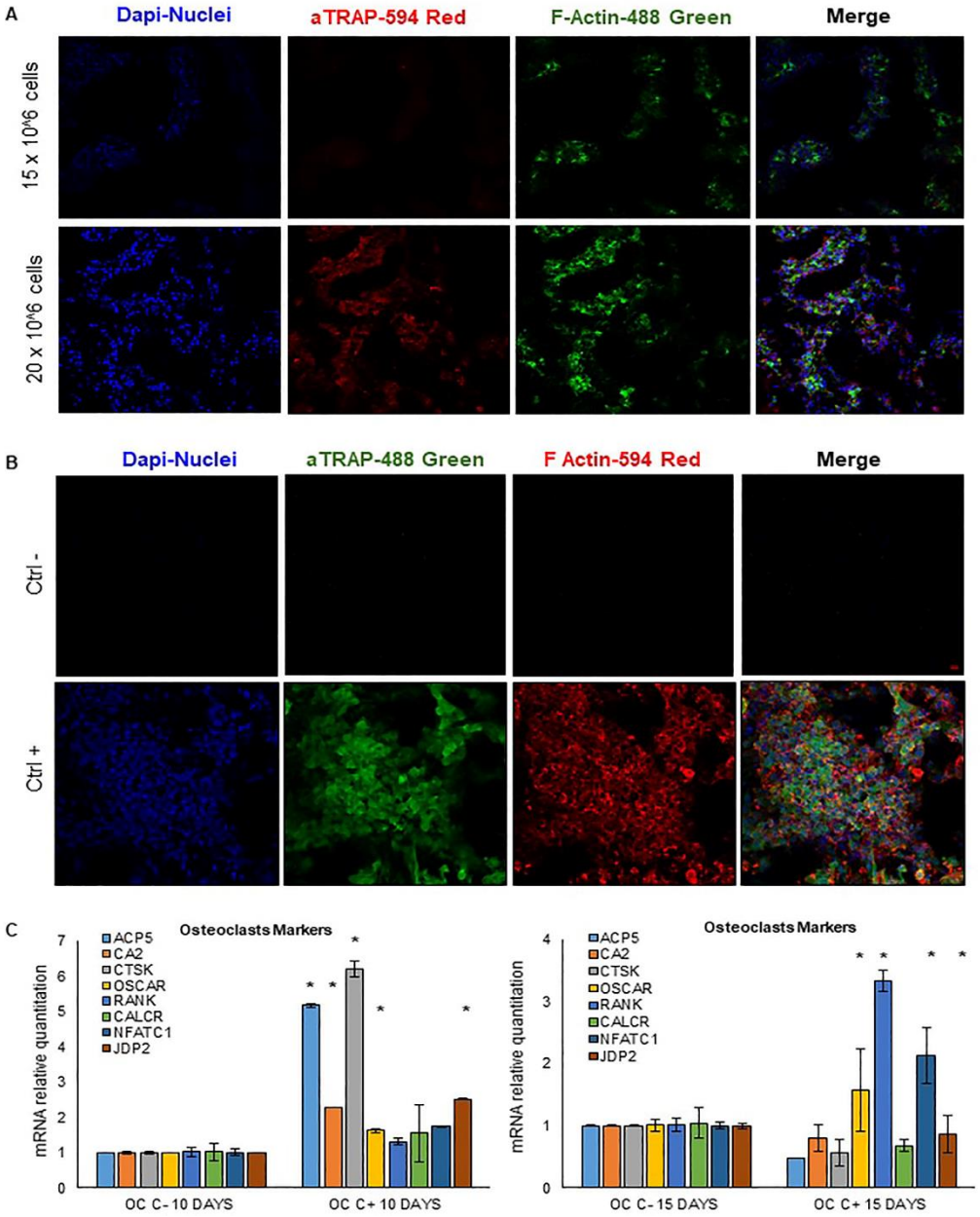

Fig. 3 3D bone biomimetic model is suitable for osteoclasts differentiation. *A) Confocal images of TRAP as osteoclasts marker in PBMCs cells differentiated towards osteoclast lineage at 15 days. Positive staining of TRAP (Alexafluor-594) indicates mature osteoclasts. Different concentrations of PBMCs were tested and 20 x10^6 cells/scaffold was defined as the optimal concentration to obtain a good cellularity within the scaffold and osteoclasts differentiation at day 15. Alexafluor-488 Phalloidin Staining was performed to detect filamentous actin (F-actin), disposed in mature osteoclasts as an F-actin ring, and nuclei were counterstained in DAPI. B) Confocal images to compare osteoclasts differentiation at 15 days of differentiation from PMBCs without differentiated factors MCS-F and RANKL (CTRL-) vs PBMCs led to differentiate with 100ng/ml of MCS-F and RANKL (CTRL+). C) RT–qPCR analysis of early and late osteoclastogenesis (ACP5, CA2, CTSK, OSCAR, RANK CALCR, NFATC1, JDP2) in PBMCs cells not differentiated (CTRL-) and differentiated (CTRL+) into osteoclast lineage at 10 and 15 days of differentiation. The values were relative to PBMCs cells not differentiated (CTRL-). Data are represented as mean ± S.E.M. (n = 3), *P < 0.05.*

4.3 Different ECM affects breast cancer cells behavior.

Once optimized the cellular components of the 3D bone biomimetic model to mimic bone metastatic niche, we next characterized the model evaluating how the extracellular matrix affects breast cancer behavior. Indeed, it is noteworthy that not only the cellular components but also the extracellular matrix (ECM) of the primary and metastatic organ can affect metastasis[202]. Hence, we compared the responses to the two different environment of collagen and HA/collagen matrix (HA/COLL, 3D mineralized scaffold) of three cell lines with different molecular patterns and clinical behavior: MDA-MB-231 cell line, triple negative cell lines connected to high grade and aggressive disease, the bone metastatic SCP2 cell line, a subclone of MDA-MB-231 *in vivo* isolated to preferentially metastasize to bone[51] (a kind gift from Prof. Yibin Kang, Princeton University, NJ, USA) and the estrogen receptor positive (ER+) Luminal A MCF7 cell line, connected to a more indolent and less aggressive disease.

First, we compared their morphology, disposition, and cell growth dynamics in the collagen-based scaffold and in the HA/COLL scaffold (3D mineralized scaffold) in a time course experiment of 10 days. Morphology and disposition within the scaffold were assessed by confocal microscopy (Fig. 4A). Cancer cells did not assume a significant different morphology or disposition within the two different environments. However, cancer cells within the 3D mineralized scaffold showed a slower growth rate compared to the collagen-based scaffold (Fig. 4B). In particular, the crucial and exponential phase of cell growth is reached for all the three different cell lines between the 72h and 7 days of growth within the scaffold, whereas at 7 days cancer cells reach a plateau. To deeper investigate how the ECM affects cancer cells behavior, we assessed the modulation of aggressiveness and osteomimicry markers at 72h and 7 days of culture (Fig. 4C). Osteomimicry occurs when cancer cells begin to express genes normally restricted to cells resident in the bone tissue. Interestingly, cells showed a more significant gene modulation at 72h of culture, meanwhile at 7 days they probably adapt to the environment. MDA-MB-231 cells at 72h showed a significant upregulation of osteomimicry markers CXCR4, JAG1 and a significant downregulation of the aggressiveness marker LOX. Similarly, SCP2 cells showed a significant upregulation of CXCR4, JAG1 and a significant downregulation of LOX and OPG gene. MCF7 cells showed a significant downregulation of LOX at 72h. Interestingly, at 7 days meanwhile MDA-MB-231 and SCP2 cells maintain a significant downregulation of LOX gene, MCF7 showed a significant upregulation of this aggressive gene. At 10 days, time point where in cancer cells showed a growth decrease, gene expression analysis did not highlight a modulation in markers analyzed, confirming an

adaptation of cancer cells to the different microenvironment (data not shown). Hence, ECM can affect cancer cell behavior in their growth dynamics and gene modulation of aggressive and osteomimicry markers.

Fig.4 Different ECM affects breast cancer cells behavior.

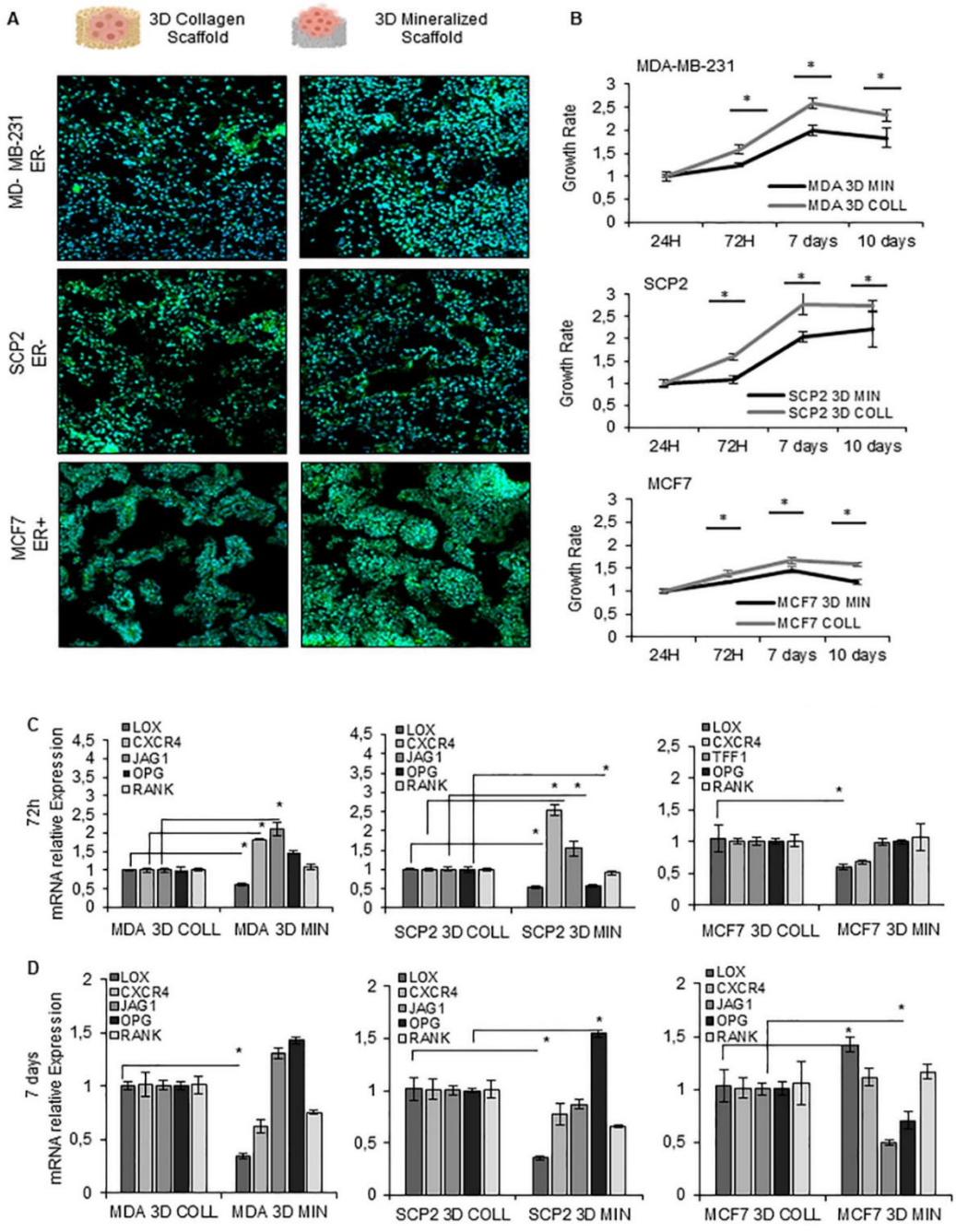

Fig.4 Different ECM affects breast cancer cells behavior. *A) Confocal images of breast cancer cells (MDA-MB-231, SCP2, MCF7 cells) cultured in 3D collagen and 3D mineralized scaffold (HA/COLL) at 10 days of culture. Breast cancer cells were stained with Alexafluor-488 Phalloidin staining to detect filamentous actin (F-actin) and DAPI to counterstain the nuclei. B) Tumor cell growth assay by MTT analysis of breast cancer cells cultured in 3D collagen and 3D mineralized scaffold. Values were normalized with respect to 24h time points. Data represent mean ± S.E.M. (n = 3). *P < 0.05, two-tailed*

*Student's t-test. C) RT–qPCR analysis of selected markers related to aggressiveness and bone metastasis (LOX, CXCR4, JAG1, OPG, RANK) in breast cancer cells cultured in 3D collagen and 3D mineralized scaffold. The values were normalized with respect to breast cancer cell line cultured in 3D collagen scaffold. Data represent mean ± S.E.M. (n = 3). *P < 0.05.*

4.4 Sensitivity of breast cancer cells to bone targeted therapy.

Since MDA-MB-231 and SCP2 cells cultured in the 3D mineralized scaffold showed an osteomimetic pattern by gene modulation, we assessed whether this model could be suitable to study breast cancer sensitivity to bone targeted drugs. Moreover, we evaluated whether their response could be different within the two different environments examined: collagen matrix, mimicking the primary tumor ECM and HA/collagen, mimicking the bone metastatic ECM. Cells were treated with Zoledronic Acid (Zol) and Denosumab (Deno, an anti-RANKL inhibitor). For ER- cell lines, MDA-MB-231 cells cultured in the collagen scaffold and in the mineralized scaffold did not show a different response to Deno, meanwhile they are more sensitive to Zol in 3D mineralized scaffold and 2D plates (Fig. 5A). SCP2 cells, cultured in the 3D mineralized matrix, showed a significant increase in sensitivity to Deno and Zol compared to 3D collagen matrix, and they are more sensitive in 2D plates, probably related to their osteotropic phenotype (Fig. 5B). For luminal A MCF7 cells, when cultured in the 3D mineralized scaffold, cells showed a significant increased sensitivity to Zol (Fig. 5C).

Fig.5 Different ECM affects breast cancer sensitivity to Bone Targeted Therapy.

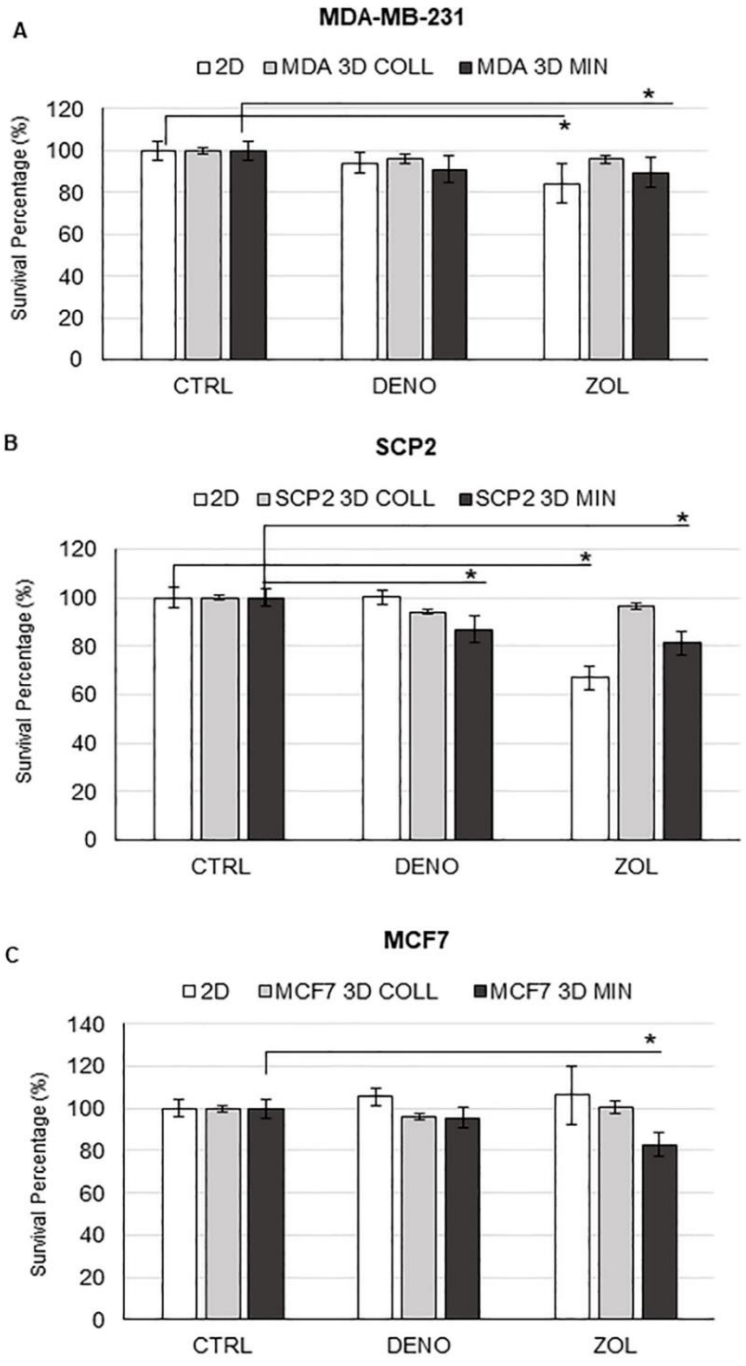

Fig.5 Different ECM affects breast cancer sensitivity to Bone Targeted Therapy. *A) Survival Percentage (%) by MTT assay in MDA-MB-231 cells cultured in 2D plates, 3D collagen scaffold (3D COLL) and 3D mineralized scaffold (3D MIN). Values were normalized to the untreated condition. Data represent mean ± S.E.M. (n = 3). *P < 0.05. B) Survival Percentage (%) by MTT assay in SCP2 cells cultured in 2D plates, 3D collagen scaffold and 3D mineralized scaffold. Values were normalized to the untreated condition. Data represent mean ± S.E.M. (n = 3). *P < 0.05. C) Survival Percentage (%) by MTT assay in MCF7 cells cultured in 2D plates, 3D collagen scaffold and 3D mineralized scaffold. Values were normalized to the untreated condition. Data are represented as mean ± S.E.M. (n = 3). *P < 0.05, two-tailed Student's t-test.*

4.5 Breast cancer cells cultured in a 3D biomimetic scaffold affect osteoclasts differentiation from PBMCs.

Then, we attempted to mimic some of the key phases of pre-metastatic niche formation. We aimed to evaluate whether the different ECM can affect the secretion, by cancer cells, of soluble factors related to osteoclasts differentiation. We compared the osteoclastogenic potential of breast cancer cell lines cultured in bidimensional model and in the collagen and mineralized based scaffold. Soluble factors secreted by breast cancer cells were collected at day 7 of culture in the three different models, and the medium was used to induce osteoclasts differentiation from precursors' cells. At 15 days of differentiation, osteoclasts were counted and defined as TRAP-positive cells with more than 4 nuclei (Fig. 6A). Factors secreted by ER- breast cancer cell lines MDA-MB-231 and SCP2 induced similarly the differentiation of PBMCs in osteoclasts cells (Fig. 6B, C). Moreover, when cancer cells were cultured in the 3D models (collagen or mineralized) the osteoclasts differentiation induced by soluble factors was increased in a significant manner compared to positive control condition. For luminal A cell line MCF7, osteoclastogenic potential of soluble factors secreted by MCF7 cultured in 2D was less than the positive control, where in differentiation is induced by adding M-CSF and RANKL to the medium. However, when MCF7 cells, cultured in both 3D models, released soluble factors are effective in differentiating PBMCs into osteoclasts in a significant manner (Fig. 6D).

Fig.6 Breast Cancer Cells cultured in a 3D bone biomimetic scaffold affect osteoclasts differentiation from PBMCs.

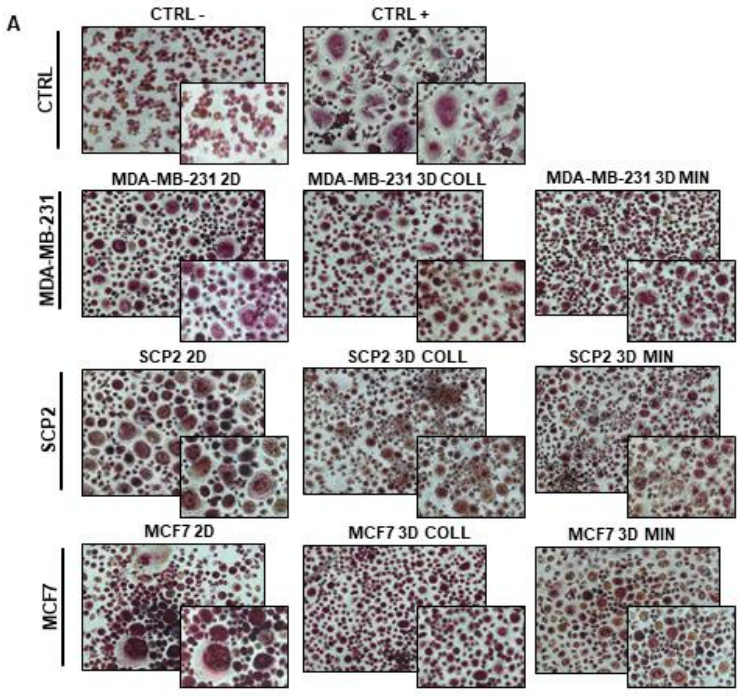

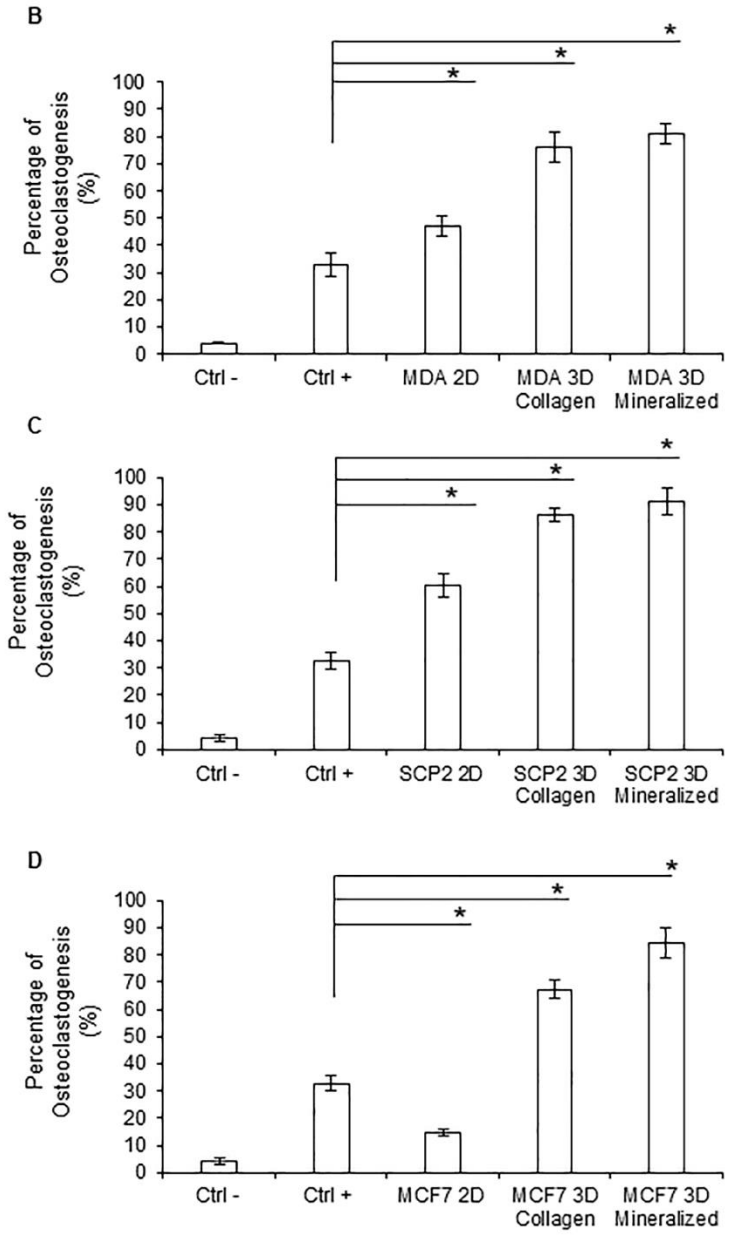

Fig.6 Breast Cancer Cells cultured in a 3D biomimetic scaffold affect osteoclasts differentiation from PBMCs. *A) Representative pictures for each condition of PBMCs and differentiated osteoclasts after 15 days of differentiation with M-CSF and RANKL (CTRL+) or with conditioned medium from breast cancer cells cultured in 2D or 3D collagen or 3D mineralized. Conditioned medium (CM) was collected at 7 days of cultures and added to complete α-MEM to obtain a CM with 20% cancer cell medium and 80% α-MEM. B) Percentage of Osteoclastogenesis (%) induced by MDA-MB-231 cells. Data were normalized to the CTRL- condition. Differentiated osteoclasts were identified as cells positive to TRAP staining and with more than 4 nuclei. Significance was related to the CTRL+ condition, PBMCs differentiated with MCS-F and RANKL (*P < 0.05, two-tailed Student's t-test) C) Percentage of Osteoclastogenesis (%) induced by SCP2 cells. D) Percentage of Osteoclastogenesis (%) induced by MCF7 cells.*

4.6 Gene expression of pro-inflammatory cytokines by breast cancer cells is affected by 3D biomimetic model.

Then, we evaluated which soluble factors secreted by breast cancer cells could be involved in the differentiation of PBMCs into osteoclasts and whether their expression and secretion are affected by the different environment. Since from gene expression analysis and ELISA assay we assessed that RANKL, the key factor for differentiation of pre-osteoclasts into mature osteoclasts, seemed not be expressed by MDA-MB-231, SCP2 and MCF7 cells (data not shown), we selected from literature some pro-inflammatory cytokines that could be involved in the differentiation of monocytes into mature osteoclasts at different levels (Fig. 7). We investigated the expression of the following pro-inflammatory cytokines: TNF-α, IL-6, IL-8, and IL-11. Interestingly, for all the three cell lines there was a significant upregulation of TNF-α expression when cells were cultured in 3D models compared to when cultured in conventional plates. Meanwhile MDA-MB-231 and SCP2 cell line showed a significant downregulation of IL-6 and IL-8 when cells were cultured in the mineralized scaffold, MCF7 cells showed a significant upregulation of IL-6.

Fig.7 Gene expression of pro-inflammatory cytokines by Breast Cancer Cells is affected by 3D biomimetic model.

A: MDA-MB-231

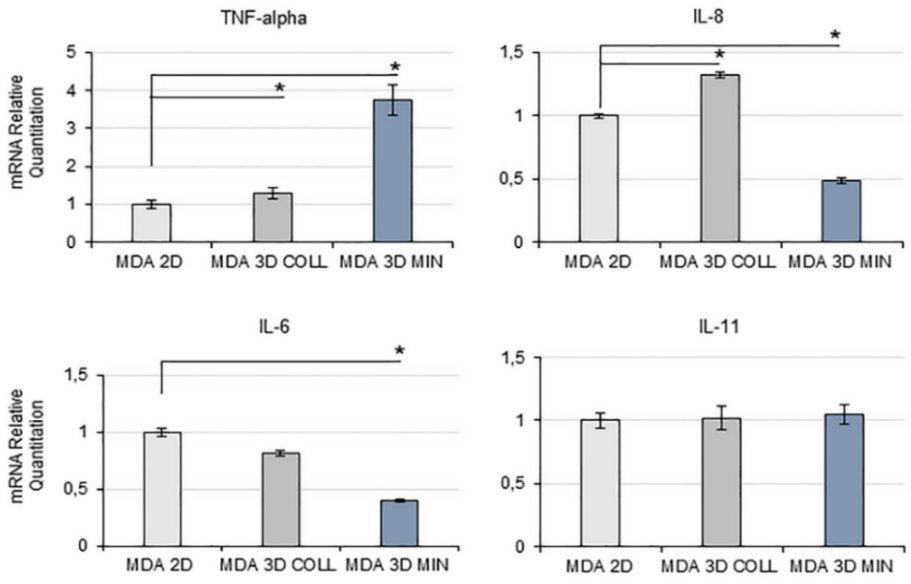

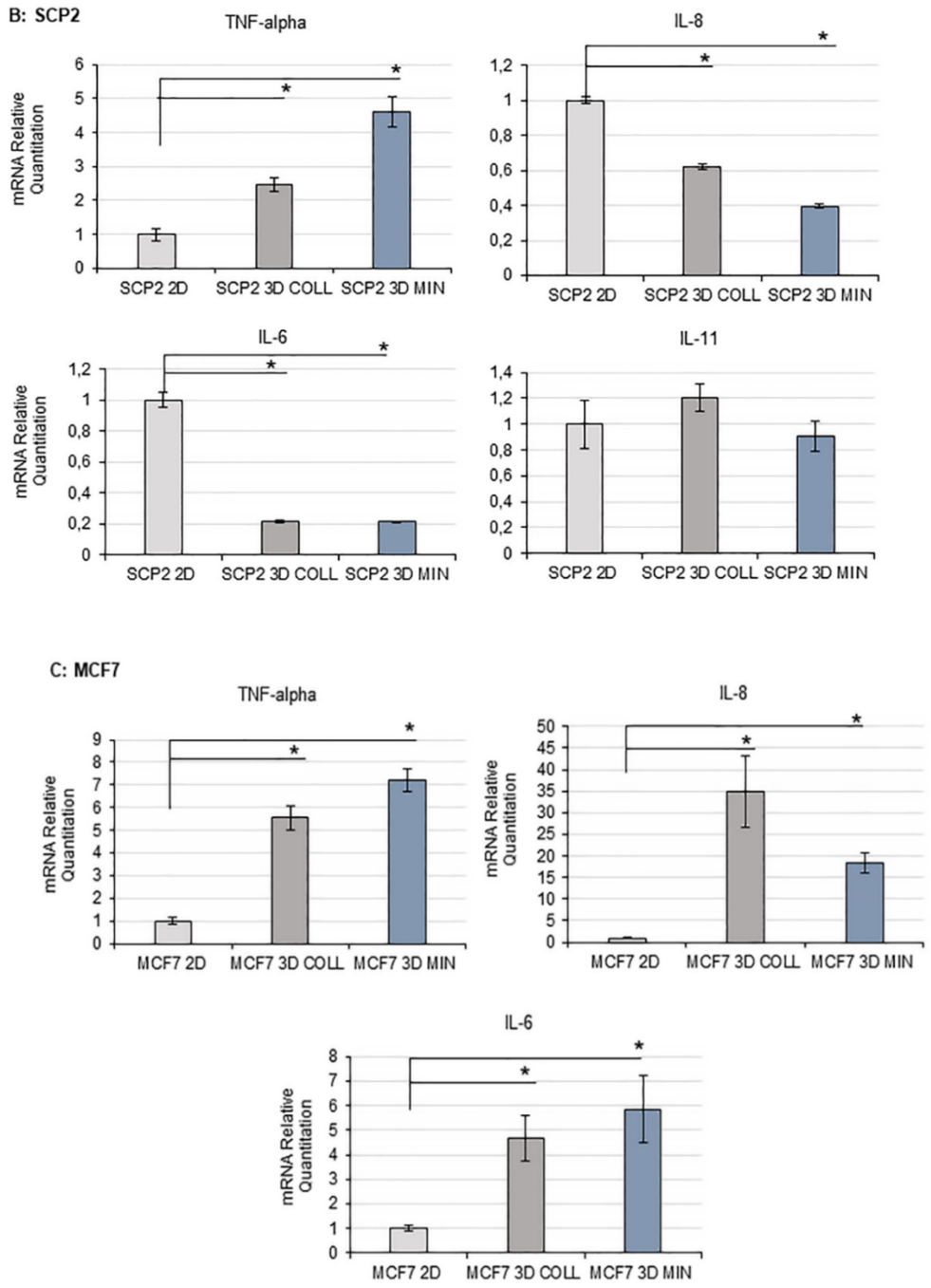

Fig.7 Gene expression of pro-inflammatory cytokines by Breast Cancer Cells is affected by 3D biomimetic model. *A) RT–qPCR analysis of pro-inflammatory cytokines (TNF-alpha, IL-8, IL-6, IL-11) gene expression by MDA-MB-231 cells cultured in 2D, 3D collagen, 3D mineralized scaffold. Values were normalized with respect to cells cultured in 2D as reference. Data represent mean ± S.E.M. (n = 3). *P < 0.05 two-tailed Student's t-test. B) RT–qPCR analysis of pro-inflammatory cytokines (TNF-alpha, IL-8, IL-6, IL-11) expression by SCP2 cells cultured in 2D, 3D collagen, 3D mineralized scaffold. Values were normalized with respect to cells cultured in 2D as reference. Data represent mean ± S.E.M. (n = 3). *P < 0.05, two-tailed Student's t-test. C) RT–qPCR analysis of pro-inflammatory cytokines (TNF-alpha, IL-8, IL-6) expression by MCF7 cells cultured in 2D, 3D collagen, 3D mineralized scaffold. Values were normalized with respect to cells cultured in 2D as reference. Data are represented as mean ± S.E.M. (n = 3). *P < 0.05, two-tailed Student's t-test.*

4.7 Osteoclasts' sensitivity to bone targeted therapy is affected by the different secretome.

Then, we evaluated whether and how osteoclast differentiation process induced by breast cancer cells secreted factors can be altered by bone targeted therapy. Secreted factors were collected from conditioned medium of breast cancer cells cultured in the three different models (2D plates, 3D collagen-scaffold and 3D mineralized scaffold) and then PBMCs were induced to differentiate for 15 days. Zoledronic Acid and Denosumab were administered at 8 days of the differentiation process since their action is predominantly in the late phase of osteoclasts differentiation. When osteoclasts are differentiated by soluble factors secreted by ER- cell line MDA-MB-231, cultured in 3D mineralized scaffold, mature osteoclasts differentiation is inhibited by Denosumab (RANKL inhibitor) treatment for 90% compared to the respective control and by Zoledronic Acid by 30% (Fig. 8A). Instead, when osteoclasts are differentiated by ER- SCP2 3D mineralized scaffold secreted factors, bone targeted therapy is less effective, and the difference in Zol treatment, compared to the respective control, is not significant (Fig. 8B). When osteoclasts are differentiated by soluble factors of SCP2 cultured in 2D or in 3D collagen scaffold, cells are more sensitive to treatment. Meanwhile, when osteoclasts are differentiated by ER+ MCF7 3D mineralized scaffold soluble factors, osteoclastogenesis is inhibited by Denosumab for 50% and by Zoledronic Acid for nearly 90% (Fig. 8C).

Fig.8 Osteoclasts' sensitivity to Bone Targeted Therapy is affected by the different secretome.

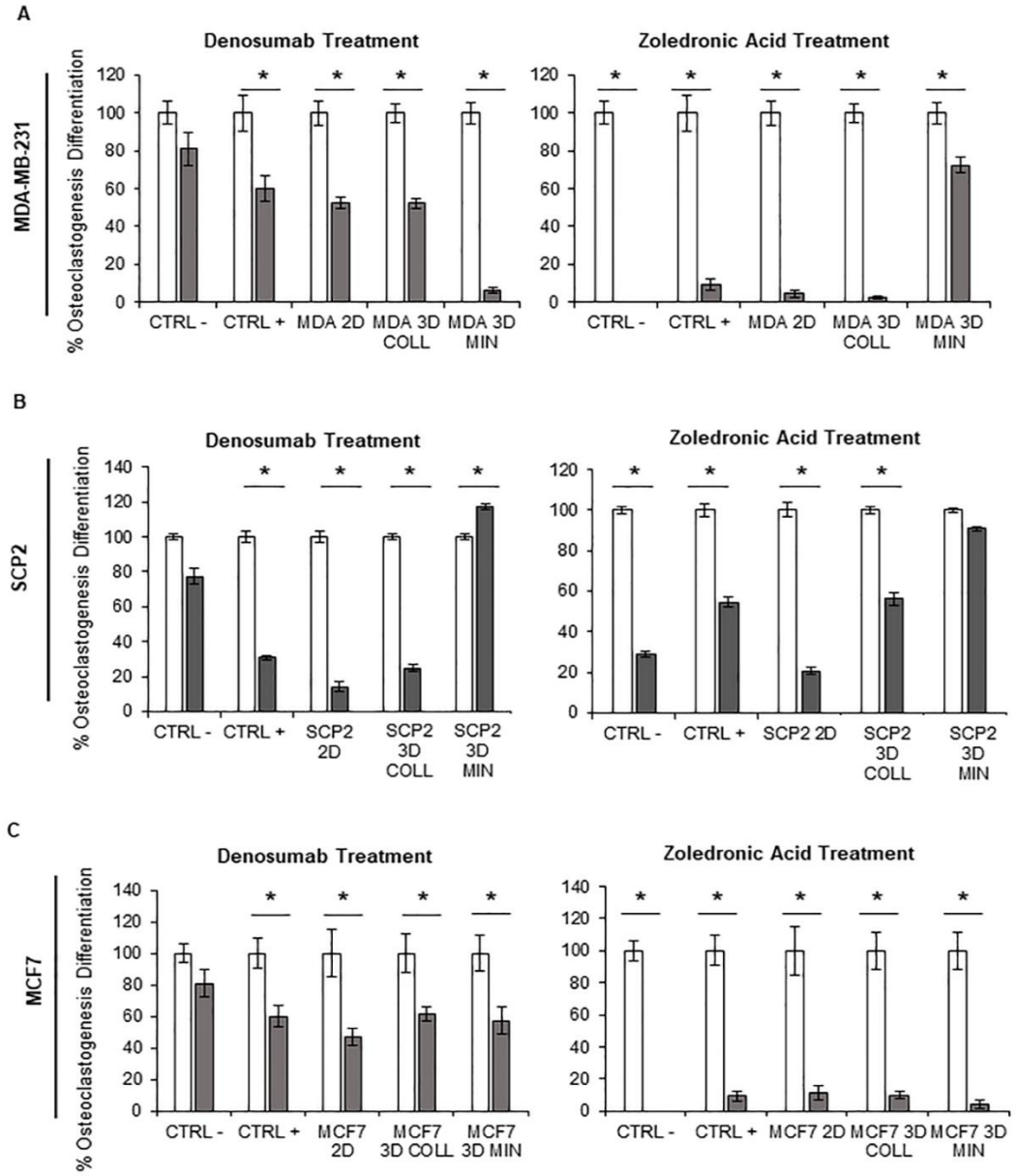

Fig.8 Osteoclasts' sensitivity to Bone Targeted Therapy is affected by the different secretome*. A) Percentage of osteoclasts differentiation induced by MDA-MB-231 conditioned medium, normalized with respect to the untreated condition. Differentiated osteoclasts were identified as cells positive to TRAP staining and with more than 4 nuclei. Significance was related to the untreated condition (*P<0.05, two-tailed Student's t-test.). B) Percentage of osteoclasts differentiation induced by SCP2 conditioned medium, normalized with respect to the untreated condition. Differentiated osteoclasts were identified as cells positive to TRAP staining and with more than 4 nuclei. Significance was related to the untreated condition (*P<0.05, two-tailed Student's t-test). C) Percentage of osteoclasts differentiation induced by MCF7 conditioned medium, normalized with respect to the untreated condition. Differentiated osteoclasts were identified as cells positive to TRAP staining and with more than 4 nuclei. Significance was related to the untreated condition (*P<0.05, two-tailed Student's t-test).*

4.8 Recreating bone metastatic niche with breast cancer cells and osteoclasts co-culture

Next, aiming to recreate the bone metastatic niche, we improved our model to enable the study of the mutual crosstalk between breast cancer cells and osteoclasts. Hence, we recreate a direct interaction between breast cancer cells and osteoclasts in the 3D mineralized scaffold and we evaluated the mutual affection between tumor cells and osteoclasts by gene expression and confocal analysis. To evaluate the gene expression of the two different cell lineages, since our technical limitation in cell sorting, we settled an indirect co-culture in two different scaffolds, placed in the same well. In this way, cells shared the same medium, and they were mutually conditioned in their growth throughout the 15 days of culture. For confocal analysis, a direct co-culture in the same scaffold was performed. Osteoclasts differentiated by MDA-MB-231 cells showed a significant upregulation of the following osteoclasts markers gene: CA2, OSCAR, RANK whereas a downregulation of ACP5, CTSK and CALCR (Fig. 9A). Then, we evaluated in breast cancer cells the modulation of osteomimicry markers (Fig. 9B). Interestingly, we showed a significant upregulation of RANKL. Then we detected the acquisition of a more pronounced pro-inflammatory phenotype in MDA-MB-231 in co-culture with osteoclasts, showed by a significant upregulation of TNF-α, IL-6, and IL-8 (Fig. 9C). Moreover, we analyzed cell plasticity markers, involved in the process of Epithelial-Mesenchymal-Transition (EMT), to evaluate how the direct interaction can affect cancer cell behavior. Interestingly, we noted a downregulation of VIM, SNAI1, ZEB1, ZEB2. (Fig. 9D). By confocal analysis, we confirmed the presence of osteoclasts cells (Fig. 9E).

For the ER- cell line SCP2, osteoclasts induced by the direct interaction, showed a significant upregulation of OSCAR, whereas a downregulation of ACP5, CTSK and CALCR (Fig. 10A). Analyzing the gene expression modulation in SCP2 cells, we showed for osteomimicry markers a significant upregulation of RANKL, ACP5 and CXCR4 whereas a downregulation of RANK, JAG1, OPG and LOX (Fig. 10B). Moreover, as for MDA-MB-231, SCP2 cells in co-culture with osteoclasts cells increase the expression of TNF-α, IL-6 and IL-8 (Fig. 10C). For EMT markers, SCP2 cells showed a significant downregulation for most of the markers, except for SNAI2 and ZEB2 whose expression is slightly increased (Fig. 10D). By confocal analysis, we evaluated the close connection between pre-osteoclasts and osteoclasts with SCP2 cells (Fig. 10E).

For ER+ cell line MCF7, osteoclasts showed a significant upregulation of CA2, OSCAR and RANK (Fig. 11A). Meanwhile MCF7 in co-culture with osteoclasts showed a significant higher expression of RANK, RANKL, ACP5, CXCR4 and a significant downregulation of JAG1 and LOX (Fig. 11B). Moreover, MCF7 cells express a pro-inflammatory phenotype as demonstrated by a significant higher expression of TNF-α, IL-6 and IL-8 (Fig. 11C). Interestingly, when evaluating the EMT markers, MCF7 cells in co-culture with osteoclasts shift to a more mesenchymal phenotype, as showed by the significant higher expression of VIM, SNAI2, TWIST1, ZEB1, and ZEB2 (Fig. 11D). This phenotype was also confirmed by confocal analysis, where in MCF7 showed a more mesenchymal spheroid-likes morphology (Fig. 11E).

Fig.9 Recreating Bone Pre-Metastatic and Metastatic Niche with Breast Cancer Cells and Osteoclasts Co-Culture: MDA-MB-231

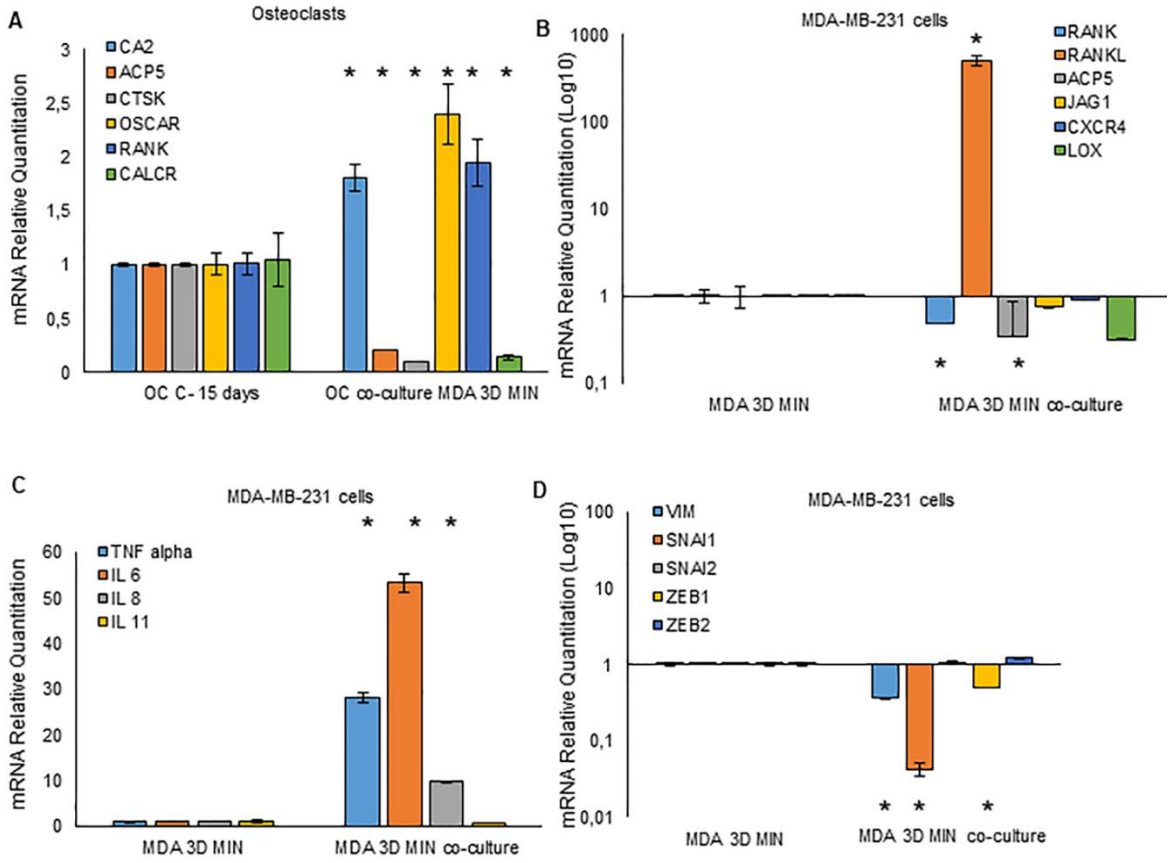

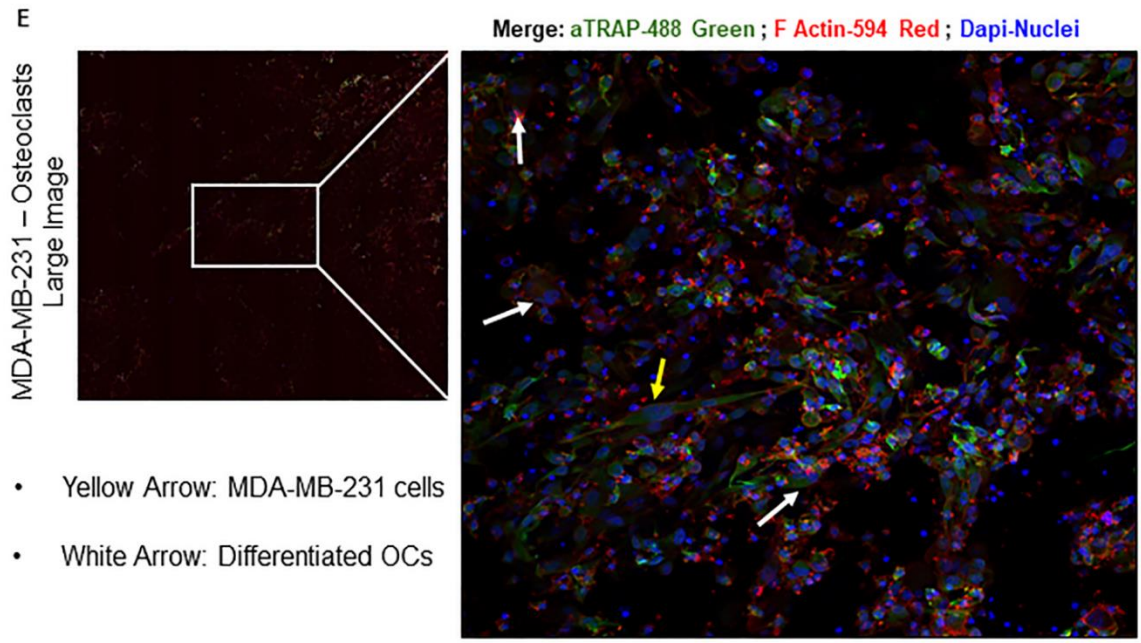

Fig.9 Recreating Bone Pre-Metastatic Niche and Metastatic Niche with Breast Cancer Cells and Osteoclasts Co-Culture: MDA-MB-231*. A) RT–qPCR analysis of osteoclasts markers (CA2, ACP5, CTSK, OSCAR, RANK, CALCR) in PBMCs cells led to differentiate by secreted factors from MDA-MB-231 cells seeded in a 3D mineralized scaffold and placed in the same well for 15 days. This enables cells to share the same medium and cells indirectly interact with secreted soluble factors. Data were normalized with respect to the PBMCs in 3D mineralized scaffold without MDA-MB-231 co-culture. *P<0.05. B) RT–qPCR analysis of selected markers related to aggressiveness and bone metastasis (RANK, RANKL, ACP5, JAG1, CXCR4, LOX) in MDA-MB-231 cells in 3D mineralized scaffold in indirect co-culture with PMBCs for 15 days of differentiation. Data were normalized with respect to MDA-MB-231 cells seeded in 3D mineralized scaffold alone. *P<0.05, two-tailed Student's t-test. C) RT–qPCR analysis of pro-inflammatory cytokines (TNF-alpha, IL-8, IL-6, IL-11) expression by MDA-MB-231 cells in 3D mineralized scaffold. *P<0.05, two-tailed Student's t-test. D) RT–qPCR analysis of EMT markers (VIM, SNAI1, SNAI2, ZEB1, ZEB2) expression by MDA-MB-231 cells in 3D mineralized scaffold in indirect co-culture with PBMCs for 15 days of differentiation. Data were normalized with respect to MDA-MB-231 cells seeded in 3D mineralized scaffold alone and graphed on a logarithmic scale. *P<0.05, two-tailed Student's t-test. E) Confocal analysis after 15 days of differentiation of osteoclasts and MDA-MB-231 cells in direct co-culture in 3D mineralized scaffold. aTRAP-Alexafluor-488 (Green), F-actin Alexafluor-594 (Red), nuclei were counterstained in DAPI.*

Fig.10 Recreating Bone Pre-Metastatic and Metastatic Niche with Breast Cancer Cells and Osteoclasts Co-Culture: SCP2

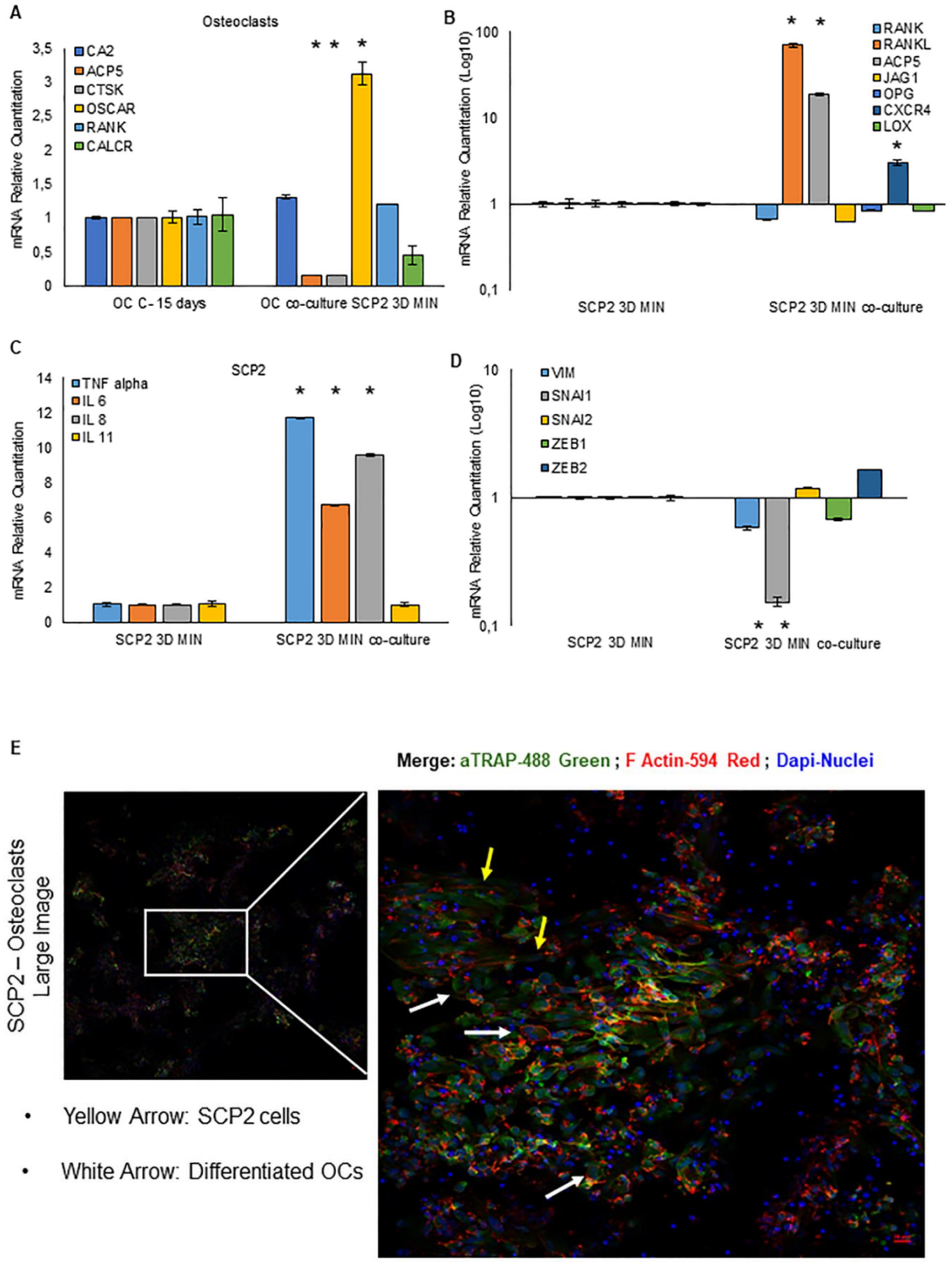

Fig.10 Recreating Bone Pre-Metastatic Niche and Metastatic Niche with Breast Cancer Cells and Osteoclasts Co-Culture: SCP2*. A) RT–qPCR analysis of osteoclasts markers (CA2, ACP5, CTSK, OSCAR, RANK, CALCR) in PBMCs cells led to differentiate by secreted factors from SCP2 cells seeded in a 3D mineralized scaffold and placed in the same well for 15 days. This enables cells to share the same medium and cells indirectly interact with secreted soluble factors. Data were normalized with respect to the PBMCs in 3D mineralized scaffold without SCP2 co-culture. *P<0.05, two-tailed Student's t-test. B) RT–qPCR analysis of selected markers related to aggressiveness and bone metastasis (RANK, RANKL, ACP5, JAG1, CXCR4, LOX) in SCP2 cells in 3D mineralized scaffold in indirect co-culture with PBMCs for 15 days of differentiation. Data were normalized with respect to SCP2 cells seeded in 3D mineralized scaffold alone. *P<0.05, two-tailed Student's t-test. C) RT–qPCR analysis of pro-inflammatory cytokines (TNF-alpha, IL-8, IL-6, IL-11) expression by SCP2 cells in 3D mineralized scaffold. *P < 0.05, two-tailed Student's t-test. D) RT–qPCR analysis of EMT markers (VIM, SNAI1, SNAI2, ZEB1, ZEB2) expression by SCP2 cells in 3D mineralized scaffold in indirect co-culture with PBMCs for 15 days of differentiation. Data were normalized with respect to SCP2 cells seeded in 3D mineralized scaffold alone and graphed on a logarithmic scale. *P<0.05, two-tailed Student's t-test. E) Confocal analysis after 15 days of differentiation of osteoclasts and SCP2 cells in direct co-culture in 3D mineralized scaffold. aTRAP-Alexafluor-488 (Green), F-actin Alexafluor-594 (Red), nuclei were counterstained in DAPI.*

Fig.11 Recreating Bone Pre-Metastatic and Metastatic Niche with Breast Cancer Cells and Osteoclasts Co-Culture: MCF7

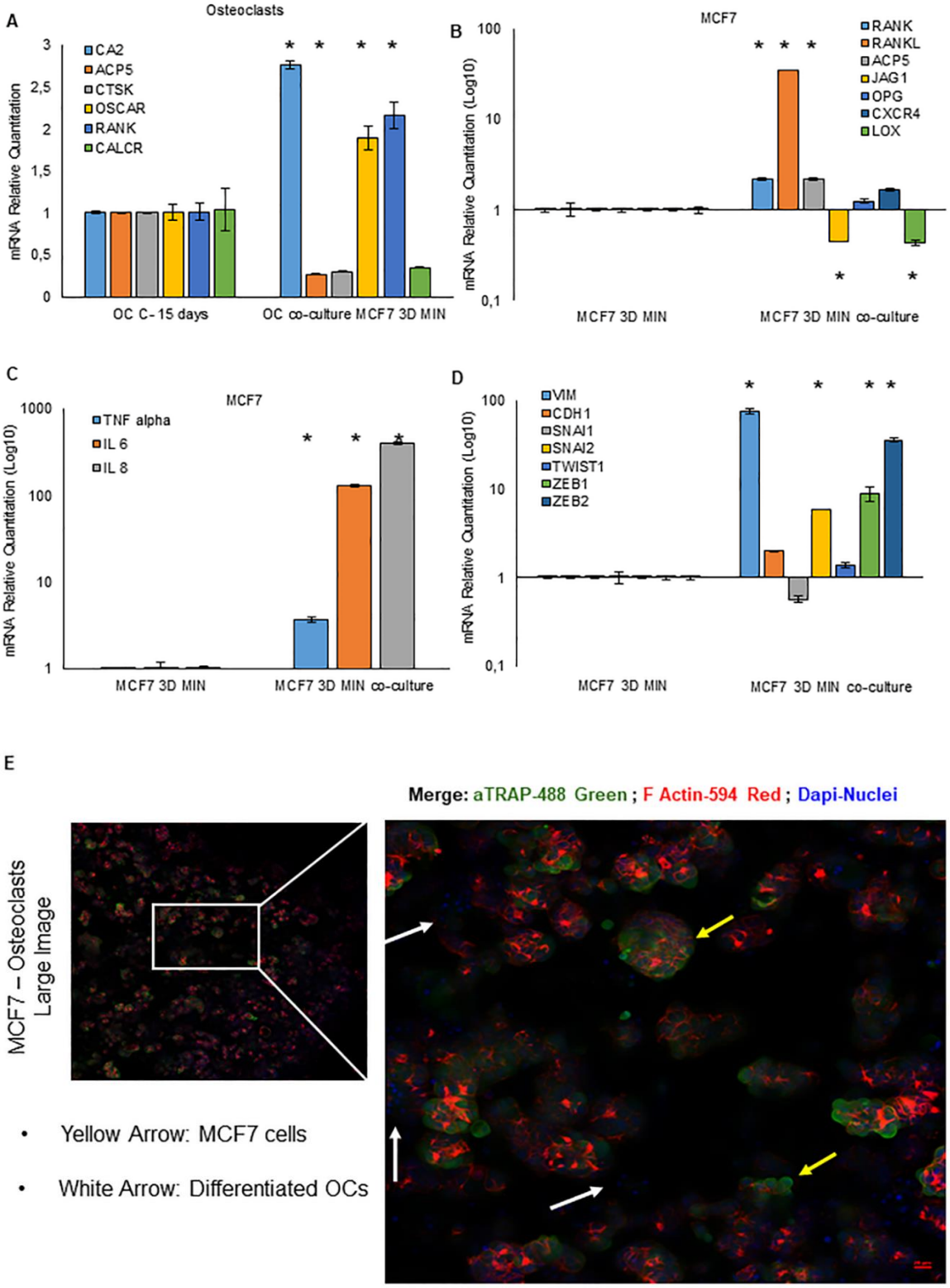

Fig.11 Recreating Bone Pre-Metastatic Niche and Metastatic Niche with Breast Cancer Cells and Osteoclasts Co-Culture: MCF7*. A) RT–qPCR analysis of osteoclasts markers (CA2, ACP5, CTSK, OSCAR, RANK, CALCR) in PBMCs cells led to differentiate by secreted factors from MCF7 cells seeded in a 3D mineralized scaffold and placed in the same well for 15 days. This enables cells to share the same medium and cells indirectly interact with secreted soluble factors. Data were normalized with respect to the PBMCs in 3D mineralized scaffold without MCF7 co-culture. *P<0.05, two-tailed Student's t-test. B) RT–qPCR analysis of selected markers related to aggressiveness and bone metastasis (RANK, RANKL, ACP5, JAG1, CXCR4, LOX) in MCF7cells in 3D mineralized scaffold in indirect co-culture with PBMCs for 15 days of differentiation. Data were normalized with respect to MCF7 cells seeded in 3D mineralized scaffold alone and graphed in a logarithm scale. *P<0.05, two-tailed Student's t-test. C) RT–qPCR analysis of pro-inflammatory cytokines (TNF-alpha, IL-8, IL-6, IL-11) expression by MCF7 cells in 3D mineralized scaffold. *P<0.05, two-tailed Student's t-test. D) RT–qPCR analysis of EMT markers (VIM, CDH1, SNAI1, SNAI2, TWIST1, ZEB1, ZEB2) expression by MCF7 cells in 3D mineralized scaffold in indirect co-culture with PBMCs for 15 days of differentiation. Data were normalized with respect to MCF7 cells seeded in 3D mineralized scaffold alone and graphed on a logarithmic scale. *P<0.05, two-tailed Student's t-test. E) Confocal analysis after 15 days of differentiation of osteoclasts and MCF7 cells in direct co-culture in 3D mineralized scaffold. aTRAP-Alexafluor-488 (Green), F-actin Alexafluor-594 (Red), nuclei were counterstained in DAPI.*

5. Discussion

Nowadays, it is well known that bone metastasis from breast cancer is the result not only of the genetic intrinsic features of breast cancer cells and their propensity to bone site, as postulated by Stephen Paget in the "Seed and Soil hypothesis"[203]. Indeed, this hypothesis should be revisited and implemented with the critical role played by the soil microenvironment, comprising bone resident cells and the extracellular matrix[44]. Hence, in this project, we aimed to develop a three-dimensional *in vitro* model able to mimic, more similarly to the *in vivo* condition, the "vicious cycle" of bone metastasis from breast carcinoma. Indeed, meanwhile two-dimensional models (2D) are a useful and suitable way to study the molecular interactions between breast cancer and bone cells in the establishment of bone metastasis, it lacks key features related to bone metastasis progression, such as microenvironment context of the tumor. With a step-by-step project, we aimed to highlight the mechanisms involved in the establishment of the pre-metastatic niche and bone metastasis, leading to the opportunity to identify new therapeutic and diagnostic strategies to block the metastatic spread at an early stage. Since the bone microenvironment is defined by a composite matrix that consists primarily of organic collagen and inorganic mineral, we developed a bone biomimetic bovine collagen scaffold functionalized with hydroxyapatite material (HA, mineralized scaffold) able to mimic the composition of the bone matrix *in vitro*. Indeed, the inorganic component of bone is primarily composed of the mineral hydroxyapatite (HA), a crystalline calcium phosphate phase with the molecular formula Ca5(PO4)3(OH)[204]. This is largely known for its role in modulating structural and mechanical properties to bone, but it also functions as a bioactive material that directly regulates the behavior of both normal and cancer cells[205,206]. Indeed, it has been demonstrated that the stiffness properties of the extracellular matrix (ECM) can affect cancer cells behavior and aggressiveness[94,95]. Interestingly, it has been recently demonstrated that primary tumor stiffness can modulate breast cancer cells' bone metastatic potential by the induction of an osteolytic phenotype, which can be maintained during cancer dissemination as "mechanical memory"[207]. However, the impact of mineralized-ECM and its stiffness in the crosstalk between bone and breast cancer cells in the establishment of bone metastasis is still not well understood. Hence, the 3D mineralized scaffold developed in our project, represented the culture system for the optimization of osteoclasts and osteoblasts differentiation from PBMCs and mesenchymal stem cells, respectively. Indeed, we demonstrated that this platform is suitable for the culture and differentiation of PBMCs in osteoclasts cells. For the optimization, we needed to define the concentration of PBMCs seeded in the scaffold and of

the soluble factors M-CSF and RANKL to induce an optimal differentiation. We defined respectively 20x10^6 cells for each scaffold and 100ng/ml as the concentration needed to successfully induce their differentiation in a period of 15 days. In order to confirm their differentiation, we evaluated by gene expression the modulation of osteoclasts markers verifying that at 10 days of differentiation cells display a higher gene expression of *JDP2* transcription factor and the modulation of *ACP5*, gene which transcribe for the TRAP (Tartrate-resistant acid phosphatase) protein, a metallo-phospho-esterase participating in osteoclast-mediated bone turnover typically expressed by mature osteoclasts, and *CTSK* (cathepsin K), gene encoding a lysosomal cysteine proteinase involved in bone remodeling and resorption. At 15 days of differentiation, osteoclasts expressed at higher level the transcription factor *NFATC1*, which regulates the expression of osteoclasts related markers, the osteoclast-associated receptor (*OSCAR*), which is a member of the leukocyte receptor complex protein family that plays critical roles in the regulation of both innate and adaptive immune responses and of *RANK* gene, coding for the RANK receptor, essential mediator of osteoclasts development by their direct interaction with the soluble factor RANKL (receptor activator of nuclear factor-κB ligand), usually expressed by osteoblasts and other stromal cells in the bone environment. Surprisingly, at 15 days of differentiation, osteoclasts expressed lower gene level of *ACP5* and *CTSK*. However, TRAP protein expression by osteoclasts cells was confirmed by immunofluorescence imaging. We next attempt to optimize the differentiation of mature osteoblasts from human mesenchymal stem cells. The issue to maintain and grow mesenchymal stem cells hampered this optimization. However, we confirmed that the model is suitable for the attachment and differentiation of MSCs into mature osteoblasts, throughout a differentiation period of 14 days. In parallel with the optimization of bone cells cultured in the 3D mineralized scaffold, to mimic the bone metastatic niche of breast cancer metastasis, we investigated how the 3D mineralized scaffold extracellular matrix can affect the cell growth dynamics, genetic and phenotypic features of breast cancer cell lines. Indeed, it has been demonstrated that mechanical features of ECM, like the matrix stiffness can significantly affect breast cancer cells behavior[94,207]. Moreover, supporting the evidence that ECM of the distant organ can affect tumor cell behavior in metastasis, it has been recently demonstrated that the bone microenvironment drives breast and prostate cancer cells to further metastasize and form multi-organ metastasis[208,209]. This mechanism is driven by epigenetic reprogramming than confers stem-like properties on disseminated cancer cells[210].

In this work, we evaluated three cell lines, with different molecular patterns and clinical behavior. The MDA-MB-231, a triple negative breast cancer cell line, highly aggressive,

invasive and poorly differentiated; the SCP2 cell line, a bone-tropic subclone of the MDA-MB-231, *in vivo* selected[51]; and the MCF7 cell line, a luminal A breast cancer cell line with a less aggressive and more differentiated phenotype, and with less propensity for migration. From a clinical point of view, different molecular subtypes exhibited differences in the prevalence of different metastatic sites and number of metastases. Indeed, despite the less aggressive phenotype and less propensity for migration compared to other breast cancer subtypes, hormone receptor-positive tumors show a predilection for bones as the first site of relapse compared to hormone-receptor-negative tumors which have a propensity to develop as visceral metastases[211,212]. Moreover, ER+ tumors may recur in distant organs years later after the primary tumor diagnosis, remaining dormant in the bone for a prolonged period, despite adjuvant therapies.

Then, we assessed the morphology and growth rate of the three breast cancer cell lines in the collagen-based scaffold, which mimic more closely the key features of the ECM of breast cancer primary tumor[200] compared to the newly synthetized 3D mineralized scaffold, mimicking more closely the key features of bone-ECM. Interestingly, meanwhile cancer cells do not assume a different morphology in the two different ECM-based scaffolds, the proliferative capacity for MDA-MB-231, SCP2 and MCF7 cells is decreased in the presence of HA. This is in contrast from previous published results[206]; however, a possible explanation could be the different cell concentration seeded and the scaffold composition. Indeed, the more compacted structure of the mineralized-scaffold compared to the collagen-based scaffold could provide resistance to breast cancer cells expansion and growth. However, for all the three cell lines tested, the exponential phase of growth is from 72h of culture to 7 days. For this reason, we evaluated the gene expression modulation of breast cancer cell lines at these two time points.

To evaluate how bone-ECM affects breast cancer behavior in the progression to bone metastasis, we evaluated the gene modulation of osteomimicry and aggressiveness markers. Indeed, in bone metastases, the interaction with the host organ is much more favored if tumor cells gain “osteomimicry”, that is the ability to resemble a resident bone cell, thus intruding in the physiology of the bone[101]. Meanwhile MCF7 cells do not seem to modulate significantly genes related to the osteomimicry process when cultured in the 3D mineralized scaffold, MDA-MB-231 and SCP2 cells at 72h significantly upregulated *CXCR4* and *JAG1*, two genes strictly related to the bone metastatic process. Indeed, CXCR4 is involved in in the CXCR4-CXCL12 axis which plays a role in the metastatic spread of breast cancer cells to the bone, moreover it has been demonstrated that CXCR4 is more likely to be expressed in bone metastases than visceral metastases[213] and it is upregulated in breast cancer that more likely metastasizes to

bone[102]. JAG1 is the Notch ligand, associated with breast cancer bone metastasis, it has been demonstrated that Jagged1-Notch signaling facilitates communication between tumor cells and the bone microenvironment to promote metastasis[137]. Indeed, it has been previously demonstrated that JAG1 is significantly upregulated in aggressive bone-tropic sublines, compared the weakly metastatic ones, in MDA-MB-231[137]. Another interesting result which underlines the difference between the triple negative cell lines (MDA-MB-231) and the Luminal A (MCF7) cell line in their adaptation to the bone-ECM is the different modulation of the *LOX* gene. LOX is an aggressiveness marker, which could be upregulated by hypoxia condition, and it acts as a collagen-crosslinker[214]. Moreover, in ER- breast cancer can drive pre-metastatic niche formation and alter ECM composition[160]. Here, it seems to be downregulated by MDA-MB-231 and SCP2 cell lines, meanwhile it is upregulated in MCF7 cell line in the presence of HA. It would be interesting to evaluate and confirm in clinical samples whether LOX gene is differently express in cancer cells that reside in primary tumor versus cancer cells in the bone metastatic site.

Next, we evaluated whether ECM could affect breast cancer cells sensitivity to bone targeted drugs (Zoledronic Acid and Denosumab). Indeed, we hypothesize that if breast cancer cells can acquire an osteomimetic phenotype, they could be affected differently by the action of bone targeted drugs. MDA-MB-231 and SCP2 cells are sensitive to Zoledronic Acid when cultured in 2D model and in the 3D mineralized scaffold. SCP2 cells when cultured in 3D mineralized scaffold are more sensitive also to Denosumab treatment. Instead, when they are cultured in 3D collagen-based scaffold, they seem more resistant to both treatments. Instead, the ER+ breast cancer cell line, MCF7, when cultured in the 3D mineralized scaffold is more sensitive to Zoledronic Acid compared to two-dimensional model and 3D collagen-based scaffold. This could suggest that different bone-ECM can affect breast cancer sensitivity to bone targeted drugs, in particular to Zoledronic Acid. The more sensitivity of breast cancer cells to Zoledronic Acid when cultured in the 3D mineralized scaffold, could be in part explained by the strong affinity of bisphosphonate for hydroxyapatite[215,216], that could increase the absorption of the drug by breast cancer cells, resulting in possibly apoptosis. Moreover, these results agree with previous *in vivo* studies in which ibandronate treatment decreased MDA-MB-231 tumor burden at the bone site, but not in the mammary fat pad[217]. Thus, this could better mimic the *in vivo* condition and the sensitivity to the drug by breast cancer cell lines.

Next, to assess a potential role of HA in the osteolytic phenotype of bone metastases, osteoclastogenesis was evaluated in response to conditioned medium. Indeed, tumor-derived soluble factors shift the balance between bone formation and bone degradation towards

osteolysis and our results indicate that HA is strongly implicated in this process. Thus, breast cancer cells, when cultured in the 3D mineralized scaffold, secrete soluble factors able to induce indirectly the differentiation of PBMCs in mature osteoclasts in a significant manner compared to when cultured in 2D. Since RANKL, which is the critical soluble factor which induce the differentiation of pre-osteoclasts into mature osteoclasts, does not seem differentially expressed by breast cancer cells cultured in the different environment, evaluating the secreted factors differentially expressed by breast cancer cells we showed a significant upregulation of TNF-α. TNF-α is a stimulator of osteoclastogenesis and plays an essential role in the regulation of bone homeostasis[218]. Interestingly, it has been found that RANKL and TNF-α can synergize to promote the differentiation of osteoclasts from precursor cells, increasing the activation of NF-kB and AP1 signaling[219,220]. However, mechanisms independent of the RANK-RANKL interaction for TNF-α induced osteoclastogenesis have also been identified *in vitro* and *in vivo*[221].

Then, we evaluated the sensitivity to bone targeted drugs of osteoclasts induced by tumor-cell derived factors. Interestingly for SCP2 cells cultured in presence of HA we showed that secreted factors can protect osteoclasts from the bone targeted treatment. This suggest that when breast cancer cells establish an interaction with bone cells, can support and protect them from the treatment. In part, this could be explained by TNF-α, which is expressed at higher level in SCP2 cells cultured in 3D mineralized scaffold. Indeed, TNF-α not solely can support osteoclasts differentiation, reducing consequently the effect of Denosumab treatment, but there are also evidences that it could support the survival of osteoclasts reducing their apoptosis, which is the main mechanism of action of Zoledronic Acid[222]. However, this effect could be cell-line and context-dependent since we did not confirm it for MDA-MB-231 and MCF7 cells.

Finally, to mimic the bone metastatic niche, we developed a model of direct co-culture of osteoclasts and tumor cells in the 3D mineralized scaffold. We then demonstrated the ability of tumor cells to induce osteoclasts differentiation of PBMCs by gene expression modulation of osteoclasts markers and by immunofluorescence of osteoclasts markers. Interestingly, when tumor cells are co-cultured directly with osteoclasts in the 3D bone-environment, they are critically affected. Indeed, all the three cell lines acquire a more pronounced pro-inflammatory phenotype, with a significant gene upregulation of different inflammatory cytokines (TNF-α, IL-6, IL-8). Moreover, meanwhile MDA-MB-231 and SCP2 cell lines acquire a more osteomimetic and epithelial-like phenotype, MCF7 cells seem to acquire an EMT-hybrid like phenotype. This demonstrated the phenotypic plasticity of breast cancer cell lines acquired in

the 3D environment and in co-culture with osteoclasts. The mechanisms underline this phenotypic plasticity still need to be clarified and will be next investigated.

6. Conclusion

In conclusion, with this project we demonstrated that the mineral matrix of the bone microenvironment could regulate the pathological bone remodeling associated with breast cancer bone metastasis. For this reason, it is strictly important to model *in vitro* the crosstalk between breast cancer and bone cells in a 3D biomimetic model to better characterize the molecular mechanisms underline this process, and to identify new therapeutic and more effective strategies to inhibit bone metastasis. Our model needs to be implemented with the tri co-culture of osteoclasts, osteoblasts, and tumor cells. Moreover, it would need to be confirmed with patients' clinical samples to increase its translational value. However, it is a first step in the development of an *in vitro* 3D biomimetic model of bone metastasis. This would enable the study and a more comprehensive delineation of the natural history of breast cancer bone metastasis, from the primary tumor to the formation of the pre-metastatic niche, till the establishment of the bone metastasis, focusing on the interaction between the extracellular matrix, tumor and bone cells.

7. Bibliography

1. Breast cancer. https://www.who.int/news-room/fact-sheets/detail/breast-cancer.

2. Amin, M. B. *et al.* The Eighth Edition AJCC Cancer Staging Manual: Continuing to build a bridge from a population-based to a more 'personalized' approach to cancer staging. *CA Cancer J Clin.* **67**, 93–99 (2017).

3. Gomes Do Nascimento, R. & Otoni, K. M. Histological and molecular classification of breast cancer: what do we know? *Mastology.* **30**, e20200024 (2020).

4. Cserni, G. Histological type and typing of breast carcinomas and the WHO classification changes over time. *Pathologica.* **112**, 25–41 (2020).

5. Tan, P. H. *et al.* The 2019 World Health Organization classification of tumours of the breast. *Histopathology.* **77**, 181–185 (2020).

6. Lacroix-Triki, M. & Roussy, G. New breast cancer classification: traditional pathology and molecular subtypes. *ESMO preceptorship on breast cancer*. (2020).

7. Harbeck, N. *et al.* Breast cancer. *Nat Rev Dis Prim.* **5**, 1–31 (2019).

8. Goldhirsch, A. *et al.* Personalizing the treatment of women with early breast cancer: highlights of the St Gallen International Expert Consensus on the Primary Therapy of Early Breast Cancer 2013. *Ann Oncol.* **24**, 2206–2223 (2013).

9. Gao, J. J. & Swain, S. M. Luminal A Breast Cancer and Molecular Assays: A Review. *Oncologist.* **23**, 556–565 (2018).

10. Parker, J. S. *et al.* Supervised risk predictor of breast cancer based on intrinsic subtypes. *J Clin Oncol.* **27**, 1160–1167 (2009).

11. Paik, S. *et al.* A Multigene Assay to Predict Recurrence of Tamoxifen-Treated, Node-Negative Breast Cancer. *N Engl J Med.* **351**, 2817–2826 (2004).

12. Van de Vijver, M. J. *et al.* A gene-expression signature as a predictor of survival in breast cancer. *N Engl J Med.* **347**, 1999–2009 (2002).

13. Anderson, W. F., Jatoi, I. & Devesa, S. S. Distinct breast cancer incidence and prognostic patterns in the NCI's SEER program: Suggesting a possible link between etiology and outcome. *Breast Cancer Res. Treat.* **90**, 127–137 (2005).

14. Cardoso, F. *et al.* Early breast cancer: ESMO Clinical Practice Guidelines for diagnosis, treatment and follow-up†. *Ann Oncol.* **30**, 1194–1220 (2019).

15. Korde, L. A. *et al.* Neoadjuvant Chemotherapy, Endocrine Therapy, and Targeted Therapy for Breast Cancer: ASCO Guideline. *J Clin Oncol.* **39**, 1485–1505 (2021).

16. Fisher, B. *et al.* Effect of preoperative chemotherapy on local-regional disease in women with operable breast cancer: findings from National Surgical Adjuvant Breast and Bowel Project B-18. *J Clin Oncol.* **15**, 2483–93 (1997).

17. Bear, H. D. *et al.* The effect on tumor response of adding sequential preoperative docetaxel to preoperative doxorubicin and cyclophosphamide: preliminary results from National Surgical Adjuvant Breast and Bowel Project Protocol B-27. *J Clin Oncol.* **21**, 4165–4174 (2003).

18. Golshan, M. *et al.* Breast Conservation After Neoadjuvant Chemotherapy for Triple-Negative Breast Cancer: Surgical Results From the BrighTNess Randomized Clinical Trial. *JAMA Surg.* **155**, e195410–e195410 (2020).

19. Spring, L. M. *et al.* Neoadjuvant Endocrine Therapy for Estrogen Receptor-Positive Breast Cancer: A Systematic Review and Meta-analysis. *JAMA Oncol.* **2**, 1477–1486 (2016).

20. Yersal, O. & Barutca, S. Biological subtypes of breast cancer: Prognostic and therapeutic implications. *World J Clin Oncol.* **5**, 412–424 (2014).

21. Cain, H. *et al.* Neoadjuvant Therapy in Early Breast Cancer: Treatment Considerations and Common Debates in Practice. *Clin Oncol (R Coll Radiol).* **29**, 642–652 (2017).

22. Foukakis, T. Carboplatin in the neoadjuvant treatment of triple-negative breast cancer—ready for prime time? *Ann Oncol.* **29**, 2278–2280 (2018).

23. Tan, W., Yang, M., Yang, H., Zhou, F. & Shen, W. Predicting the response to neoadjuvant therapy for early-stage breast cancer: tumor-, blood-, and imaging-related biomarkers. *Cancer Manag Res.* **10**, 4333 (2018).

24. Cordoba, O., Carrillo-Guivernau, L. & Reyero-Fernández, C. Surgical Management of Breast Cancer Treated with Neoadjuvant Therapy. *Breast Care.* **13**, 238–243 (2018).

25. Clarke, M. *et al.* Effects of radiotherapy and of differences in the extent of surgery for early breast cancer on local recurrence and 15-year survival: an overview of the randomised trials. *Lancet.* **366**, 2087–2106 (2005).

26. Cardoso, F. *et al.* 5th ESO-ESMO international consensus guidelines for advanced breast cancer (ABC 5). *Ann Oncol.* **31**, 1623–1649 (2020).

27. Bonadonna, G. *et al.* 30 years' follow up of randomised studies of adjuvant CMF in operable breast cancer: cohort study. *BMJ.* **330**, 217–220 (2005).

28. Martin, M. & López-Tarruella, S. Emerging Therapeutic Options for HER2-Positive Breast Cancer. *Am Soc Clin Oncol Educ Book.* **35**, e64-70 (2016).

29. Gao, H. F. *et al.* Adjuvant CDK4/6 inhibitors combined with endocrine therapy in HR-positive, HER2-negative early breast cancer: A meta-analysis of randomized clinical trials. *Breast.* **59**, 165–175 (2021).

30. Burstein, H. J. *et al.* Neratinib, an irreversible ErbB receptor tyrosine kinase inhibitor, in patients with advanced ErbB2-positive breast cancer. *J Clin Oncol.* **28**, 1301–1307 (2010).

31. Peoples, G. E. *et al.* Clinical trial results of a HER2/neu (E75) vaccine to prevent recurrence in high-risk breast cancer patients. *J Clin Oncol.* **23**, 7536–7545 (2005).

32. Salemme, V., Centonze, G., Cavallo, F., Defilippi, P. & Conti, L. The Crosstalk Between Tumor Cells and the Immune Microenvironment in Breast Cancer: Implications for Immunotherapy. *Front Oncol.* **11**, 610303 (2021).

33. Barzaman, K. *et al.* Breast cancer immunotherapy: Current and novel approaches. *Int Immunopharmacol.* **98**, 107886 (2021).

34. Lan, H. R. *et al.* Role of immune regulatory cells in breast cancer: Foe or friend? *Int Immunopharmacol.* **96**, 107627 (2021).

35. Issam, M., Mohammad, A., Ahmed, A. & Kieber-Emmons, T. Breast Cancer Immunotherapy: An Update. *Breast Cancer Basic Clin Res.* **12**, 1–15 (2018).

36. Thomas, R., Al-Khadairi, G. & Decock, J. Immune Checkpoint Inhibitors in Triple Negative Breast Cancer Treatment: Promising Future Prospects. *Front Oncol.* **10**, 600573 (2021).

37. Loi, S. *et al.* Pembrolizumab plus trastuzumab in trastuzumab-resistant, advanced, HER2-positive breast cancer (PANACEA): a single-arm, multicentre, phase 1b–2 trial. *Lancet Oncol.* **20**, 371–382 (2019).

38. Bindal, P., Gray, J. E., Boyle, T. A., Florou, V. & Puri, S. Biomarkers of therapeutic response with immune checkpoint inhibitors. *Ann Transl Med.* **9**, 1040 (2021).

39. Zhu, Y., Zhu, X., Tang, C., Guan, X. & Zhang, W. Progress and challenges of immunotherapy in triple-negative breast cancer. *Biochim Biophys Acta Rev Cancer.* **1876**, 188593 (2021).

40. Strickler, J. H., Hanks, B. A. & Khasraw, M. Tumor Mutational Burden as a Predictor of Immunotherapy Response: Is More Always Better? *Clin Cancer Res.* **27**, 1236–1241 (2021).

41. Singh, K., Yadav, D., Jain, M., Singh, P. K. & Jin, J. O. Immunotherapy for the Breast Cancer treatment: Current Evidence and Therapeutic Options. *Endocr Metab Immune Disord Drug Targets.* (2021)

42. Schmidts, A. & Maus, M. V. Making CAR T Cells a Solid Option for Solid Tumors. *Front Immunol.* **9**, 2593 (2018).

43. Zhao, Z. *et al.* Chimeric antigen receptor T cells in solid tumors: a war against the tumor microenvironment. *Sci China Life Sci.* **63**, 180–205 (2020).

44. Fidler, I. J. The pathogenesis of cancer metastasis: the 'seed and soil' hypothesis revisited. *Nat Rev Cancer.* **3**, 453–458 (2003).

45. Kang, Y. & Pantel, K. Tumor cell dissemination: emerging biological insights from animal models and cancer patients. *Cancer Cell.* **23**, 573–81 (2013).

46. Zhang, X. H. F. *et al.* Selection of Bone Metastasis Seeds by Mesenchymal Signals in the Primary Tumor Stroma. *Cell.* **154**, 1060 (2013).

47. Kennecke, H. *et al.* Metastatic behavior of breast cancer subtypes. *J Clin Oncol.* **28**,

3271–3277 (2010).

48. Wang, R. *et al.* The Clinicopathological features and survival outcomes of patients with different metastatic sites in stage IV breast cancer. *BMC Cancer.* **19**, 1091 (2019).

49. Coleman, R. *et al.* Bone metastases. *Nat Rev Dis Prim.* **6**, 83 (2020).

50. Coleman, R. *et al.* Bone health in cancer: ESMO Clinical Practice Guidelines. *Ann Oncol.* **31**, 1650–1663 (2020).

51. Kang, Y. *et al.* A multigenic program mediating breast cancer metastasis to bone. *Cancer Cell.* **3**, 537–549 (2003).

52. Spadazzi, C. *et al.* Trefoil factor-1 upregulation in estrogen-receptor positive breast cancer correlates with an increased risk of bone metastasis. *Bone.* **144**, 115775 (2021).

53. Pantano, F. *et al.* Integrin alpha5 in human breast cancer is a mediator of bone metastasis and a therapeutic target for the treatment of osteolytic lesions. *Oncogene.* **40**, 1284–1299 (2021).

54. Clarke, B. Normal bone anatomy and physiology. *Clin J Am Soc Nephrol.* **3**, S131-9 (2008).

55. Florencio-Silva, R., Sasso, G. R., Sasso-Cerri, E., Simões, M. J. & Cerri, P. S. Biology of Bone Tissue: Structure, Function, and Factors That Influence Bone Cells. *Biomed Res Int.* **2015**, 421746 (2015).

56. Tanaka, Y., Nakayamada, S. & Okada, Y. Osteoblasts and osteoclasts in bone remodeling and inflammation. *Curr Drug Targets Inflamm Allergy.* **4**, 325–328 (2005).

57. Kular, J., Tickner, J., Man Chim, S. & Xu, J. An overview of the regulation of bone remodelling at the cellular level. *Clin Biochem.* **45**, 863–73 (2012).

58. Rodan, G. A. Bone homeostasis. *Proc Natl Acad Sci U. S. A.* **95**, 13361–13362 (1998).

59. Lerner, U. H., Kindstedt, E. & Lundberg, P. The critical interplay between bone resorbing and bone forming cells. *J Clin Periodontol.* **46**, 33–51 (2019).

60. Föger-Samwald, U., Dovjak, P., Azizi-Semrad, U., Kerschan-Schindl, K. & Pietschmann, P. Osteoporosis: Pathophysiology and therapeutic options. *EXCLI J.* **19**, 1017 (2020).

61. Palagano, E., Menale, C., Sobacchi, C. & Villa, A. Genetics of Osteopetrosis. *Curr Osteoporos Rep.* **16**, 13–25 (2018).

62. Boyden, L. M. *et al.* High Bone Density Due to a Mutation in LDL-Receptor–Related Protein 5. *N Engl J Med* .**346**, 1513–1521 (2009).

63. Teitelbaum, S. L. Bone resorption by osteoclasts. *Science.* **289**, 1504–1508 (2000).

64. Mun, S. H., Park, P. S. U. & Park-Min, K. H. The M-CSF receptor in osteoclasts and beyond. *Exp Mol Med.* **52**, 1239–1254 (2020).

65. Zaidi, M., Blair, H. C., Moonga, B. S., Abe, E. & Huang, C. L. H. Osteoclastogenesis, Bone Resorption, and Osteoclast-Based Therapeutics. *J Bone Miner Res.* **18**, 599–609 (2003).

66. Lacey, D. L. *et al.* Osteoprotegerin ligand is a cytokine that regulates osteoclast differentiation and activation. *Cell.* **93**, 165–176 (1998).

67. Ono, T., Hayashi, M., Sasaki, F. & Nakashima, T. RANKL biology: bone metabolism, the immune system, and beyond. *Inflamm Regen.* **40**, 1–16 (2020).

68. Boyce, B. F. & Xing, L. Functions of RANKL/RANK/OPG in bone modeling and remodeling. *Arch Biochem Biophys.* **473**, 139–46 (2008).

69. Siddiqui, J. A. & Partridge, N. C. Physiological Bone Remodeling: Systemic Regulation and Growth Factor Involvement. *Physiology (Bethesda).* **31**, 233–45 (2016).

70. Weitzmann, M. N. The Role of Inflammatory Cytokines, the RANKL/OPG Axis, and the Immunoskeletal Interface in Physiological Bone Turnover and Osteoporosis. *Scientifica (Cairo).* **2013**, 1–29 (2013).

71. Ten Dijke, P. *et al.* Identification of type I receptors for osteogenic protein-1 and bone morphogenetic protein-4. *J Biol Chem.* **269**, 16985–16988 (1994).

72. Horst, G. V. D., Farih-Sips, H., Löwik, C. W. & Karperien, M. Hedgehog stimulates only osteoblastic differentiation of undifferentiated KS483 cells. *Bone.* **33**, 899–910 (2003).

73. Kato, M. *et al.* Cbfa1-independent decrease in osteoblast proliferation, osteopenia, and persistent embryonic eye vascularization in mice deficient in Lrp5, a Wnt coreceptor. *J Cell Biol.* **157**, 303–14 (2002).

74. Chen, H., Senda, T. & Kubo, K. Y. The osteocyte plays multiple roles in bone remodeling and mineral homeostasis. *Med Mol Morphol.* **48**, 61–68 (2015).

75. Bellido, T. Osteocyte-Driven Bone Remodeling. *Calcif Tissue Int.* **94**, 25–34 (2014).

76. Boskey, A. L. Bone composition: relationship to bone fragility and antiosteoporotic drug effects. *Bonekey Rep.* **2**, 447 (2013).

77. Baylink, D. J., Finkelman, R. D. & Mohan, S. Growth factors to stimulate bone formation. *J. Bone Miner Res.* **8**, S565-72 (1993).

78. Canalis, E., McCarthy, T. & Centrella, M. Growth factors and the regulation of bone remodeling. *J Clin Invest.* **81**, 277–281 (1988).

79. Poste, G. & Fidler, I. J. The pathogenesis of cancer metastasis. *Nature.* **283**, 139–146 (1980).

80. Fidler, I. J. The organ microenvironment and cancer metastasis. *Differentiation.* **70**, 498–505 (2002).

81. Kalluri, R. & Weinberg, R. A. The basics of epithelial-mesenchymal transition. *J Clin*

Invest. **119**, 1420 (2009).

82. Lu, W. & Kang, Y. Epithelial-mesenchymal plasticity in cancer progression and metastasis. *Dev Cell.* **49**, 361–374 (2019).

83. Roche, J. The Epithelial-to-Mesenchymal Transition in Cancer. *Cancers (Basel).* **10**, 52 (2018).

84. Lambert, A. W., Pattabiraman, D. R. & Weinberg, R. A. Emerging Biological Principles of Metastasis. *Cell.* **168**, 670–691 (2017).

85. Thiery, J. P. Epithelial–mesenchymal transitions in tumour progression. *Nat Rev Cancer.* **2**, 442–454 (2002).

86. Kim, D. H. *et al.* Epithelial Mesenchymal Transition in Embryonic Development, Tissue Repair and Cancer: A Comprehensive Overview. *J Clin Med.* **7**, 1 (2018).

87. Yang, J. *et al.* Guidelines and definitions for research on epithelial–mesenchymal transition. *Nat Rev Mol Cell Biol.* **21**, 341–352 (2020).

88. Thiery, J. P. & Sleeman, J. P. Complex networks orchestrate epithelial–mesenchymal transitions. *Nat Rev Mol Cell Biol.* **7**, 131–142 (2006).

89. Craene, B. D. & Berx, G. Regulatory networks defining EMT during cancer initiation and progression. *Nat Rev Cancer.* **13**, 97–110 (2013).

90. Aiello, N. M. *et al.* Metastatic progression is associated with dynamic changes in the local microenvironment. *Nat Commun.* **7**, 12819 (2016).

91. Cheng, J. C. & Leung, P. C. Type I collagen down-regulates E-cadherin expression by increasing PI3KCA in cancer cells. *Cancer Lett.* **304**, 107–116 (2011).

92. Mihalko, E. P. & Brown, A. C. Material Strategies for Modulating Epithelial to Mesenchymal Transitions. *ACS Biomater. Sci. Eng.* **4**, 1149–1161 (2017).

93. Pasini, A. *et al.* Perfusion Flow Enhances Viability and Migratory Phenotype in 3D-Cultured Breast Cancer Cells. *Ann Biomed Eng.* (2021) doi:10.1007/s10439-021-02727-w.

94. Liverani, C. *et al.* Investigating the Mechanobiology of Cancer Cell–ECM Interaction Through Collagen-Based 3D Scaffolds. *Cell Mol Bioeng.* **10**, (2017).

95. Wei, S. C. *et al.* Matrix stiffness drives epithelial-mesenchymal transition and tumour metastasis through a TWIST1-G3BP2 mechanotransduction pathway. *Nat Cell Biol.* **17**, 678–688 (2015).

96. Lamouille, S., Xu, J. & Derynck, R. Molecular mechanisms of epithelial–mesenchymal transition. *Nat Rev Mol Cell Biol.* **15**, 178–96 (2014).

97. Aiello, N. M. & Kang, Y. Context-dependent EMT programs in cancer metastasis. *J Exp Med.* **216**, 1016–1026 (2019).

98. Janiszewska, M., Primi, M. C. & Izard, T. Cell adhesion in cancer: Beyond the migration of single cells. *J Biol Chem.* **295**, 2495–2505 (2020).

99. Santini, D. *et al.* Expression pattern of receptor activator of NFκB (RANK) in a series of primary solid tumors and related bone metastases. *J Cell Physiol.* **226**, 780–784 (2011).

100. Blake, M. L., Tometsko, M., Miller, R., Jones, J. C. & Dougall, W. C. RANK expression on breast cancer cells promotes skeletal metastasis. *Clin Exp Metastasis.* **31**, 233–245 (2014).

101. Rucci, N. & Teti, A. Osteomimicry: How the Seed Grows in the Soil. *Calcif Tissue Int.* **102**, 131–140 (2017).

102. Sacanna, E. *et al.* The role of CXCR4 in the prediction of bone metastases from breast cancer: a pilot study. *Oncology.* **80**, 225–231 (2011).

103. Müller, A. *et al.* Involvement of chemokine receptors in breast cancer metastasis. *Nature.* **410**, 50–56 (2001).

104. Jung, Y. *et al.* Regulation of SDF-1 (CXCL12) production by osteoblasts; a possible mechanism for stem cell homing. *Bone.* **38**, 497–508 (2006).

105. Guo, Y., Hangoc, G., Bian, H., Pelus, L. M. & Broxmeyer, H. E. SDF-1/CXCL12 Enhances Survival and Chemotaxis of Murine Embryonic Stem Cells and Production of Primitive and Definitive Hematopoietic Progenitor Cells. *Stem Cells.* **23**, 1324–1332 (2005).

106. Wang, J., Loberg, R. & Taichman, R. S. The pivotal role of CXCL12 (SDF-1)/CXCR4 axis in bone metastasis. *Cancer Metastasis Rev.* **25**, 573–587 (2006).

107. Carvalho, M. S., Cabral, J. M. S., da Silva, C. L. & Vashishth, D. Bone Matrix Non-Collagenous Proteins in Tissue Engineering: Creating New Bone by Mimicking the Extracellular Matrix. *Polymers (Basel).* **13**, 1095 (2021).

108. Lin, X., Patil, S., Gao, Y. G. & Qian, A. The Bone Extracellular Matrix in Bone Formation and Regeneration. *Front. Pharmacol.* **11**, 757 (2020).

109. Duong, L. T. & Rodan, G. A. Integrin-mediated signaling in the regulation of osteoclast adhesion and activation. *Front Biosci.* **3**, 757–68 (1998).

110. Rolli, M., Fransvea, E., Pilch, J., Saven, A. & Felding-Habermann, B. Activated integrin αvβ3 cooperates with metalloproteinase MMP-9 in regulating migration of metastatic breast cancer cells. *Proc Natl. Acad Sci. U. S. A.* **100**, 9482–9487 (2003).

111. Felding-Habermann, B. *et al.* Integrin activation controls metastasis in human breast cancer. *Proc Natl Acad Sci. U. S. A.* **98**, 1853 (2001).

112. Esposito, M., Guise, T. & Kang, Y. The Biology of Bone Metastasis. *Cold Spring Harb Perspect Med.* **8**, (2018).

113. Banyard, J. & Bielenberg, D. R. The Role of EMT and MET in Cancer Dissemination. *Connect Tissue Res.* **56**, 403–413 (2015).

114. Williams, E. D., Gao, D., Redfern, A. & Thompson, E. W. Controversies around epithelial–mesenchymal plasticity in cancer metastasis. *Nat Rev Cancer.* **19**, 716–732 (2019).

115. Korpal, M., Lee, E. S., Hu, G. & Kang, Y. The miR-200 Family Inhibits Epithelial-Mesenchymal Transition and Cancer Cell Migration by Direct Targeting of E-cadherin Transcriptional Repressors ZEB1 and ZEB2. *J Biol Chem.* **283**, 14910–14914 (2008).

116. Gollavilli, P. N. *et al.* The role of miR-200b/c in balancing EMT and proliferation revealed by an activity reporter. *Oncogene.* **40**, 2309–2322 (2021).

117. Esposito, M. *et al.* Bone vascular niche E-selectin induces mesenchymal-epithelial transition and Wnt activation in cancer cells to promote bone metastasis. *Nat Cell Biol.* **21**, 627–639 (2019).

118. Harjes, U. E-selectin fills two needs for metastasis. *Nat Rev Cancer.* **19**, 301 (2019).

119. Macedo, F. *et al.* Bone Metastases: An Overview. *Oncol Rev.* **11**, 321 (2017).

120. Jinnah, A. H., Zacks, B. C., Gwam, C. U. & Kerr, B. A. Emerging and Established Models of Bone Metastasis. *Cancers (Basel).* **10**, 176 (2018).

121. Suva, L. J., Washam, C., Nicholas, R. W. & Griffin, R. J. Bone metastasis: mechanisms and therapeutic opportunities. *Nat Rev Endocrinol.* **7**, 208–18 (2011).

122. Christenson, R. H. Biochemical markers of bone metabolism: an overview. *Clin Biochem.* **30**, 573–593 (1997).

123. Yin, J. J., Pollock, C. B. & Kelly, K. Mechanisms of cancer metastasis to the bone. *Cell Res.* **15**, 57–62 (2005).

124. Tsuda, E. *et al.* Isolation of a novel cytokine from human fibroblasts that specifically inhibits osteoclastogenesis. *Biochem Biophys Res Commun.* **234**, 137–142 (1997).

125. Udagawa, N. *et al.* Osteoprotegerin produced by osteoblasts is an important regulator in osteoclast development and function. *Endocrinology.* **141**, 3478–3484 (2000).

126. Soki, F. N., Park, S. I. & McCauley, L. K. The multifaceted actions of PTHrP in skeletal metastasis. *Futur Oncol.* **8**, 803–17 (2012).

127. Bouizar, Z., Spyratos, F. & De Vernejoul, M. C. The parathyroid hormone-related protein (PTHrP) gene: Use of downstream TATA promotor and PTHrP 1-139 coding pathways in primary breast cancers vary with the occurrence of bone metastasis. *J Bone Miner Res.* **14**, 406–414 (1999).

128. Boyle, W. J., Simonet, W. S. & Lacey, D. L. Osteoclast differentiation and activation. *Nature.* **423**, 337–342 (2003).

129. Zhang, Y. & Derynck, R. Regulation of Smad signalling by protein associations and signalling crosstalk. *Trends Cell Biol.* **9**, 274–279 (1999).

130. Massagué, J. TGF-beta signal transduction. *Annu Rev Biochem.* **67**, 753–791 (1998).

131. Wu, X. *et al.* RANKL/RANK System-Based Mechanism for Breast Cancer Bone Metastasis and Related Therapeutic Strategies. *Front Cell Dev Biol.* **8**, 76 (2020).

132. Bendre, M. S. *et al.* Interleukin-8 stimulation of osteoclastogenesis and bone resorption is a mechanism for the increased osteolysis of metastatic bone disease. *Bone.* **33**, 28–37 (2003).

133. Coon, D., Gulati, A., Cowan, C. & He, J. The role of cyclooxygenase-2 (COX-2) in inflammatory bone resorption. *J Endod.* **33**, 432–436 (2007).

134. Hiraga, T., Myoui, A., Choi, M. E., Yoshikawa, H. & Yoneda, T. Stimulation of Cyclooxygenase-2 Expression by Bone-Derived Transforming Growth Factor-β Enhances Bone Metastases in Breast Cancer. *Cancer Res.* **66**, 2067–2073 (2006).

135. D'Amico, L. & Roato, I. Cross-talk between T cells and osteoclasts in bone resorption. *Bonekey Rep.* **1**, 82 (2012).

136. Ponzetti, M. & Rucci, N. Updates on Osteoimmunology: What's New on the Cross-Talk Between Bone and Immune System. *Front Endocrinol.* **10**, 236 (2019).

137. Sethi, N., Dai, X., Winter, C. G. & Kang, Y. Tumor-derived Jagged1 Promotes Osteolytic Bone Metastasis of Breast Cancer by Engaging Notch Signaling in Bone Cells. *Cancer Cell.* **19**, 192–205 (2011).

138. Lampreia, F. P., Carmelo, J. G. & Anjos-Afonso, F. Notch Signaling in the Regulation of Hematopoietic Stem Cell. *Curr Stem Cell Reports.* **3**, 202–209 (2017).

139. Li, X. *et al.* Wnt signaling in bone metastasis: mechanisms and therapeutic opportunities. *Life Sci.* **208**, 33–45 (2018).

140. Patel, K. D. & Nguyen, D. X. Condensing and constraining WNT by TGF-β. *Nat Cell Biol.* **23**, 213–214 (2021).

141. Esposito, M. *et al.* TGF-β-induced DACT1 biomolecular condensates repress Wnt signalling to promote bone metastasis. *Nat Cell Biol.* **23**, 257–267 (2021).

142. Fang, J. & Xu, Q. Differences of osteoblastic bone metastases and osteolytic bone metastases in clinical features and molecular characteristics. *Clin Transl Oncol.* **17**, 173–179 (2014).

143. Cecchini, M. G., Wetterwald, A., van der Pluijm, G. & Thalmann, G. N. Molecular and biological mechanisms of bone metastasis. *EAU Updat. Ser.* **3**, 214–226 (2005).

144. Feeley, B. T. *et al.* Influence of BMPs on the formation of osteoblastic lesions in metastatic prostate cancer. *J Bone Miner Res.* **20**, 2189–2199 (2005).

145. Davenport, A. P. *et al.* Endothelin. *Pharmacol Rev.* **68**, 357–418 (2016).

146. Yin, J. J. *et al.* A causal role for endothelin-1 in the pathogenesis of osteoblastic bone metastases. *Proc Natl Acad Sci. U. S. A.* **100**, 10954–10959 (2003).

147. Nelson, J. B. *et al.* New bone formation in an osteoblastic tumor model is increased by

endothelin-1 overexpression and decreased by endothelin A receptor blockade. *Urology.* **53**, 1063–1069 (1999).

148. Tsai, T. L., Wang, B., Squire, M. W., Guo, L. W. & Li, W. . Endothelial cells direct human mesenchymal stem cells for osteo- and chondro-lineage differentiation through endothelin-1 and AKT signaling. *Stem Cell Res. Ther.* **6**, 1–14 (2015).

149. Zilberberg, L. *et al.* Specificity of latent TGF-ß binding protein (LTBP) incorporation into matrix: role of fibrillins and fibronectin. *J Cell. Physiol.* **227**, 3828 (2012).

150. Rabbani, S. A. *et al.* An amino-terminal fragment of urokinase isolated from a prostate cancer cell line (PC-3) is mitogenic for osteoblast-like cells. *Biochem Biophys Res Commun.* **173**, 1058–1064 (1990).

151. Ren, G., Esposito, M. & Kang, Y. Bone metastasis and the metastatic niche. *J Mol Med.* **93**, 1203–12 (2015).

152. Méndez-Ferrer, S. *et al.* Mesenchymal and haematopoietic stem cells form a unique bone marrow niche. *Nature.* **466**, 829–834 (2010).

153. Frenette, P. S., Pinho, S., Lucas, D. & Scheiermann, C. Mesenchymal stem cell: keystone of the hematopoietic stem cell niche and a stepping-stone for regenerative medicine. *Annu Rev Immunol.* **31**, 285–316 (2013).

154. Morrison, S. J. & Scadden, D. T. The bone marrow niche for haematopoietic stem cells. *Nature.* **505**, 327–334 (2014).

155. Weilbaecher, K. N., Guise, T. A. & McCauley, L. K. Cancer to bone: a fatal attraction. *Nat Rev Cancer.* **11**, 411–425 (2011).

156. Doglioni, G., Parik, S. & Fendt, S. M. Interactions in the (Pre)metastatic Niche Support Metastasis Formation. *Front Oncol.* **9**, 219 (2019).

157. Cox, T. R., Gartland, A. & Erler, J. T. The pre-metastatic niche: is metastasis random? *Bonekey Rep.* **1**, 80 (2012).

158. Fares, J., Fares, M. Y., Khachfe, H. H., Salhab, H. A. & Fares, Y. Molecular principles of metastasis: a hallmark of cancer revisited. *Signal Transduct Target Ther.* **5**, 1–17 (2020).

159. Esposito, M. & Kang, Y. Targeting tumor-stromal interactions in bone metastasis. *Pharmacol Ther.* **141**, 222–233 (2014).

160. Erler, J. T. *et al.* Hypoxia-induced lysyl oxidase is a critical mediator of bone marrow cell recruitment to form the premetastatic niche. *Cancer Cell.* **15**, 35–44 (2009).

161. Kolb, A. D. & Bussard, K. M. The Bone Extracellular Matrix as an Ideal Milieu for Cancer Cell Metastases. *Cancers (Basel).* **11**, 1020 (2019).

162. Bonnans, C., Chou, J. & Werb, Z. Remodelling the extracellular matrix in development and disease. *Nat Rev Mol Cell Biol.* **15**, 786–801 (2014).

163. Feng, X. Chemical and Biochemical Basis of Cell-Bone Matrix Interaction in Health and Disease. *Curr Chem Biol.* **3**, 189–196 (2009).

164. Stock, S. R. The Mineral–Collagen Interface in Bone. *Calcif Tissue Int.* **97**, 262 (2015).

165. Poltavets, V., Kochetkova, M., Pitson, S. M. & Samuel, M. The Role of the Extracellular Matrix and Its Molecular and Cellular Regulators in Cancer Cell Plasticity. *Front Oncol.* **8**, 431 (2018).

166. González Díaz, E. C., Sinha, S., Avedian, R. S. & Yang, F. Tissue-engineered 3D models for elucidating primary and metastatic bone cancer progression. *Acta Biomater.* **99**, 18–32 (2019).

167. Hofbauer, L. C. *et al.* Novel approaches to target the microenvironment of bone metastasis. *Nat Rev Clin Oncol.* **18**, 488–505 (2021).

168. Habli, Z., AlChamaa, W., Saab, R., Kadara, H. & Khraiche, M. L. Circulating Tumor Cell Detection Technologies and Clinical Utility: Challenges and Opportunities. *Cancers (Basel).* **12**, 1–30 (2020).

169. Mazel, M. *et al.* Frequent expression of PD-L1 on circulating breast cancer cells. *Mol Oncol.* **9**, 1773–1782 (2015).

170. Rachner, T. D. *et al.* Prognostic Value of RANKL/OPG Serum Levels and Disseminated Tumor Cells in Nonmetastatic Breast Cancer. *Clin Cancer Res.* **25**, 1369–1378 (2019).

171. Mundy, G. R. Metastasis to bone: causes, consequences and therapeutic opportunities. *Nat. Rev. Cancer.* **2**, 584–593 (2002).

172. Clézardin, P. Anti-tumour activity of zoledronic acid. *Cancer Treat. Rev.* **31 Suppl 3**, 1–8 (2005).

173. Reszka, A. A. & Rodan, G. A. Mechanism of action of bisphosphonates. *Curr Osteoporos Rep.* **1**, 45–52 (2003).

174. Mönkkönen, H. *et al.* A new endogenous ATP analog (ApppI) inhibits the mitochondrial adenine nucleotide translocase (ANT) and is responsible for the apoptosis induced by nitrogen-containing bisphosphonates. *Br J Pharmacol.* **147**, 437–445 (2006).

175. Neville-Webbe, H. L. & Coleman, R. E. Bisphosphonates and RANK ligand inhibitors for the treatment and prevention of metastatic bone disease. *Eur J Cancer.* **46**, 1211–1222 (2010).

176. Bosch-Barrera, J., Merajver, S. D., Menéndez, J. A. & Van Poznak, C. Direct antitumour activity of zoledronic acid: preclinical and clinical data. *Clin Transl Oncol.* **13**, 148–155 (2011).

177. Santini, D. *et al.* Mechanisms of disease: Preclinical reports of antineoplastic synergistic action of bisphosphonates. *Nat Clin Pr Oncol.* **3**, 325–338 (2006).

178. Haider, M. T., Holen, I., Dear, T. N., Hunter, K. & Brown, H. K. Modifying the osteoblastic niche with zoledronic acid in vivo—Potential implications for breast cancer

bone metastasis. *Bone* **66**, 240–250 (2014).

179. Rogers, T. L. & Holen, I. Tumour macrophages as potential targets of bisphosphonates. *J Transl Med.* **9**, 1–17 (2011).

180. Carrascal, M. A. *et al.* Inhibition of fucosylation in human invasive ductal carcinoma reduces E-selectin ligand expression, cell proliferation, and ERK1/2 and p38 MAPK activation. *Mol Oncol.* **12**, 579–593 (2018).

181. Neville-Webbe, H. L., Evans, C. A., Coleman, R. E. & Holen, I. Mechanisms of the synergistic interaction between the bisphosphonate zoledronic acid and the chemotherapy agent paclitaxel in breast cancer cells in vitro. *Tumour Biol.* **27**, 92–103 (2006).

182. Ottewell, P. D. *et al.* Anticancer mechanisms of doxorubicin and zoledronic acid in breast cancer tumor growth in bone. *Mol Cancer Ther.* **8**, 2821–2832 (2009).

183. Dell'Aquila, E. *et al.* Denosumab for cancer-related bone loss. *Expert Opin Biol Ther.* **20**, 1261–1274 (2020).

184. Tsourdi, E., Rachner, T. D., Rauner, M., Hamann, C. & Hofbauer, L. C. Denosumab for bone diseases: translating bone biology into targeted therapy. *Eur J Endocrinol.* **165**, 833–840 (2011).

185. Ford, J. A. *et al.* Denosumab for treatment of bone metastases secondary to solid tumours: systematic review and network meta-analysis. *Eur J Cancer.* **49**, 416–430 (2013).

186. Fizazi, K. *et al.* Denosumab versus zoledronic acid for treatment of bone metastases in men with castration-resistant prostate cancer: a randomised, double-blind study. *Lancet.* **377**, 813–822 (2011).

187. Stopeck, A. T. *et al.* Denosumab compared with zoledronic acid for the treatment of bone metastases in patients with advanced breast cancer: a randomized, double-blind study. *J Clin Oncol.* **28**, 5132–5139 (2010).

188. Salamanna, F., Contartese, D., Maglio, M. & Fini, M. A systematic review on in vitro 3D bone metastases models: A new horizon to recapitulate the native clinical scenario? *Oncotarget.* **7**, 44803–44820 (2016).

189. Krishnan, V., Vogler, E. A., Sosnoski, D. M. & Mastro, A. M. In vitro mimics of bone remodeling and the vicious cycle of cancer in bone. *J Cell Physiol.* **229**, 453–462 (2014).

190. Liverani, C. *et al.* CSF-1 blockade impairs breast cancer osteoclastogenic potential in co-culture systems. *Bone.* **66**, (2014).

191. Mercatali, L. *et al.* The effect of everolimus in an in vitro model of triple negative breast cancer and osteoclasts. *Int J Mol Sci.* **17**, (2016).

192. Mercatali, L. *et al.* Tumor-stroma crosstalk in bone tissue: The osteoclastogenic potential of a breast cancer cell line in a co-culture system and the role of EGFR inhibition. *Int J Mol Sci.* **18**, (2017).

193. Spadazzi C. *et al.* mTOR inhibitor and bone-targeted drugs break the vicious cycle between clear-cell renal carcinoma and osteoclasts in an in vitro co-culture model. *J Bone Oncol.* (2019) doi:doi: 10.1016/j.jbo.2019.100227.

194. Joyce, J. A. & Pollard, J. W. Microenvironmental regulation of metastasis. *Nat Rev Cancer.* **9**, 239–52 (2009).

195. Smalley, K. S., Lioni, M. & Herlyn, M. Life isn't flat: taking cancer biology to the next dimension. *In Vitro Cell Dev Biol Anim.* **42**, 242–7 (2006).

196. Krishnan, V. *et al.* Dynamic interaction between breast cancer cells and osteoblastic tissue: Comparison of Two- and Three-dimensional cultures. *J Cell Physiol.* **226**, 2150–2158 (2011).

197. Mastro, A. M. & Vogler, E. A. A three-dimensional osteogenic tissue model for the study of metastatic tumor cell interactions with bone. *Cancer Res.* **69**, 4097–4100 (2009).

198. Reddy, M. S. B., Ponnamma, D., Choudhary, R. & Sadasivuni, K. K. A Comparative Review of Natural and Synthetic Biopolymer Composite Scaffolds. *Polymers.* **13**, 1105 (2021).

199. Pathi, S. P., Lin, D. D. W., Dorvee, J. R., Estroff, L. A. & Fischbach, C. Hydroxyapatite nanoparticle-containing scaffolds for the study of breast cancer bone metastasis. *Biomaterials.* **32**, 5112 (2011).

200. Liverani, C. *et al.* A biomimetic 3D model of hypoxia-driven cancer progression. *Sci Rep.* **9**, 1–13 (2019).

201. Liverani, C. *et al.* Lineage-specific mechanisms and drivers of breast cancer chemoresistance revealed by 3D biomimetic culture. *Mol Oncol.* (2021) doi:10.1002/1878-0261.13037.

202. Eble, J. A. & Niland, S. The extracellular matrix in tumor progression and metastasis. *Clin Exp Metastasis.* **36**, 171–198 (2019).

203. Ribatti, D., Mangialardi, G. & Vacca, A. Stephen Paget and the 'seed and soil' theory of metastatic dissemination. *Clin Exp Med.* **6**, 145–149 (2006).

204. Wu, X., Walsh, K., Hoff, B. L. & Camci-Unal, G. Mineralization of Biomaterials for Bone Tissue Engineering. *Bioengineering.* **7**, 1–24 (2020).

205. Balasundaram, G. & Webster, T. J. Nanotechnology and biomaterials for orthopedic medical applications. *Nanomedicine.* **1**, 169–176 (2006).

206. Pathi, S. P., Kowalczewski, C., Tadipatri, R. & Fischbach, C. A Novel 3-D Mineralized Tumor Model to Study Breast Cancer Bone Metastasis. *PLoS One.* **5**, e8849 (2010).

207. Watson, A. W. *et al.* Breast tumor stiffness instructs bone metastasis via maintenance of mechanical conditioning. *Cell Rep.* **35**, 109293 (2021).

208. Zhang, W. *et al.* The bone microenvironment invigorates metastatic seeds for further dissemination. *Cell.* **184**, 2471-2486.e20 (2021).

209. Seton-Rogers, S. Metastases arrive at other organs via bone. *Nat Rev Cancer.* **21**, 411 (2021).

210. Bado, I. L. *et al.* The bone microenvironment increases phenotypic plasticity of ER+ breast cancer cells. *Dev Cell.* **56**, 1100-1117.e9 (2021).

211. Pareek, A. *et al.* Bone metastases incidence and its correlation with hormonal and human epidermal growth factor receptor 2 neu receptors in breast cancer. *J Cancer Res Ther.* **15**, 971–975 (2019).

212. Yang, H. *et al.* Impact of molecular subtypes on metastatic behavior and overall survival in patients with metastatic breast cancer: A single-center study combined with a large cohort study based on the Surveillance, Epidemiology and End Results database. *Oncol Lett.* **20**, 87 (2020).

213. Cabioglu, N. *et al.* Chemokine receptors in advanced breast cancer: differential expression in metastatic disease sites with diagnostic and therapeutic implications. *Ann Oncol.* **20**, 1013–1019 (2009).

214. Cox, T. R. *et al.* LOX-Mediated Collagen Crosslinking Is Responsible for Fibrosis-Enhanced Metastasis. *Cancer Res.* **73**, 1721–1732 (2013).

215. Zielińska, M., Chmielewska, E., Buchwald, T., Voelkel, A. & Kafarski, P. Determination of bisphosphonates anti-resorptive properties based on three forms of ceramic materials: Sorption and release process evaluation. *J Pharm Anal.* **11**, 364–373 (2021).

216. Leu, C. T., Luegmayr, E., Freedman, L. P., Rodan, G. A. & Reszka, A. A. Relative binding affinities of bisphosphonates for human bone and relationship to antiresorptive efficacy. *Bone* **38**, 628–636 (2006).

217. Michigami, T. *et al.* The effect of the bisphosphonate ibandronate on breast cancer metastasis to visceral organs. *Breast Cancer Res. Treat.* **75**, 249–258 (2002).

218. Osta, B., Benedetti, G. & Miossec, P. Classical and Paradoxical Effects of TNF-α on Bone Homeostasis. *Front Immunol.* **5**, 48 (2014).

219. Lam, J. *et al.* TNF-alpha induces osteoclastogenesis by direct stimulation of macrophages exposed to permissive levels of RANK ligand. *J Clin Invest.* **106**, 1481–1488 (2000).

220. Marahleh, A. *et al.* TNF-α Directly Enhances Osteocyte RANKL Expression and Promotes Osteoclast Formation. *Front Immunol.* **10**, 2925 (2019).

221. Kobayashi, K. *et al.* Tumor necrosis factor alpha stimulates osteoclast differentiation by a mechanism independent of the ODF/RANKL-RANK interaction. *J Exp Med.* **191**, 275–285 (2000).

222. Lee, S. E. *et al.* Tumor Necrosis Factor-α Supports the Survival of Osteoclasts through the Activation of Akt and ERK. *J Biol Chem.* **276**, 49343–49349 (2001).